Personalized local drug delivery by intra-operative custom made implant coating

A Dissertation

Submitted in Partial Fulfilment of the Requirements
for the Degree of Doctor rerum naturalism (Dr. rer. nat.)

to the Department of Biology, Chemistry and Pharmacy
of Freie Universität of Berlin

by

BRANKO TRAJKOVSKI

Berlin, 2012

Supervisor: Univ.-Prof. Dr.-Ing. Georg N. Duda

Second examiner: Univ.-Prof. Dr. sc. nat. Andreas Lendlein

Date of the viva voce/defense: 15.08.2013

Acknowledgments

My deepest and sincere gratitude goes to both my supervisors, Prof. Georg Duda and Dr. Ansgar Petersen for their patience, advices and continuous support towards this project and myself. The have provided me with both academic and personal guidance throughout the years of this research project. It was a pleasure and I am grateful that I had the opportunity to be able to work with them.

I would like to express my enormous gratitude towards our collaborators Prof. Andreas Lendlein, Dr. Christian Wischke, Dr. Nico Scharnagl and Dr. Wolfgang Wagermaier, for the generous technical and advisory support. Their work and insights were critical towards the goal achievements in the project.

I would also like to thank my colleagues and friends that I made through the years in the laboratory. I will always cherish the full support of Dr. Sabine Bartosch and the Berlin-Brandenburg School for Regenerative Therapies. I will always remember the discussions and all the fun we had together with the other BSRT students-also my dear friends.

I am also grateful for all the love and support that I got from my family, their understanding and encouragement kept me going forward and to never give up.

Abstract

Bone is among the few tissues in the human body that has high endogenous healing capacity. However, failure of the healing process presents a tremendous burden for the individual; it has related health and economic consequences and leads to significant clinical challenge. Various concepts for a local drug delivery to bone have been developed during the last decades in order to overcome such healing deficits. Nevertheless, in most cases these concepts do not specifically meet the surgeon's requirements who must use these strategies; neither have they satisfied the individual patient's needs who should benefit from them. In this dissertation, it is first described the current available methods for local drug delivery as well as their therapeutic limitations. Various solutions for drug delivery systems aiming at clinical applications are discussed. Intra-operative drug delivery by implant coating and strategies for controlled drug release are highlighted. Then a new set of design and performance requirements for intra-operatively customized implant coatings for controlled drug delivery is proposed.

Local application of drugs can be used to promote the regeneration, prevent infection, or treat post-surgical pain. If used in combination with implants, the coating strategies should allow the choice of a drug or combination of drugs, their doses, localization and release due to intra-operative considerations. The current implant coating technologies are distant to personalized medicine strategies. The goal of the present study was to realize a personalized, intra-operative strategy for drug delivery by using a polyvinylalcohol (PVA) patch. PVA patch was rapidly attached to test implant surfaces by a cyanoacrylate (CA) adhesives. Their polymerization to poly(alkyl-2-cyanoacrylate) [PACA] was initiated by water uptake of the patch due to an exposure to a humid environment. A tensile tester was used to measure the coating strength that depended on the type of the PACA, the time of external pressing load, the properties of the patch, the amount of humidity provided, and the type and properties of the implant surface. According to the Wide Angle X-ray Scattering (WAXS), Small Angle X-ray Scattering (SAXS), Raman and Infrared microscopy, CA adhesive did not change the morphology but penetrated into and polymerized within the patch without deactivation of the embedded bioactive molecules. Coomassie Plus Assay was used to define a formulation of the PVA patches so that protein release pattern was minimally affected by the attachment to the implant surface. Flow cytometry (FACS) and Alamar Blue Assay proved that the use of PACA in combination with the PVA patch was non-cytotoxic in vitro. Furthermore, the glued

PVA patches were able to provide a release profile of Dexamethasone that was mainly controlled by the embedded and pre-loaded PLGA microparticles.

The addition of hydroxyapatite (HA) nanoparticles within the PVA changed the morphology of the patch. The presence of HA did not significantly affect the coating strength but it was able to successfully prevent the cyanoacrylate penetration within the patch. That also prevented the swollen patch detachment from some of the implant surfaces. In addition, the release of Dexamethasone from the patch was not influenced by the presence of HA. That could be of a great advantage to safely deliver drugs from a drug loaded particles that can be additionally incorporated within the patch.

Intra-operative drug delivery by implant coating can meet the surgeon's requirements and can satisfy the individual patient's needs. Possible solution could be if the drug delivery systems in a form of patch are rapidly attached to test implant surfaces by a cyanoacrylate (CA) adhesives. Hydrophilic patch composites such as PVA/HA could enable quick water uptake and initiate the CA polymerization. This could result in a strong patch attachment and safe drug delivery due to the amorphous/crystalline composite combination. Finally, this technology platform opens the possibility for personalized medicine to locally administer drugs due to intra-operative requirements.

Table of Contents

1. Introduction (Clinical need to locally stimulate healing of bone and other regenerative tissues) -in parts published [1]

The number of patients suffering from musculoskeletal diseases and injuries is in continuous rise [2]. Due to that fact and because of the increasing age of the patient population, an increased numbers of joint replacement surgeries, spinal surgeries and age-related fractures such as in hip are being observed in Europe and across the U.S. [3-7]. In all those cases, implants are used in mechanically highly loaded areas to replace joints, stabilize fractures, and realign bone fragments or vertebras [8]. Despite the sophistication of the current implant techniques, a "biological problems" are still present and can lead to implant loosening, delayed or non-healing fractures, infection, or non-union in spinal fusion surgery [9-15].

Based on the data of the National Center for Health statistics of the Centers for Disease Control and Prevention [16], almost 16.2 million fractures were treated in physicians' offices, emergency and outpatient clinics, and hospitals in 2006/2007 in USA, accounting for 26% of the 61.2 million musculoskeletal injuries treated. Nearly 3.0 million of these occurred in young males under the age of 18, while a further 2.5 million occurred in females aged 65 and over. Fractures are the most common musculoskeletal condition requiring hospitalization among Medicare enrolees of age 65 and over. Approximately 621,000 patients needed a surgical reduction of the fracture and 403,000 required an additional internal fixation. The total number of fractures of the upper and lower extremities treated in USA has remained fairly constant in the period between 1998 and 2006. Upper limb fractures account for 53-59% of the total fractures treated, while lower limb fractures accounted for 42-48% in the same period. In about 37% of the patients, the long bones of the upper (27%) and lower limb (10%) were fractured. In 2006/2007 the average stay in hospital for a fracture was 5.0 days, giving a total of 4.2 million hospital days and the average hospital charge per patient was $35,000, giving a total cost of $29.08 billion [17].

From 1998 to 2008, the rates of spinal fusion surgery in the U.S. rose constantly from 174,223 to 413,171 per year. During the same period, the average total hospital charges per patient associated with spinal fusion discharges have more than tripled, from $24,676 to $81,960. The overall annual costs for spinal fusion surgery have increased by 7.9 fold, from $4.3 billion in 1998 to about $33.9 billion in 2008 [18]. Especially in the U.S., the costs for spinal fusion surgery were further exacerbated by the use of growth factors (BMP's) as biological stimulation for spinal fusion [19]. Their rate of usage rose from 0.69 % to 24.89%

in 2006, resulting in an increase of between 11% and 41% of the inpatient hospital charges for spinal fusion procedures [19].

Due to the differences in the reporting and recording of health statistics in European countries, directly equivalent regional data cannot be presented here, but the trends and the cost per patient are similar [20-24]. In 2000, the treatment costs associated with hip, spine and wrist fractures reached 32 billion Euros in Europe [25]. In 2002, the age-adjusted incidence of a limb fracture was 7.3 per 1000 person-years in men and 19 per 1000 person-years in women, similar to that in the U.S. [21]. A useful indicator of the increase in Europe of spinal fusion surgical procedures is the market value of spinal fusion surgical instrumentation products. A recent market analysis report concluded that total sales of these products of $528.9 million in 2010 would rise at a compound annual rate of 5.5% to reach an estimated value of $730.9 million in 2016.[26].

Regardless of the geographic location, approximately 5-10% of bone fractures exhibit impaired healing and require additional treatment, with corresponding additional costs [27]. Today, infection rates after joint replacement surgery are reported to be between 0.5% and 12% [15, 28-32]. The non-union rate after spinal fusion surgery ranges from about 10-15% [6, 7, 33, 34]. Depending on the diagnosis and the age and the extension of surgery, the infection rates after spinal fusion surgery range between 0.9% and 5.4% [35]. In most cases, these “biological problems” result from a combination of several local and systemic individual patient characteristics such as: perfusion, previous operations, age, immune-suppression, medication, hormonal status, gender, and metabolic diseases [10, 14, 15, 36-44]. With a rising number of patients suffering from these complications, the associated costs increase dramatically [45].

Fractures of the tibia are the most frequent fractures and are prone to prolonged or delayed healing [46]. They therefore present a good example of the need to focus on and carry out further research on what has been previously described as “biological problems”. The final outcome after tibial fracture depends on multiple local and systemic factors such as the intensity of injury, the amount of the closed or open soft tissue trauma, the existence of an open wound, the amount of fracture fragments, the presence of vascular or nerve injury, the location of the injury, and the selected method of fixation [47]. Even in simple fracture types, tibial fracture healing requires roughly 20 weeks for a successful outcome.

Even when initial treatment is adequate, complications such as delayed fracture healing, non-unions and extensive osseous infections still occur [48]. Delayed unions are defined as fractures that do not heal within the expected period [10]. The frequency is about 16% to

60% for less severe fractures and about 43% for more severe fractures. Non-unions occur if fragment motion persists and no healing is visible by radiology after 6 months. The rate of non-unions of tibial fractures ranges between 4% and 10%. Non-unions are associated with severe pain and lack of limb function [47]. Complications may occur after complex, commuted fractures; open fractures involving a significant amount of soft tissue injury and the risk of infection; inadequate (too early or too late) mobilization; lack of sufficient blood supply and nutrition, or presence of chronic disease such as is found in immune-compromised patients [49]. The described multiple complications after tibial fracture are also known to occur in joint replacement or non-union after spinal fusion surgery [12, 15, 42-44].

Accelerating the regeneration process, especially in bone healing, is a broadly accepted strategy to address these fracture complications and overcome the remaining limitations of impaired healing. After an optimization of the mechanical stabilization the most important aim is to optimize the endogenous biological potential. If the latter is absent, potential strategies such as the use of osteogenic cells, osteoinductive scaffolds, or the delivery of growth factors is required [10].

The biological process of bone healing is considered to be dependent on the availability of osteoprogenitor cells and their precursors, the mesenchymal stem cells (MSC's) [50, 51]. The MSC's can be found in the bone marrow and the periosteum [52]. MSC activation and chemotactic migration from nearby tissue to the injury site is assumed to be a key to the onset of regeneration; MSC's play a crucial role in callus formation and thus the multiple phases of the healing cascade [50, 51]. The bone marrow MSC's have been shown to be effective in repair of bone defects [53]. Still, the use of osteogenic cells in clinical treatments appears to be hindered by many challenges, safety concerns, and debates about the expansion conditions [54]. The combination of MSC's and growth factors like BMP-2 seems to be more effective in new bone formation when compared to the cells acting alone [55]. However, solution of this kind would require a combination device strategy and therefore very complicated approval procedures.

Various growth factors, hormones and other biologically active molecules have shown to have specific effects on bone regeneration [56]. BMPs, VEGF, PDGF, IGFs and TGFβ are known to be directly involved in bone regeneration. Proteins and growth factors (GF`s) are released at the injury site during different stages of the healing cascade and work in an interactive manner i.e. hematoma formation, inflammation, angiogenesis, cartilage formation (with subsequent calcification, cartilage removal and then bone formation) and bone remodelling [57, 58].

BMP`s are TGFβ homo/heterodimeric cytokine molecules secreted by cells. They represent hydrophobic, low molecular weight, dimeric molecules consisting of two polypeptide chains and are connected by a single disulfide bond. Nevertheless, they are bioactive both as homodimers and heterodimers. To date, about 20 different proteins in humans have been identified as BMP's. The osteogenic BMP's are divided into several subgroups: Group 1. BMP-2, BMP-4; Group 2. BMP-5, BMP-6, BMP-7, BMP-8; and Group 3: BMP-9, BMP-10 [56, 59]. The BMP's diffuse by concentration gradients and can cause autocrine, paracrine and endocrine effects [60, 61].

Once secreted, BMP's might act directly and/or might be temporarily stored in the extracellular matrix. In bone, they are generally involved in bone remodelling, bone formation, chondrogenesis, angiogenesis, extracellular matrix formation, mesenchymal cell infiltration and proliferation [59, 62]. BMP's are effective by binding Type I and Type II serine/threonine kinase receptors on the target cells and initiate a number of signalling cascades such as Smad or Mitogen-activated protein kinase (MAPK) pathways [56, 59]. Moreover, BMP-2, BMP-7, and their combinations, promote the osteoblast adhesion and growth onto substrates. They also regulate the osteocalcin secretion (presumably via the IL-6 pathway), and support the extracellular matrix formation by inhibition of MMP secretion (using the TIMP pathway)[62]. Both BMP-2 and BMP-7 increase the alkaline phosphatase (ALP) production, but rhBMP-2 is noticeably more effective then rhBMP-7 [59].

Deregulation in the BMP signalling pathways can lead to various pathological conditions; obesity, diabetes, vascular diseases and cancer have been linked to BMP-2. It has been demonstrated that BMP-2 can stimulate progenitors into white adipogenic lineage. Furthermore, BMP-2 is upregulated in endothelial cells that are present at the atherosclerotic plaques. Various cancers also over-express BMP-2, probably due to its function as an angiogenic factor, thus leading to neovascularisation of melanoma cells [61].

Furthermore, the FGF family members stimulate bone healing, but can also regulate cell proliferation and increase osteoclastic bone remodelling. Equally important, VEGF stimulates proliferation and migration of endothelial cells, leading to the formation of tubular blood vessels. IGF provokes proliferation and chemotactic migration of various cell types [63]. In addition, PDGF seems to recruit osteoblast precursors during bone remodelling and repair. Glucocorticoids have a positive effect on osteoblasts and their mineralization potential; however, in higher concentrations they may significantly decrease mineralization capacity leading to a reduced bone mineral density [56]. All of the above mentioned molecules can

find possible treatment solution for certain indications if delivered properly via drug delivery systems.

Controlled delivery of required drug doses that are readily and rapidly adjustable for specific clinical situations is highly desirable in order to achieve effective bone healing [64]. Therefore, intra-operative customized strategies for personalized treatment and bone regeneration are increasingly important. Formulation and application of new drugs and new drug delivery systems should be achieved in such versatile modes that the specific needs of the individual patients are adequately addressed [1]. The current 'one-size-fits-all' devices do not fulfil this demand nor do the therapeutic procedures that also have little customization ability. Although localized drug delivery is, by designation, a personalized therapy, current strategies often fail to address the specific biological needs of the individual patients. That is due to the use of pre-defined and fixed dosages and pre-coated implants for local administration of drugs [1]. There are certain restrictions with these procedures. For instance, high temperatures and non-physiological conditions are used during the actual coating process in order to prepare inorganic implant coatings. After the coating has been applied they can be drug-loaded with growth factors by adsorption but this can lead to burst and uncontrolled drug release profiles [65]. On contrary, non-ceramic coatings can be customized in their release kinetics as they are drug-loaded during preparation and that can result in controlled drug delivery profiles. They seem to be appropriate for release of small molecule therapeutics (e.g. gentamicin) as well as complex molecules such as recombinant human BMPs. However, their preparation in principle requires long preparation times [66] and the use of harsh solvents [67], both of which limits their use as intra-operative customization strategies. Some of the implant coatings that are coming to market (e.g. Expert Tibial Nail PROtect, Synthes Inc, Nanomagnetic drug delivery, Biophan Technologies Inc) are prepared directly outside the operating room and they contain prefabricated formulations with fixed doses of defined drugs. Such coatings are usually applied not just at the locations where the drug is needed but over the entire implant surface. In order to ensure drug stability during storage periods, the pre-coated implants also require careful quality control monitoring.

The first part of this dissertation discusses the current clinically approved methods for local drug delivery in bone. The provision of localized concentration of drugs is not well achieved by prefabricated solutions and their versatility is limited by the existing procedures. These limiting and inflexible current strategies are the motivation for developing interesting new technologies that could be adapted to meet the challenge of real-time-rapid customization of drug delivery within an operating room setting. Therefore, a new concept of an intra-

operative, custom-made implant coating is proposed. This is a step towards versatility as the surgeon would be able to select an optimal dosage of a suitable drug determined by the specific needs of the individual patient, thus providing personalized-patient specific medical treatment in surgery at its best.

1.1. Combination devices for drug delivery

The drug-device combination products are pioneering biomedical structural devices with the additional feature of delivering drugs to a desired location. Supporting the link between the core device technology and additional components is the general concept of such products [68]. Medical device and pharmaceutical companies have both shown great interest to clarify certain well-known clinical problems associated with the device implantation. The mutual reinforcing effect of the combination device products offer advantages over application of the drug and the device individually. Defined by the US FDA, combination devices comprise two or more regulated components that are combined or mixed and produced as a single product, or appear as two or more products packed collectively. Unfortunately, these products often do not meet the expected effectiveness. The main reason could be that they have not been designed to improve each other and the drug delivery capability serves as an add-on feature that is poorly adapted to the device [69]. Since none of the current combination medical devices have been specifically designed to deliver drugs, new technologies that will combine drug, biologics and device are expected to become available as a new generation of combination devices while establishing a new high-value market [68].

The regulatory process for device and drug/biologic products has important influence on time and cost for approval and market [70]. Previously, FDA assigned the regulatory authority to two or more different centers which raised concerns about the management of entire review process. Therefore, a new Office for Combination Products (OCP) was created in order to specify the appropriate new product regulatory review assignment, and consistent and appropriate post-market regulation after suitable and efficient review [71].

This presents a significant opportunity for the orthopaedic field experts to promote new strategies and accelerate the bone healing outcomes in difficult clinical cases. The currently available orthopaedic, device-based drug delivery systems that are used to treat bone infections consist of antibiotics loaded bone cement, polymethylmethacrylate (PMMA), or PMMA beads. The antibiotic-loaded PMMA cements provide initial burst release followed by a long-lasting and incomplete release up to several months. They are effective in reduction

of infections but their drug release profiles are unsatisfactory and they have poor bonding strength to implant surfaces. PMMA is not biodegradable and thus requires additional surgical procedure for its removal. From that aspect the biomimetic synthetic hydroxyapatites (HAP) are much more appealing in terms of non-toxicity and new bone tissue formation. They can be used for controlled antibiotic release as an anionic collagen:HAP composite paste. These biodegradable polymer cements are superior to the PMMA cements due to the fact that there is no need for second-removal surgery and moreover, they are able to provide longer release of higher concentrations of antibiotics. The biodegradable and FDA-approved polyesters (PLA, PGA, PLGA) have also been widely used for pharmaceutical and biomedical applications. Their molecular weight, copolymer composition, bead size, polymer to antibiotic mass ratio and various processing procedures influence their release kinetics [69].

1.2. Current clinically approved methods for local drug delivery to bone

The limitations in the existing understanding of the timely interaction of proteins and growth factors that influence bone regeneration have led to new principles that target and promote the endogenous regeneration cascades [72]. However, the current surgical procedures in orthopaedics and trauma entail the use of autogenous materials, allogenic bone, and platelet rich plasma (PRP) as a stimuli and a source of growth factors [73]. PRP seems to provide patient-dependent potency and seems not to be effective in all cases [74]. Since the discovery of the strong BMPs potency to produce new bone, an entirely new concept of local administration of growth factors has emerged. The use of recombinant gene technology enables large quantities of defined biological drugs such as several rhBMPs to be produced under well-controlled conditions [75].

1.2.1. FDA approved devices for BMP delivery and their complications

The FDA so far has clinically approved only two BMPs (rhBMP-2 as INFUSE™ from Medtronic and rhBMP-7 OP-1 from Olympus Biotech). In the first one-INFUSE, rhBMP-2 is mixed during the time of surgery and is added to an absorbable collagen sponge that is intended for use in spine fusion. On the other hand, rhBMP-7 is added to collagen granules. The drug application procedure in both these cases takes at least 15 minutes for protein absorption from reconstituted aqueous solution [49]. For example, the INFUSE bone graft

(Medtronic) requires rhBMP-2 to be first gently agitated in sterile water in order to dissolve and then the reconstituted rhBMP-2 is dispensed by a sterile syringe over the thin collagen sponge. After the wetted sponge has been allowed to stand for 15 minutes, it is finally inserted into a metal spinal cage followed by implantation into the spine. These products are limited to being used in anterior application in lumbar spinal interbody fusion (rhBMP-2), postero-laterally in lumbar spinal non-unions (rhBMP-7) and in acute tibial fractures and non-unions (rhBMP-7). Collagen-based scaffolds are used to keep in place and deliver these growth factors to the site of injury in order to initiate the onset of bone formation [75, 76]. The application of rhBMP-2 in lumbar spinal fusion surgeries resulted in increased fusion rates in animal studies [77-81]. In the FDA approval study about lumbar fusion, it was found that the fusion rates seem to be higher with rhBMP-2 when compared to autologous spongiosa (94% vs. 88%); while, at the same time, avoiding donor site morbidity [82]. Other studies have shown that the fusion rates are higher with rhBMP-2, the duration of bony consolidation seems to be shorter although the clinical outcome is similar to that without application of rhBMP [83-85].

In addition, the possibilities of complications arise with the use of BMP's. Due to observed ectopic ossifications rates of 20% to 75% [86, 87]; extensive soft tissue swelling (8% to 50%) followed by dysphagia [88-91]; increased rates of infection [92, 93]; vertebral osteolysis [94, 95]; occurring radiculitis [96, 97]; and graft sintering [98] in the cervical spine, rhBMP's have not yet received their approval. The high dosage used in "off-label" studies in cervical fusion seems to be related to the problem of osteolysis. Such a high-dosage administration appears to additionally activate osteoclasts next to osteoblasts, especially with local presence of inflammatory interleukins [99, 100]. When the bone growth is excessive, such as with ectopic formations, a possible loss of sensory or motor function may occur due to the newly formed bone impinging or compressing the spinal cord or the radices of the spinal nerves in the neuroforaminae [75].

The scaffold material that is used for the growth factor delivery seems to notably impact the effects of BMP's [81, 101]. The effective clinical BMP-2 dose that is considered to be given by some devices that are coming on the market may be as much as 40 mg per application (FDA, P050036). This is in conflict with the clinical requirements to use only minimal doses of BMP for spinal fusion [75]. One trial showed the results of increased healing rates with a higher dose of 1.5 mg/ml of rhBMP-2 compared to a dose of 0.75 mg/ml in acute and open tibial fractures [49]. However, the rhBMP-2 doses used by this drug delivery system are still very high. There are issues regarding the cost and safety because also it does not provide the

desired controlled release profile [64]. Complications associated with high-dose rhBMP-2 treated tibial fractures can be ectopic bone formation, bone resorption, as well as erythema and oedema [76].

1.2.2. Synthetic bone graft scaffolds

The FDA has also approved synthetic bone graft substitutes that are supposed to be osteoconductive without the delivery of growth factors. These grafts typically comprise calcium phosphates used alone or in combination with collagen or other polymers. For example, currently available products are Maxresorb (Botiss), ChronOS (Synthes), Cerasorb (Curasan), Collagraft (Zimmer) [102] or CarriGen (ETEX). These products still do not have approval as combination devices, therefore their use in combination with drugs is considered to be an “off-label”.

The potential failure of the devices for BMPs delivery associated with their high cost has led to alternative combination products. For instance, rhPDGF-BB, known also as pro-angiogenic growth factor, up-regulates the VEGF expression and therefore stimulates the bone and soft tissue regeneration. The combination of rhPDGF-BB with ß-tricalcium phosphate (ß-TCP) (GEM 21S®; Luitpold,) is currently approved for periodontal use in the US, Europe and Canada. In addition, Augment® Bone Graft (BioMimetic Therapeutics, Inc, USA) is a synthetic bone graft replacement material comprising rhPDGF-BB and ß-TCP. The Injectable Augment® Bone Graft also includes rhPDGF-BB and a matrix prepared of β-TCP and collagen (80:20, w:w). Spine fusion models in sheep showed that the effect of Augment® Bone Graft is comparable to an autograft. Therefore, the limitations and morbidities related to the allograft could be avoided. Augment® Bone Graft has received approval for foot and ankle arthrodesis in Canada but is not yet approved by the FDA [103].

1.2.3. Demineralized Bone Matrix (DBM) material

Another source for administration of growth factors in the clinic is demineralized bone matrix (DBM). DBM is a material that is being chemically extracted from allograft bone. The process of preparation involves acidic dissolution of the bone mineral, leaving behind collagen fibres and non-collagen proteins such as BMPs [104]. Due to the extensive processing, it is less immunogenic option when compared to other types of allografts [49].

DBM is considered to be "minimally treated" human tissue and, as such, it has not been a subject of thoroughly testing by the FDA [105].

The commercial DBM is available as a solid, a strip or piece, and as semi-solid pastes bone-filling devices. The variability of the ”osteo-inductive index” of DBM is not subject to control by the tissue bank sources, resulting in their use and efficacy to still remain controversial [104]. DBM can be combined with various biomaterials and devices that can influence the clinical outcome. For example, the moldable soft DBM putty that comprises DBM solid powder and water-soluble polymers, such as sodium hyaluronate or carboxymethylcellulose, or anhydrous water-miscible solvents such as glycerol, is highly preferred for surgical procedures. DBM can be adjusted off-label as a versatile device for local delivery of one or more desired drugs [106]. Local drug delivery to the implant location by intra-operative-on-demand and according to the surgical needs can be achieved by a drug-loaded nano- or micro- particles or capsules addition into the DBM. In order to meet various therapeutic needs, small molecules such as antibiotics, analgesics and anti-inflammatory drugs, as well as proteins, genes, small interfering (siRNA) therapeutics and cells can be formulated into and delivered by DBM [106]. In summary, DBM and DBM/carrier formulations lay basis of a promising combination device technology platform.

1.2.4. Implant coatings

In ideal case, as addition to the mechanical stability, the surgical implant’s adjacent to or at the site of injury should also provide the missing biological factors that are needed to support the healing process. Nevertheless, most research in the field of drug delivery by implant coating is concentrated on improving already existing technologies, and on finding suitable applications rather than focusing on the clinical requirements. Up to date, there is no implant coating strategy that can be customized rapidly during the time of operation in the operating room and the existing off-site coating technologies do not appear to be suitable in all cases.

1.2.4.1. Inorganic implant coatings

The osteoinductivity of calcium phosphate coatings has attracted significant interest by using various coating techniques including magnetron sputtering, plasma spraying, hot isostatic pressing, electrophoretic deposition, sol-gel deposition, ion beam dynamic mixing deposition,

pulsed laser deposition, biomimetic deposition, electro-spray deposition, and electrolytic deposition [65]. However, the majority of these inorganic implant coating techniques do not provide a uniform coating, require highly controlled conditions, have low mechanical strength and are time consuming. Some of them also require high temperatures, non-physiological conditions, specialized equipment and expertise, all representing major drawbacks for drug incorporation during the coating process while performing surgery [65].

For example, absorption of BMP-2 and hyaluronic acid over hydroxyapatite coating enhances the gap healing in bone without influence on the interface shear strength and bone implant contact [107]. On the other hand, the mutant rhBMP-2 with lacking glycosylation has decreased solubility, which in turn leads to delayed release from the application site. Consequently, drying of non-glycosylated BMP-2 onto the hydroxyapatite surface contributes to osteointegration of the implant. A very small BMP-2 release from such a surface has been observed during the first 4 days. More specifically, a coating loaded with 100 µg/cm^2 of BMP-2 released 0.65 µg (or 21%) during a period of 16 days. It was also shown that the loading concentration had influence on the release kinetics, i.e. a coating with 10 µg/cm^2 loading had only 0.06 µg (or 0.18%) of the BMP-2 *in vitro* release [108]. Even though growth factors adsorption on inorganic coatings significantly improves the implant incorporation in cortical bone, gap healing and bone in-growth [109-111], incorporation of the drug into the coating still resulted in a better outcome than if the BMP-2 is just adsorbed [112]. For instance, coatings with incorporated BMP-2 cause an osteoinductive effect up to 70 times more than that of the coatings with adsorbed BMP-2. This is probably due to the fact that the adsorbed BMP-2 depot provides initial burst release and over-stimulation of osteoclast activity [113, 114].

1.2.4.2. Non-ceramic implant coatings

Apart from the above discussed inorganic coatings, most of the non-ceramic implant coating methods permit drug incorporation during the coating process. For example, Synthes has already launched the first antibiotic-coated tibial nail to prevent bacterial colonization on the implant surface (Expert Tibial Nail PROtect) [115]. It represents a thin film of PDLLA polymer loaded with gentamicin sulfate and being prepared by dip-coating of the metallic nail. The dip-coating method can be used to control the drug release profile by the use of only one polymer [67]. It is also called "cold coating" technique and is based on implant dipping in a polymer/solvent/drug solution lasting just a several seconds. The dipped implants are

consequently dried and, during solvent evaporation, a drug-incorporated PDLLA coating is formed. During the first 48 hours, 54% of IGF-I and 48% of TGF-ß1 were eluted from such a coating *in vitro*. Furthermore, after 42 days, 76% of IGF-I and 71% of TGF-ß1 were released [116]. This coating has already been shown to deliver BMP-2 as well, and can also be effective in bone healing [117, 118]. Unfortunately, concern may well arise from the use of harsh solvents such as chloroform and ethyl acetate. To illustrate this, their handling requires strict safety precautions, and the need to remove residual harsh solvents from the coating requires longer drying times, both of which are disadvantageous in an intra-operative situation.

Recently, the layer-by-layer (LbL) coating technique has attracted significant interest for drug elution by implants. The LbL technique includes subsequent dipping of the implant in positively and negatively charged polymer solutions in order to prepare a multilayer, structured film. Great potential lies in the LbL technique for fine-tuning of the drug incorporation and its controlled delivery. Macdonald *et al.* achieved microgram-scale delivery of BMP-2 by increasing the number of layers and the coating thickness. Most of the BMP-2 (80%) was released within two days and was followed by a linear release *in vitro* during the study period of 14 days [66]. The LbL technique requires a series of alternate dippings in polymer and drug solution, each followed by washing and drying, and each lasting several minutes. Unfortunately, due to the need of a long preparation time, this technique cannot be easily customized and used intra-operatively. An additional concern is the durability of these coatings during routine orthopaedic handling and placement.

1.2.5. Injectable biomaterials and their disadvantages

Injectable medical devices in current commercial use, such as Spineplex Radiopaque Bone Cement (Stryker), Spine-Fix Biomimetic Bone Cement (Teknimed), Staxx Fx System (Spine Wave, Inc), Confidence High Viscosity Bone Cement (Disc-O-Tech Medical Technologies, LTD.), Cortoss (Orthovita, Inc), are bone cements that are used as bone augmentation materials. It is well known that these bone cements result in incomplete drug release; they do not provide the desirable release profiles and their exothermic polymerization can kill surrounding tissue and inactivate loaded drugs [69].

It was hypothesized that a heparin-loaded fibrin-fibronectin matrix is an ideal injectable drug delivery system [119]. However, these fibrin-fibronectin systems can have certain safety drawbacks such as allergies, anaphylaxis and transmission of viral diseases [120]. Therefore,

the use of synthetic carrier polymers that can be injected has attracted much more attention. For example, poly(ester-anhydrides), that are based on sebacic acid and ricinoleic acid, harden to a semi-solid just after addition of the buffer and consequently release drugs during gradual degradation [121]. At room temperature, poly(sebacic-co-ricinoleic-esteranhydride) P(SA-RA) is a pasty material that allows integration of drugs by gentle mixing without use of any additives or solvents . The biomaterial can later be injected at the selected location and, as soon as it gets into contact with body fluids, it gels and entraps the drugs [122]. Furthermore, an attractive drug delivery system for intra-operative customization is the synthetic poly-d,l-lactic acid-para-dioxanone-polyethylene glycol (PLA-DX-PEG) copolymer because it undergoes temperature-dependent liquid-semisolid transition (liquid at 60°C, semisolid at 37°C). The PLA-DX-PEG copolymer that is loaded with BMP-2 can be heated, injected as a liquid and, at body temperature, it then turns into a semisolid [123].

Nevertheless, such injectable materials are always at risk of interfering with the biological healing process in some way. In contrast to scaffolds or combination products, they merely supply drug and their depot positioned adjacent to the injury and healing zone should not negatively influence the biological processes in the zone itself. Since bone healing is a mechano-biologically driven process, additional parts of biomaterials that only indirectly interact with the healing zone can cause additional inflammatory cascades. If the presence of such injectable biomaterial is too far away from the healing zone, the dosage of delivered drugs has to be increased and their efficiency is reduced. In ideal case, the implant device properties already deliberately used in place to provide the requisite mechanical framework for bone healing should be partnered with appropriate biological factors as the release kinetics and dosing will provide simultaneous additional stimuli for bone regeneration.

1.3. The need for development of new intra-operatively customized implant coating strategies

While a wide choice of potential injectable depot-based drug delivery candidates that can be customized intra-operatively according the individual patient’s needs are available, this is not the case with drug delivery by implant coating. There are not enough methods that can apply sustained, controlled release drug delivery systems as intra-operatively customized implant coatings, controlling kinetics, dosing, different drug formulation requirements and local pharmacology. Currently, surgeons are limited to the use of only approved pre-coated, pre-loaded implants as prescribed by and received from the manufacturer. This type of coating

has a defined drug loading and dose, as well as location over the surface of the implant. In most cases, this seems to be a preferred option in order to treat the "average" patient. However, in some cases it is highly desirable that the surgeon has the facility to choose which drugs, coatings, and doses to best are applied at which specific spatial locations on the device or implant surface.

In view of previously stated limitations, the development of new intra-operative, versatile, custom-made implant coating technologies is highly beneficial. It would be of a great advantage if these technologies could allow localized drug dosing and administration during surgical procedures according to the particular needs of each individual patient. These implant coatings should be custom-shaped and efficiently loaded with clinically relevant drugs using methods capable of avoiding any loss of expensive materials such as growth factors. In addition, their bioactivity should be preserved while ensuring proper loading, release and dosing. One option to provide these capabilities is to pre-fabricate certain coating components independently under controlled sterile formulations conditions to be made available for surgical assembly and use. Implant coating should not only be able to be rapidly applied over the implant surface, also in patterns or only in localized areas, it should also be capable of providing controlled drug release of either single or multiple drug administrations**.** An ideal implant coating system of that kind would facilitate the surgeon to deploy it quickly within the surgical location based on intra-operative decisions determined by local patient and disease requirements, thus applying local therapies to patients according to their individual needs.

1.3.1. Current perspectives of intra-operative implant coating

In order to allow such intra-operative and rapid implant coating, new delivery systems have to be developed that meet criteria such as biocompatibility, biodegradability, low immunogenicity, preservation of drug bioactivity, ease and low cost of large-scale production, facility for proper storage and reliable shelf-life, stability and handling, sterilization, and the provision of a controlled drug release profile, or perhaps several possible release profile choices. The attempt to use glycosoaminoglycans and proteins as implant coatings to deliver drugs has already been considered. In this case, collagen/chondroitin sulphate and collagen/chondroitin sulphate/BMP-4 coatings appeared to be more effective in bone formation than the collagen coating only [124]. Unfortunately, most of the research in this direction has used only well-known coating techniques such as fibrillogenesis and has

not yet addressed the development of newer approaches that can be used for more versatile intra-operative customized coatings.

1.3.1.1. Sleeve coating concepts

Nano- and micro-encapsulation of biologically active components is another extensively studied strategy for controlled and sustained drug release. Present approaches for using micro/nano-carriers involve combining, dispersing, incorporating and sintering them into 3-D porous scaffolds [56]. Subsequently, they can be included in gels [125-127], fibrous scaffolds [128], pastes [129], composite scaffolds [130, 131], and ceramic materials [56]. The most commonly used biomaterial for preparation of micro-spheres and micro-particles is PLGA [132, 133]. PLGA micro-spheres have already been immobilized in a polyvinyl alcohol (PVA) hydrogel as a coating for implantable devices in order to deliver dexamethasone [134, 135].

Furthermore, placing the device implant inside a drug-impregnated thin degradable sleeve during the surgery offers a good intra-operative solution for applying drugs over the implant surface. A sleeve-based approach has already been used for delivery of rhBMP-2 by PLGA micro-particles. In this case, a porous polypropylene fumarate (PPF) was tested as the sleeve for a solid PPF intra-medullary rod. Such porous sleeve was pre-wetted and then loaded with a polymer Pluronic F-127 gel/PLGA micro-particle aqueous suspension. In order to achieve the desired drug loading, the mixture was pipetted into the sleeve followed by application of a vacuum. The mixture penetrated throughout the scaffold and was then incubated at 37^0C for 10 minutes in order to accomplish matrix gelling within the pores [136]. This seems to be a very promising strategy for adapting the type and dose of drugs, but may still be too tedious and time consuming for intra-operative needs.

If the sleeve is used as provided by the manufacturer, the surgeon does not need to prepare any drug delivery formulation, thus ensuring standardized drug delivery conditions. The sleeves can be entirely loaded with gel/drugs or just partially loaded at specific locations onto the sleeve. In such way, the surgeon can select the precise locations on the implant surface to position the drug releasing part of the sleeve [137]. Unfortunately, this method is currently restricted by the high temperatures required during the sleeve manufacturing process, preventing its combination with various biologic drugs and growth factors.

Sleeves provided by Synthes Inc., USA, comprise synthetic degradable co-polyester prepared from glycolide, caprolactone, trimethylene carbonate and lactide. In a sheep model, such

sleeves were placed over a metallic compression plate just before stabilization of an osteotomy of the tibia. They released gentamicin and triclosan without any irritation of the bone and with a foreign body response in the physiological limits [138]. Another example is a gentamicin-polyurethane-coated sleeve that was able to deliver the antibiotic for 26 weeks *in vitro*. These sleeves are known under the name OrthoGuard AB (Smith & Nephew Inc.) and have FDA clearance for coating pins and wires that are used with external fixation devices [139].

1.3.1.2. Sticky strip coating concepts

An interesting alternative for a versatile intra-operative platform technology would be for the drug delivery system to be prepared prior to the implantation. In this case, an apparatus and standard method would be required for producing the drug delivery system that comprises a device that would dispense drugs or drug-loaded particles from multiple drug cartridges by using a pen or a brush system (Fig. 1a) onto a sterile implantable device in a sterile field during surgery. This could be a generic biomaterial matrix or sheet that absorbs the loaded drug and is pre-coated by a surgical adhesive for implant attachment. An adjustable device for cutting could be located below the dispenser in order to adjust and optimize the size and shape of the sticky strip prepared from the biocompatible and bioresorbable adhesive material. Immediately before use, the chosen drugs would be applied to the sticky strip which is then fixed onto the implant surface using a surgical adhesive (Fig. 1b) [140]. A limitation of this drug delivery platform is that generally only aqueous setting can be used as a solvent or dispersant for the drugs (even though some organic solvents are approved for topical oral/gingival drug delivery e.g. NMP). Organic solvents usage to disperse the drugs could result in residual solvent in the strip and associated toxicity/safety issues or proof of elimination. Other drawback of this strategy is the difficulty in obtaining proper adhesion to the implant surface, especially in cases with surfaces that have a protective oxide layer or poor interfacial adhesion (e.g., rough surfaces, many polymers). Here, the strip adhesion would have to rely only to the mechanical interlocking with the implant surface micro-roughness. If the adhesive is coated onto the sticky tape, there will be lack of opportunity for the adhesive to penetrate into the rough structure of the implant surface and, with the resultant poor bonding, the coating may fail during the implantation procedure. An additional risk is that the coating may detach after device implantation and cause problems such as

irritation and displacement of the localized drug delivery. Therefore, the development of other more reliable coating methods needs to be further investigated.

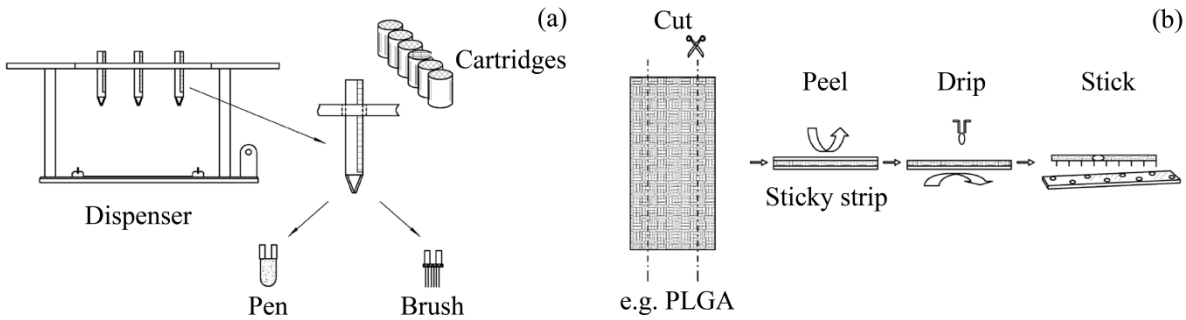

Figure 1. Apparatus for drugs to be loaded on the sticky strip (a). Optimized sticky strip dimensions, drug loading and application to the implant surface (b). Taken from patent application US20090182425A1.

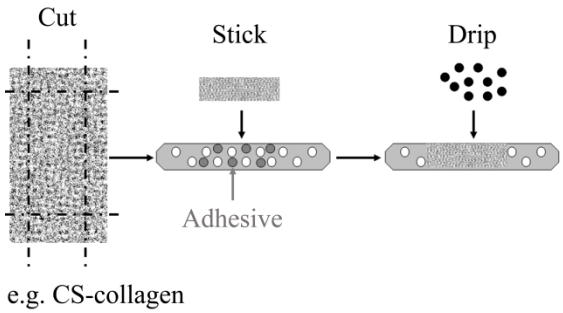

Figure 2. Drug-releasing strip dimensions optimization (left), application of the strip to the implant surface by adhesive -- e.g. fixation plate (middle), and drug loading of the strip (right).

Collagen is a material that can be easily processed as a porous matrix and be modified with additional functional polymers, such as chondroitin sulphate (CS). The presence of CS into the collagen scaffold results in an increased number of polar groups. As a result, the hydrophilicity of the scaffold is increased and could thus absorb much greater amounts of rhBMP-2. The scaffolds prepared of CS-collagen had better osteoinductive activity in rabbit mandibular bone defects as a consequence of the high initial release of rhBMP-2 [141]. The processing of this material into highly porous strips could have great potential for intra-operative customization. First, the drug-free strip can be custom-shaped according to the implant needs. Second, the strip could be fixed over the implant surface by medical adhesive. In a final step, pre-loaded and pre-validated nano- or micro-spheres or particles with certain

known drug doses per mass fraction could be loaded into the strip according the surgeon's discretion. The same principles that valid for the porous sleeve [136] could be also adopted for a porous strip (Fig. 2). This strategy is highly versatile but also time consuming within a timeframe of minutes, which is not desired in many surgical situations.

1.3.2. Local and rapid gluing of drug delivery patches

The drawbacks of the previously mentioned intra-operative coating strategies have inspired further ideas for the creation of new coating platforms that would better fulfil the following requirements: strong implant adhesion and rapid attachment to the implant surface; no time consuming preparations and the ability to deliver various types of drugs, including temperature-sensitive drugs such as biologics and growth factors. Preparation of prefabricated and drug-loaded patches seems to be a promising approach in this direction. Such patches should be able to provide mechanical support and allow a controlled drug-delivery. Medical adhesives could be used to accomplish a rapid intra-operative implant coating strategy by attaching drug-loaded patches of specific doses and calibrated by strip size/area at the specific locations of interest on the implant surface.

1.3.2.1. Optional adhesives and sealants for intra-operative coating

Out of all current FDA-approved medical adhesives, cyanoacrylates appear to be most appropriate for attachment of drug-releasing patches to implant surfaces [142, 143]. Cyanoacrylate adhesives have certain advantages over fibrin glues (e.g., Tisseel), bovine albumin/glutaraldehyde glue (e.g., BioGlue), polyethylene glycol-based sealants (e.g., FocalSeal-L, CoSeal, AdvaSeal-S, DuraSeal, ProGel) and the collagen-based adhesives (e.g., FloSeal, Proceed, CoStasis) which are actually formulations that mechanically seal areas of tissue trauma, leakage or bleeding. Some of them can also swell by up to 600% and this could potentially result in their detachment from the implant surface. Cyanoacrylate pre-polymers and monomers, on the other hand, can penetrate within the micro-roughness of the implant surface, polymerize inside, and form highly crystalline and hydrophobic poly(alkyl-2-cyanoacrylates). The cyanoacrylate adhesives have much stronger bonding properties than any of the above mentioned glues and sealants, which makes them great candidates for the intra-operative implant coating [142-146]. The strong and durable bond is of significant

advantage if the coating must remain attached to the implant surface for a long time after the initial implantation.

However, due to their degradation products such as formaldehyde and alkyl cyanoacetate, the cyanoacrylates remain a major concern for the FDA and there are currently no FDA-approved cyanoacrylate-based adhesive products for long-term implantation into the human body. Nevertheless, the cyanoacrylates have already been widely used for various clinical applications such as thoracic, gastrointestinal, neurologic, cardiovascular, ophthalmologic, and vascular surgery as well as in cartilage and bone grafting procedures [142]. In order to ensure that cyanoacrylate adhesives can be safely used for long-term implantation, it would be a great benefit to include some additional components such as those in drug-loaded patch itself. In the first place, the humidity in the patch would initiate the cyanoacrylate polymerization after the monomers had penetrated the micro-roughness of the implant surface. Then the patch would represent a barrier between the cyanoacrylate adhesive and the surrounding tissue, thereby greatly retarding the diffusion of dangerous degradation products from the cyanoacrylate adhesives. An option would be for the degradation products to be safely neutralized by the patch before they could diffuse away from it into the surrounding tissue.

1.3.2.2. Sticky drug delivery patch design

To incorporate many of the requested design features for surgical performance and versatility, the ideal patch would have to comprise of at least two layers. The first, or barrier, layer would be in contact with the adhesive and could consist of a biomaterial that interacts with the cyanoacrylate in order to form an interpenetrating polymeric network. The thickness of the barrier layer should prevent the diffusion of the cyanoacrylate monomers so that these monomers do not penetrate and chemically interact with the drugs in the second drug delivery layer (Fig. 3). On the other hand, the barrier layer should not swell to such an extent that it would result in patch detachment from the implant surface. If the patch were to deform and swell excessively, the polycyanoacrylate network and the polycyanoacrylate within the micro-roughness of the implant surface would also deform to adjust this dimensional change. As a result, the patch would most certainly detach from the implant surface if there is no chemical interaction with the substrate and cause complications such as bone irritation, loss of structural integrity and de-localization of the patch.

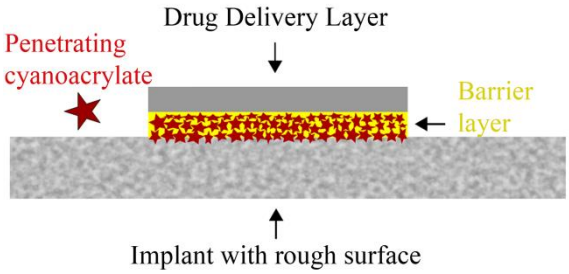

Figure 3. Drug delivery patch rapidly attached to the implant surface by a cyanoacrylate adhesive.

The second layer of the patch would carry out the role of drug delivery system. In order to accomplish the desired drug release profiles, the drugs would have to be pre-loaded into the patch or in micro- or nano-particles or spheres that are immobilized within during fabrication. The proper choice of particle/patch combination would permit the provision of specifically designed properties over a wide range of single or multiple drug release profiles. In ideal case, the patch itself would minimally influence the release profiles provided by the embedded particles. Such a technology platform would be universal for any designed drug loaded particle, drug or release profile and suitable for numerous clinical applications.

This patch design is similar to the multilayer transdermal drug delivery patches that is currently classified as combination device and is used in millions of pieces world-wide annually for multiple major drug classes. These patches usually consist of backing film, drug reservoir layer and adhesive that contacts the skin. In some cases, semi-permeable membrane between the drug reservoir and the adhesive is used as rate-limiting barrier. It is also possible to have matrix system of two layers by incorporating the drug directly into the adhesive [147, 148]. Nevertheless, the presence of backing film provides limitation for drug to be released in a direction towards the adhesive and its substrate, which is not desirable for drug delivery by implant coating. Furthermore, the non-degradable polymers that are used for transdermal external use by this technology do not fulfil the criteria for internal implantation in the body.

1.3.2.3. Application of the drug delivery patch over the implant

In order to achieve reproducible and reliable patch attachment over the implant, the proposed patch could be mounted into a humidity chamber for a short period to activate the adhesive. There, the patch would absorb sufficient amount of humidity to serve as an initiator for cyanoacrylate polymerization. In the meantime, the cyanoacrylate adhesive would be applied

at the desired location on the implant surface. The low viscosity of the cyanoacrylate adhesive would allow the monomers sufficient time to penetrate within the micro-roughness of the implant surface. Then the humidified patch would be positioned just above the desired implant location and pressed against the adhesive. This will require the design of a new device incorporating a slot for locating the implant in the position where the adhesive is supposed to be applied. A slot for positioning of the drug-loaded patch could also be part of incorporated humidification chamber. Finally, an orifice below the patch would be opened to allow the patch to be pressed from above using an elastic disk to distribute forces equally during application pressure (Fig. 4). A few seconds would be sufficient to achieve full bonded adhesion of the patch to the implant surface.

New intra-operatively customized solutions of this type would appear to be mandatory in order to achieve the desired results. Most importantly, such a drug delivery coating platform would have to be universal in general design and able to support controlled release of single or multiple drugs. For this purpose, in this thesis, we propose a combination of a well-tuned drug delivery patch model and a suitable adhesive for a fast and intra-operatively applicable attachment.

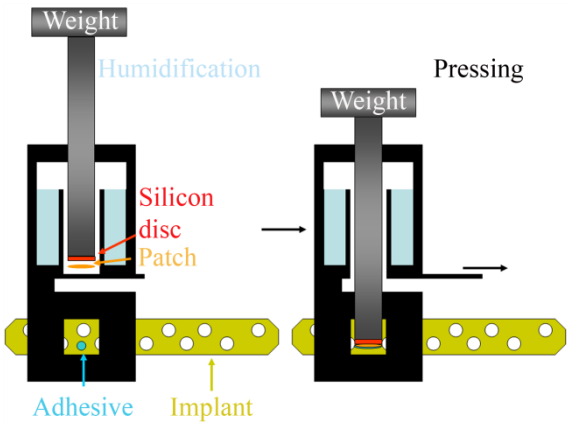

Figure 4. Humidification and positioning of the patch above the desired implant location (here a fracture fixation plate) for patch application and coating (left). Once pressed against the adhesive, the patch is glued directly and rapidly onto the implant surface.

1.4. Possible strategies in order to provide controlled drug delivery from patches

In order to control their release profiles, drugs can generally be physically entrapped [149], adsorbed [150], be involved in non-covalent (hydrogen bonds, electrostatic bonds, Van der Waals forces, hydrophobic interactions) [151], or undergo covalent interaction [152] and

complexation [153] with the biomaterials. It is widely accepted that proteins such as BMP's need to be stabilized by controlled drug delivery systems in order to prevent them from enzymatic degradation [154]. Additionally, the drug delivery systems have to fulfil requirements such as: control of release kinetics and dosing, localization at specific sites, stabilization, and bioactivity protection against molecule denaturation. The attempts to use glycosoaminoglycans and drug loaded particles for implant coating have already been investigated [124, 134, 135]. There is still a lack of techniques that can apply sustained, controlled release, drug delivery systems as intraoperative, customized implant coatings. Anyway, the use of glycosoaminoglycans and micro- and nanocarriers appears to be the best current strategy for controlled drug release profiles and they should remain in focus for future patch designs.

1.4.1. Glycosoaminoglycans

A very promising strategy to control drug delivery profiles is the use of highly anionic, sulphated glycosoaminoglycans such as heparin, heparan sulfate and hyaluronic acid [119, 151, 154-159]. Actually, the heparan sulfate proteoglycans represent reservoirs and co-receptors that present the growth factors to the cell receptor, thereby altering the growth factor-receptor interaction [154]. Heparin has the highest anionic charge density of any known biological molecule and represents a multivalent binding agent for many molecules [151]. As a result, the positively charged amino acids on proteins form ion pairs with the negatively charged sulfo- or carboxyl groups on the heparin chain. These ion pairs represent the main type of interaction between heparin and proteins; however, hydrogen bonding and hydrophobic forces are also present [160]. For example, heparin conjugated to fibrin can prolong the release period of BMP-2. This injectable system was able to achieve about 89.4% of *in vitro* BMP-2 release in 13 days, whereas the fibrin only system released about 83.7% in 3 days. A release of 1 µg of BMP-2 from this system was sufficient to induce ectopic bone formation in rats [157].

On the other hand, if heparin is stabilized in an ionic complex by other biopolymers like chitosan, then BMP-2 is released in accordance with the degradation rate of chitosan. In this case, the chitosan protects the heparin from enzymatic degradation and heparin stabilizes the growth factor. As a result, a heparin/chitosan complex loaded with 50 µg of BMP-2 induced abundant ectopic bone formation in the muscle of a rat when compared to collagen gel formulation [154]. In order to tune the controlled release of bFGF, other biomaterials like

PEG can also be cross-linked with heparin via covalent [151, 155] or protein-polysaccharide interactions as described below [156, 158]. For example, maleimide functionalized, high molecular weight heparin was cross-linked into a hydrogel with thiol-functionalized PEG. This hydrogel was able to achieve 15-30% *in vitro* release of bFGF in a period of 7 days. Actually, the release profile showed a very little to slight burst release [151]. Furthermore, thiol-modified heparin was cross-linked with thiol-modified hyaluronan or chondroitin sulphate with PEG-diacrylate in order to prepare hydrogels. The increase of the heparin percentage in the hydrogels was able to retard the bFGF release *in vitro* and was able to achieve a cumulative release in a period of 35 days. These hydrogels dramatically increased the neovascularization in subcutaneous pockets in mice [155]. Platelet factor 4 (PF4) is probably the strongest heparin binding protein. In order to form a hydrogel, the PF4-functionalised star-PEG (PF4-PEG) was reacted with low molecular weight heparin-functionalised star-PEG (LMWH-PEG). The release kinetics of bFGF out from this hydrogel had an initial burst release *in vitro* of about 25%. The release continued linearly and reached 35-40% over 10 days [158].

1.4.2. Microcarriers and nanocarriers

The micro- or nano-carriers can be prepared by polymerisation and preformed polymers. Furthermore, the micro-carriers favour longer release rates because of the smaller surface area than compared to the nano-carriers. The size, form, properties, rate of degradation and drug release profile of the micro/nano-carriers are controlled by choosing the correct polymers, concentrations, stabilizers, and conditions and techniques of preparation [161, 162]. In order to achieve the drug loading by diffusion, the micro- or nano-carriers can be immersed in a solution of growth factors [125, 127, 163] or the solution can be applied onto the dry micro/nano-particles [164, 165]. The growth factors can also be incorporated during the preparation of the carriers, for example, by using double-emulsion techniques [129], coacervation [166] or by crosslinking polyelectrolyte complexes [149].

For example, heparan sulphate-immobilized onto hyaluronic acid-based hydrogel particles can contribute to a minimal burst release followed by a linear release of BMP-2 for a period of 15 days [167]. PLGA is the most commonly used biomaterial for preparation of microspheres and micro-particles [132, 133]. Nevertheless, the short half-life *in vivo* of BMP-2 and depletion of its therapeutic dose when delivered by INFUSE (Medtronic), has been the inspiration for many attempts to achieve sustained BMP-2 release out of PLGA

microparticles. More recently, it has been demonstrated that using a plasticiser (PLGA-PEG) with the PLGA microparticles can result in sustained BMP-2 release for over 2 weeks [168]. In order to provide a prolonged release of BMP-2, and thus induce osteogenesis, PLGA can also be prepared as microcysts [169]. For instance, the composition of hydroxyapatite and PLGA is able to modify the release of BMP-2. As a result, these microspheres show that a faster sustained-controlled release results in better bone healing than does a slower release. It is of a great importance to have a sustained release of growth factor but if the daily released dose is below a certain concentration, then it may be of no effect at all in bone healing. In this case, 20 ng/ml of constant BMP-2 release for 7 days induced significant bone formation in a mice tibia model [64]. Moreover, hydroxyapatite-coated poly(lactide-co-glycolide) microspheres also seem to be a very promising system for controlled delivery of proteins. They have a high protein binding potential and can maintain sustained bovine serum albumin (BSA) release for 30 days *in vitro*. This is probably controlled by the mineral dissolution and the high coating porosity [170]. Certainly, drug delivery by PLGA microspheres or microparticles can also be modulated by using different PLGA resomers [163, 171]. Here, two types of implants were prepared by incorporating BMP-2 loaded PLGA microspheres in a carboxymethyl cellulose (CMC) implant. Different PLGA resomers were used to achieve an immediate (65% initial burst) and a sustained (45-55% initial and 75-80% for 42 days) BMP-2 release formulation. As a result, the sustained formulation lead to faster and complete bone healing in an animal model [163]. The nature of the 3D scaffolds can significantly influence the release profile of BMP-2-loaded PLGA microspheres incorporated within the scaffold. In fact, the BMP-2 loaded PLGA microspheres/poly(propylene fumarate) scaffold can result in 56 days of linear *in vitro* release [129]. Moreover, the burst BMP-2 release profile also depends on whether or not ectopic or orthotopic scaffold implantation is being used. More specifically, a minimal burst BMP-2 release of about 4.8% for ectopic and 9.5% for orthotopic implantation in rats was observed for the PLGA microspheres/poly(propylene fumarate) scaffold [172].

Poly-L-Lysine (PLL) and polyethyleneimine (PEI) coated Bovine serum albumin (BSA) nanoparticles are also promising delivery systems for BMP-2. For instance, the polyethyleneimine coating effectively reduced the initial burst release of BMP-2 but that did not induce any ectopic bone formation in the rat. The cationic character of polyethyleneimine, its toxicity and dose release below the effective concentration, might be the reason for lack of osteoinductivity [166, 173, 174]. In order to provide a sustained and lower burst release, PLGA nanoparticles and nanospheres can also be functionalised with

heparin, then loaded with BMP-2 and included in fibrin gel [126]. The bone regeneration with BMP-2 loaded nanoparticles-fibrin was more effective than the fibrin gel with or without BMP-2 or the nanoparticles-fibrin without any BMP-2 [125]. The heparin-conjugation over the PLGA nanospheres enabled the *in vitro* sustained delivery of BMP-2. The long-term release for 4 weeks with no initial burst was much more effective in ectopic bone formation than the short-term delivery formulation (BMP-2 loaded fibrin gel having normal PLGA nanospheres) [127]. Furthermore, the combination of this drug delivery system with undifferentiated bone marrow-derived MSC's, was able to induce more effective ectopic bone formation when compared to the osteogenically differentiated or undifferentiated MSC's [55].

Recently, smart polymeric systems have attracted significant attention in bone tissue engineering [175]. These systems are supposed to respond according the individual needs of the patient and deliver therapeutic levels of drugs in coordination with the biological status. For example, BMP-2 loaded glycidyl methacrylated dextran (Dex-GMA)/PEG microspheres can be embedded in a temperature sensitive glycidyl methacrylated dextran (Dex-GMA)/gelatine hybrid microporous hydrogel scaffold. At 37.2°C the hydrogel network collapses, which might be the reason for entrapping the residual BMP-2 and consequently retarding its release [131]. Moreover, this system is capable of dual delivery of IGF-1 and BMP-2 and has an effect on periodontal ligament fibroblasts (PDLF's) [176].

The use of micro- and nano-particles, spheres, and capsules provides a wide opportunity of choice in terms of dual drug delivery. For example, BMP-2-loaded PLGA nano-capsules and BMP-7-loaded poly(3-hydroxybutyrate-co-3-hydroxyvalerate) (PHBV) nano-capsules incorporated in a chitosan fibrous scaffold are capable of achieving sequential drug delivery [128, 177]. Indeed, such a sequential drug delivery can mimic natural processes and thereby have a synergetic impact on bone healing [149, 178].

2. Motivation, Objectives and Project Strategy-in parts published [1]

While the biomechanical situation in trauma and orthopaedic surgeries can usually be controlled by employing modern implant designs, enhancements of the individual patient's tissue biological environment seems to be a key requirement in better and more directly addressing biological deficits in individual patients that seem not to respond or who have an insufficient response to classical treatment regimes. Applications of advanced therapeutics via combination devices could exploit local drug dosing, tissue therapeutic needs and

pharmacologies, and the surgical placement of the implant. Unfortunately, medical implant devices were never designed to deliver drugs so they were originally approved without any drug delivery capability. Re-engineering existing devices to deliver drugs is one possible option. From a clinical view, the current manipulative approaches such as bone graft scaffold materials, demineralised bone matrix, implant coatings and FDA-approved devices for delivery of BMPs to bone do not appear to be fully reliable or effective in all cases. One simple description is that the surgeon is not yet able to select a suitable dosage of a required drug as determined by the specific needs of the individual patient, and is thus not providing personalized medicine in orthopedic repair surgery at its best. Consequently, the establishment of new treatment solutions such as local drug delivery approaches is considered of great benefit for patients as well as surgeons. The development of combination device technologies presents a big opportunity to use their drug delivery capabilities and thereby improve the clinical outcomes during routine surgical manipulations.

While injectable drug delivery depot systems are capable of intra-operative customization, the surgeon is still limited to pre-manufactured solutions of implants and drug-delivery coatings. These prefabricated combinations and their versatility are limited by the existing available coatings. Depots are also acting in order to deliver drugs and therefore lacking all other implant benefits (including biomechanical or structural properties for musculoskeletal repair). In order to address these limitations, new concepts of intra-operative custom-made implant coatings were already suggested [1].

Intra-operative drug loading of implant sleeves is an emerging versatile technology for manipulation of the location of application, the drug type and their doses. Pre-loaded and drug-eluting sleeves provide a less time-consuming strategy for coating implants and supplying them with local pre-formulated drug release. Unfortunately, the current processing techniques for these sleeves limit this strategy to delivery of robust small molecules and antibiotics, not biologics. The preparation of drug-loaded “sticky” or adhesive strips during surgery and their subsequent application over the implant surface seems to work only if the implant surface is not protected by a passive oxide layer or non-stick polymer. In addition, the preparation of the sticky strip or adhesive fabric itself may also take valuable time during surgery. The same problem is valid if the drug-loaded sleeve concept is translated into a sticky strip technology. Finally, a drug-loaded patch with defined drug release profiles can be prepared by various pre-processing techniques, including drug loading, laminate designs and adhesive pre-cursor pre-application. Such drug delivery patches can then be activated in situ and attached to the implant surface using a surgical (e.g., cyanoacrylate) rapid-set adhesive in

an intra-operative setting. In fact, rapid attachment can then be achieved by humidifying the drug-loaded adhesive patch and pressing it against the implant. This procedure initiates immediate polymerization of the adhesive and takes only few seconds of the valuable surgeon's time. The major advantages of such a coating strategy are localized dosing and drug administration in a custom-shaped and tailored approach readily realized during the surgical operation time. The implants could be able to provide controlled release of single or multiple drugs and could be efficiently loaded without any loss of expensive drugs or other materials (Fig. 3).

Any successful intra-operative, drug delivery implant coating platform has to satisfy certain criteria such as: fulfil local dosing and administration requirements; meeting the individual patients' needs; having a fast manipulation time during surgery and providing controlled release of either single or multiple drugs. Furthermore, the implant coatings should also be custom-prepared without any associated loss of expensive drugs (e.g. growth factors). In order to achieve such goals, the drug delivery coating should be prefabricated and stored as provided by the manufacturer and not prepared during the time of surgery. During surgery, the surgeon should have the freedom of choice as which coating containing which drug(s) to be applied at which locations on the implant. For this to be realized, it should be possible to unpack the sterile laminates or coatings and rapidly apply them to the implant surface in just a few seconds.

One solution to achieve such a local drug release platform is to realize a reproducible production of patches. For example, polyvinyl alcohol (PVA) is a highly interesting biomaterial for biomedical and pharmaceutical usage due to its hydrophilic nature. Further, PVA has relevant mechanical [179], film forming and substrate coating characteristics [180]. Drug loaded micro/nano spheres or particles could be embedded in a PVA hydrogel that is physically cross-linked by repeated freeze thawing [134, 181]. The freeze thawing eliminates the need for toxic chemical cross-linkers and organic solvents. The PVA alone allows high diffusion rates for proteins [182] leaving a drug release characteristics to be mainly controlled by loaded particles or their combinations [134]. Apparently, there is a lack of information about the biodegradation characteristics of PVA [183]. Nevertheless, it is a neutral linear molecule which makes even the high molar mass PVA (195,000 g/mol) to be safely excreted through the kidney [184]. PVA can be chemically cross-linked [159, 185-189], physically cross-linked [179, 182, 190-192] or both [193]. It is reported that PVA alone or in combination with other biomaterials has potential benefits for wound healing [188, 194] and has been used as stent coating [191, 195, 196]. It may be used in vascular [189, 197],

cartilage [198-201] and bone tissue engineering concepts [159, 202]. Production of biosensors [134, 203], soft contact lenses [204], arterial embolization [205] antibacterial activity [193] as well as drug delivery [159, 181, 188, 196, 206-208] are under investigation.

HA nanoparticles have already been used in order to influence the PVA morphology and produce bioactive nano-composite polymer hydrogels [209]. Even though the dispersion of hydroxyapatite in polymer matrices can be a critical challenge [210], still the formation of hydrogen bonding between the HA nanoparticles and PVA can contribute to formation of uniform dispersions [211]. The colloidal solution comprising PVA and HA nanoparticles can be processed as nanofibers [212] as well as membranes [213]. Due to the highly crystalline HA nanoparticles in the HA/PVA composite membranes, the membranes have reduced hydrophilicity, reduced tensile strength and elongation but increased Young`s modulus. In addition, these membranes have good biocompatibility and hold a great potential to be used in guided bone regeneration [213].

In a second step, a gluing of the patch to implant surfaces should be achieved to allow intra-operative coating of implants. For example medical cyanoacrylate adhesives can be used in order to achieve rapid patch attachment. The cyanoacrylate adhesives exist as liquid monomers that upon presence of water or base fluid undergo rapid polymerization. The resulting polymer then forms strong adhesive bonds to many substrates like metal and tissue. Cyanoacrylates have been widely used in clinics for six decades but still have limited FDA approval. The reason for that are their accompanying degradation products like formaldehyde and alkyl cyanoacetate. On the one hand, with increase in the alkyl side chain (octyl, butyl, ethyl), the biocompatibility, the degradation time, the curing time and the flexibility of the formed polymers increases, but the gluing strength decreases. There is no current cyanoacrylate adhesive approved by FDA that can be used for a long-term implantation in the human body. Yet, they find application as alternatives in many surgical procedures also including cartilage and bone grafting [143]. For instance, the cyanoacrylate adhesive has been successful in fixation of osteochondral fractures [214, 215]. On the other hand, the addition of hydroxyapatite to cyanoacrylate adhesive contributes to increased tensile strength and could be used for reinforcing of bone replacement materials [216].

2.1. Hypothesis

In this thesis we hypothesized that a humidified PVA patch could initiate rapid CA polymerization and thus provides a platform to combine standard surgical implants with adjustable coating localization and selection of drugs and their corresponding dosage-all in one step as required for intra-operative use. If such local drug delivery platform is to be achieved, it has to fulfil certain criteria such as immediate patch attachment, controlled delivery of drugs and not detaching from the implant surface. The goal of the current study was to establish a new intra-operative implant coating platform that can provide a drugs combination, dosage customization, and a free selection over the specific localization of a drug release. The suitability of this concept involving preparation of PVA patches, their morphology and possible effects of CA penetration into the patches, the binding strength and shear resistance of patches, the loading, release, and functionality of model proteins as well as the in vitro cytotoxicity were investigated in this study. The influence of the patch on the drug release profile controlled by pre-loaded PLGA microparticles and embedded within was also examined. The change in the patch morphology due to the addition of HA nanoparticles and their influence on the CA penetration within the patch, detachment after swelling, shear strength and influence on the drug release profile was also analysed. Various formulations of PVA/HA patches can be used to prepare double-layered patches where the first (drug free layer) can come in contact with the CA adhesive and the second layer can be drug loaded and adjusted to control the release profile (Fig 3).

3. Materials and Methods

3.1. Preparation of the PVA patches

In order to prepare the patches, different types of PVA were used: PVA with different water solubility based on a variation of their molecular weight and degree of partial hydrolysis of acetyl side chains (DH), namely Mowiol 6-98 (M_w ~47000, DH 98.0-98.8 mol%, Sigma-Aldrich, Germany), PVA-Sigma (M_w 13,000-23,000, DH 98 mol%, Sigma-Aldrich), and Mowiol 4-98 (M_w ~27000, DH 98.0-98.8 mol%, donated by Kuraray Europe GmbH, Germany). The PVA was dissolved by water in an ultrasonic bath at 80° C for 5 hours until

complete dissolution. With this procedure, 10 grams of 5 wt% (5% PVA), 10 wt% (10% PVA) and 15 wt% (15% PVA) solutions were obtained. They were casted in a stainless steel mould (depth: 1 mm, area: 60 mm x 120 mm) and the excess solution was wiped off with the edge of a culture plate under angle of 45 degrees. When amorphous films were prepared, the casted PVA solution was dried at room temperature until a film was obtained. The film thickness was always measured by magnetic thickness gage (Magna-Mike, Model 8000) and it proved to be within 27±7, 58±3 and 80±5 µm for 5%, 10% and 15% PVA solutions respectively. In contrast, the PVA films with increased crystallinity [182] were achieved by 3 repetitive cycles of freeze-thawing (2 hours freeze at -20° C/1 hour thaw) and then drying at room temperature. The obtained dry PVA films were then punched to prepare standardized patch sizes (8 mm and 15 mm (∅)).

PVA films with embedded HA nanoparticles (nanopowder <200nm, Sigma-Aldrich, Germany) were achieved by dispersing the HA in the Mowiol 6-98 solution. Double-layered patches PVA/HA films (HA/PVA 1.5 + 300/100 PVA/HA) in first place were prepared by dispersing 200mg HA nanoparticles in 6.41 g distilled water in an ultrasonic bath at 40° C for 15 minutes. Then 886 mg of 15 wt% Mowiol 6-98 solution (133mg PVA) were added to the HA dispersion followed by treatment in ultrasonic bath at 40° C for 30 minutes and incubated on a tube roller for 15 minutes before casting in the mould. These values were adjusted in order to achieve 7. 5 g of dispersion that was needed to fill up the total mould volume. It was of a great importance in all cases to have a total dispersion volume to avoid wiping of the extra material after casting and to maintain reproducibility. That is due to the low viscosity of this formulation resulting in fast sedimentation of HA that can lead to non-reproducible HA distribution within the film. After overnight drying at room temperature and formation of the first layer (HA/PVA 1.5), a second layer of PVA/HA as described below, was casted over the first layer.

The above mentioned dispersing procedure was used to prepare 7.5 g of 300/100, 600/200, 750/250, 900/300, 570/230 and 540/260 (PVA/HA in mg) dispersions. These dispersions were incubated on a tube roller for 24 hours before casting in the mould. Only the 300/100 PVA/HA dispersion was casted over the first layer (HA/PVA 1.5) and double-layered films (HA/PVA 1.5 + 300/100 PVA/HA) with 58.8±3.9 µm thickness were prepared. The thickness for single-layered films proved to be within 31.7±4.6, 65.2±2.6, 85±3.5, 100.8±5.4, 64.2±2 and 66.1±2.4 µm for 300/100, 600/200, 750/250, 900/300, 570/230 and 540/260 dispersions respectively. When subjected to 3 cycles of freeze-thawing as described before, the thickness

for single-layer films increased up to 77.1±1.6, 77.3±2 and 74.5±4.8 µm for 600/200, 570/230 and 540/260 dispersions respectively. These values were obtained by magnetic thickness gage mentioned above and Scanning Electron Microscopy (SEM, Gemini Supra™ 40 VP, Carl Zeiss NTS) was used to analyse the double- and single-layered patches.

3.2. Attachment of the PVA patches over test implant surfaces

In a second step, the attachment of the patch to test implant surfaces had to be achieved in order to evaluate the intra-operative coating strength to an implant surface. For that purpose, disks prepared out of anodized Titanium (12 mm (∅) x 3,5 height-gluing part and 15 mm (∅) x 3mm height-fixating part) were produced and donated by Synthes GmbH, Switzerland. For comparison, anodized Titanium Ti-6Al-44 and tumbled/electropolished CrNi 1.4441 steel disks (donated by AAP Implantate AG, Germany) with the same dimensions were also used. The surface properties of these metal disks were identical to standard osteosynthetic plates as certified and validated by both manufacturers. To compare the difference between attachment to a metal and other type of surface, custom made Poly (methyl methacrylate) [PMMA] disks of identical dimensions were made from PMMA rod (Grünberg Kunststoffe GmbH) by the Medical Technology Laboratory of the Charité. Scanning Electron Microscopy (SEM, Gemini Supra™ 40 VP, Carl Zeiss NTS) and Optical Profilometry (MicroProf, FRT; scan size 4*0.25 mm^2) were used to characterize the surface properties of the test implant surfaces.

Three types of CA monomers were used to glue the patch to the test implant surface and to obtain: poly(n-butyl cyanoacrylate) [PBCA] from Indermil (donated by P.J Dahlhausen & Co. GmbH, Germany), poly(octyl cyanoacrylate) [POCA] from Dermabond (Johnson & Johnson MEDICAL GmbH, Germany), poly(ethyl cyanoacrylate) [PECA] from Epiglu (Meyer-Haake GmbH, Germany), and as an internal control adhesive poly(methyl cyanoacrylate) [PMCA] from Loctite 496 (Henkel; obtained from Conrad Electronics GmbH, Germany as local distributer).

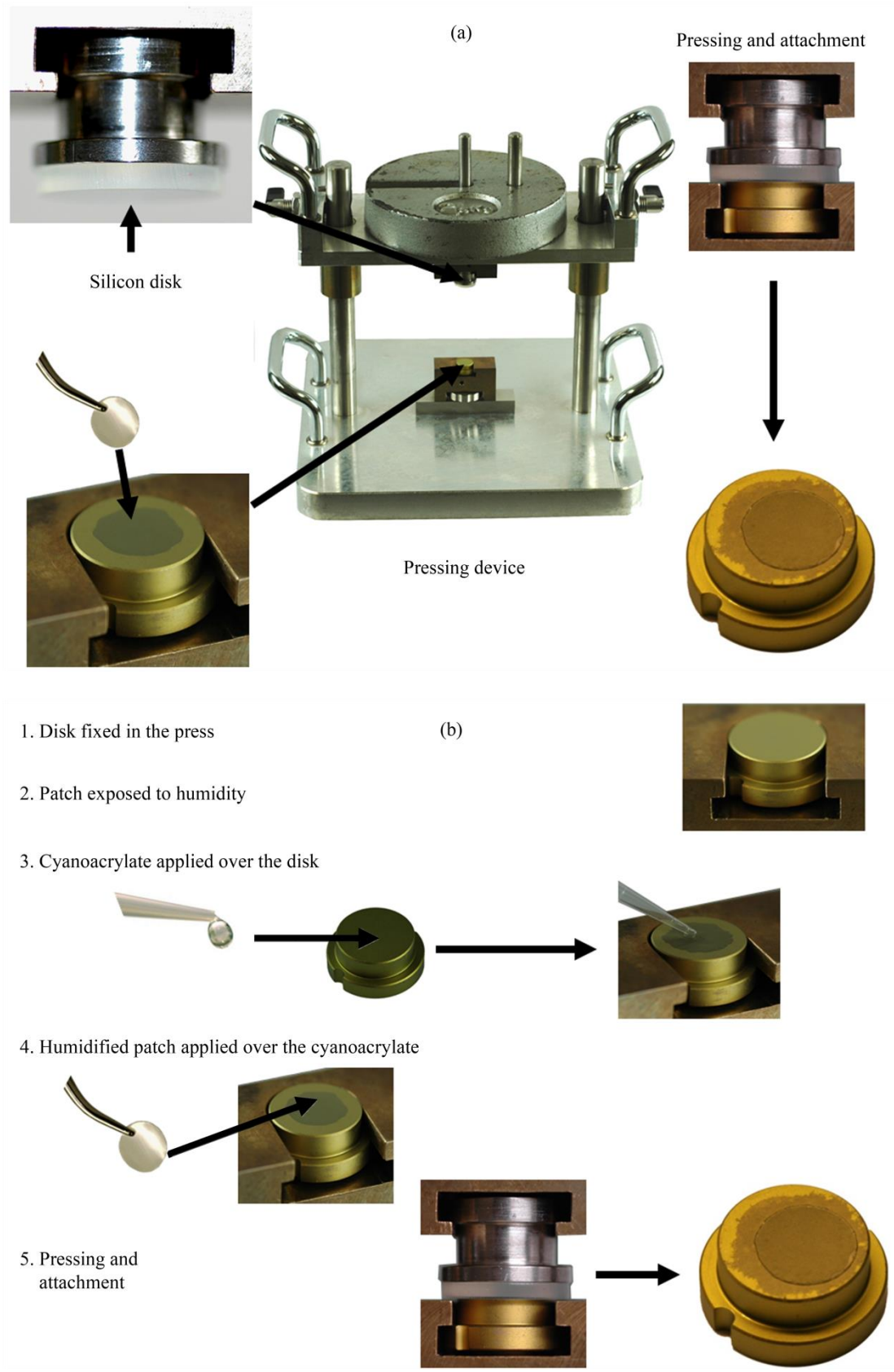

Figure 5. The drug delivery patch is attached on the test implant surface by using a pressing device (a). Required steps to apply the patch (b).

In order to obtain reproducible intra-operative coating of the implant test surfaces, a pressing device was constructed (Fig. 5a). Briefly, an upper and vertically moving platform was used to apply 2.5 kg of weight. To achieve equal pressure distribution during gluing, a silicon disk was fixed in the holder of the upper platform. The static platform at the base had a slot to fix the larger 15 mm (∅) side of the disk while leaving the 12 mm (∅) side free for attachment of the patches (Fig. 5a).

Before applying the PVA patch over the implant test surfaces, the patch was first exposed to a controlled level of humidity. The absorption of water molecules by the patch was an important condition to initiate the rapid polymerization of the CA adhesives. Water uptake by the patches was facilitated by placing them for a defined period of time in a homemade humidity tube. The humidity tube consist of a 50ml Falcon tube filled up with 20 ml of water and containing a cell strainer that is fixed in its upper part to serve as a slot for the patch. In order to achieve 100% relative humidity, the tube with a closed lid was placed in an oven at 37° C for at least 1 hour before being used. To prepare the PVA patch for initiation of CA polymerization and gluing, it was placed in the humidity tube in the oven to expose the patch to controlled humidity conditions. Meanwhile, 1 µl of CA adhesive was applied and spread over the disk surface where the patch would be glued. Then, the humidified 8 mm (∅) PVA patch was placed by tweezers onto the CA at the test implant surfaces, immediately followed by pressing (Fig. 5b). One minute of humidity exposure and 1 minute of pressing were sufficient for the patch attachment for all CA types.

In case of testing the shear strength (to avoid leakage of CA) and some other investigations of biomaterial properties (to peel off the patch), patches with larger (∅) were required than the available test implant surface models of implants. Therefore, the disk was first fixed in the upper holder of the device. Second, 5 µl of CA adhesive was applied over the disk in this case due to the bigger patch and the need to better apply and spread the CA. Then, the humidified 15mm (∅) patch was placed onto a silicon disk that was fixed in the lower holder of the press. Immediately after the humidified patch was placed onto the silicon disk, the upper holder was pressed against the humidified patch. In order to prevent any unwanted adhesions and to absorb the extra CA during pressing, sticky tape (3M™ Transpore™ White) was fixed around the disk. One minute of humidity exposure and 1 minute of pressing were enough for the patch attachment by PBCA and PECA, as POCA required 10 minutes of pressing (Table 1).

To ensure constant metal surface properties and to allow the interlocking of PACA into the microroughness (according to the mechanical theory of adhesion) [217], the disks were cleaned by Acetone (≥99,5%) and Micro-90 cleaning solution obtained from Sigma-Aldrich, Germany as well as by Ethanol 96%. If disks were re-used as in some cases, they were cleaned in ultrasonic bath at 40° C as follows: 1) 15 min /acetone 99.5%, 2) 15 min/2% Micro-90 and 3) 15 min/ethanol 100%. It was also necessary to ensure that the patches will stay attached in a wet state during certain tests such as evaluation of protein bioactivity, protein release, and biocompatibility testing. To do so, Titanium disks (Synthes) were first treated by sand paper in order to remove the protective oxide layer and then were cleaned according the above mentioned cleaning procedure. On the other hand, to examine the wet-detachment of the patches from the intact test implant surfaces, they were glued over the disks after 1 minute of humidity exposure and 1 minute of pressing. Then each sample was placed in 2 ml PBS (1x) and incubated in an oven at 37-38° C.

In order to introduce micro-roughness on the flat PMMA surface-as received, the PMMA disks were first treated with sand paper. Second, they were cleaned by using ultrasonic bath with 2% Micro-90 at 40° C for 15 minutes followed by rinsing with distilled water.

Table 1.

Overview of experimental details for the individual tests performed (no HA nanoparticles present, Dexamethasone release not included).

Test:	Shear Strength (Fig. 8)	Biomaterial properties (Fig. 11, 12, 13, 14)	Preservation of molecule bioactivity (Fig. 18)	Protein release (Fig. 19)	Biocompatibility (Fig. 20)
Disks	- Influence of disk material and surface roughness: Titanium alloy (Synthes, AAP); CrNi steel (AAP); PMMA (Charite) - Influence of pressing time and humidity-Titanium alloy (Synthes)-multiple use	Titanium alloy (Synthes)	Titanium alloy (Synthes)-sand papered	Titanium alloy (Synthes)-sand papered	Titanium alloy (Synthes)-sand papered

Patches	- 80µm thick patches, (∅) 15 mm (Mowiol 6-98) - 3 freeze-thaw cycles - no freeze-thaw	- 27, 58, 80µm thick patches, (∅) 15 mm (Mowiol 6-98, 3 freeze-thaw cycles) - 80µm, (∅) 15 mm for IR microscopy (Mowiol 6-98, 3 freeze-thaw cycles)	- 80µm thick patches, (∅) 8 mm (Mowiol 6-98, 3 freeze-thaw cycles)	- 27, 58, 80µm thick patches, (∅) 8 mm (Mowiol 6-98, 3 freeze-thaw cycles) - 80µm thick patches, (∅) 8 mm (Mowiol 4-98, PVA-Sigma, 3 freeze-thaw cycles)	- 80µm thick patches, (∅) 8 mm (Mowiol 6-98, 3 freeze-thaw cycles)
Glue	5µl POCA, PBCA, PECA	1. 5µl POCA, PBCA, PECA for SAXS and WAXS 2. 5µl PBCA for Raman and IR microscopy	1µl POCA, PBCA, PECA	1µl PBCA	1µl POCA, PBCA, PECA
Gluing conditions	0, 1, 3 and 5 minutes humidity exposure, pressing 1 minute for PBCA and PECA, 10 minutes for POCA	1 minute humidity exposure, 1 minute pressing for PBCA and PECA, 10 minutes for POCA	1 minute of humidity exposure, 1 minute pressing for all	1 minute of humidity exposure, 1 minute pressing for all	1 minute of humidity exposure, 1 minute pressing for all

Table 2.

Overview of experimental details for the individual tests performed including HA. Dexamethasone release not included.

Test:	SEM (Fig. 9)	Raman Microscopy (Fig. 15, 16)	Shear Strength (Fig. 10)	Wet-detachment test (Fig. 17)
Disks	Without gluing	Titanium alloy (Synthes)	Titanium alloy (Synthes)	Titanium alloy (Synthes, AAP); CrNi steel (AAP); PMMA (Charite); Titanium alloy (Synthes)-multiple use
Patches	- 31.7±4.6 µm thick for single-layered (300/100) and 58.8±3.9 µm thick for double-layered (HA/PVA 1.5+300/100) patches, (∅) 8 mm (Mowiol 6-98, HA nanopowder <200 nm) - prepared without freeze-thawing - glued after 1 minute humidity exposure of the patch, 1 minute pressing, by 5µl PBCA for Shear Testing and 1µl PBCA for Raman Microscopy and wet-detachment test			

3.3. Shear Strength of the implant coating

An important feature of a surface coating is the resistance shear force. Therefore, the glued disk/patch construct was placed in the lower holder of a press. An additional disk was fixed in the upper holder and glued to the patch by PMCA that served as internal control because of its highest adhesive strength. A 15 mm (∅) patch was used for this purpose. The patch was larger than the 12 mm (∅) test implant surfaces to make sure that there is no direct gluing-interface between the two disks. This disk/patch/disk construct was placed in the custom made holder (Fig. 6) and placed in a tensile tester (Zwick/Roell Z010, load cell Xforce K, Germany). Using a displacement rate of 1 mm/min, the shear force and displacement were measured until failure of the construct occurred. Each of the tested groups involved 6 samples.

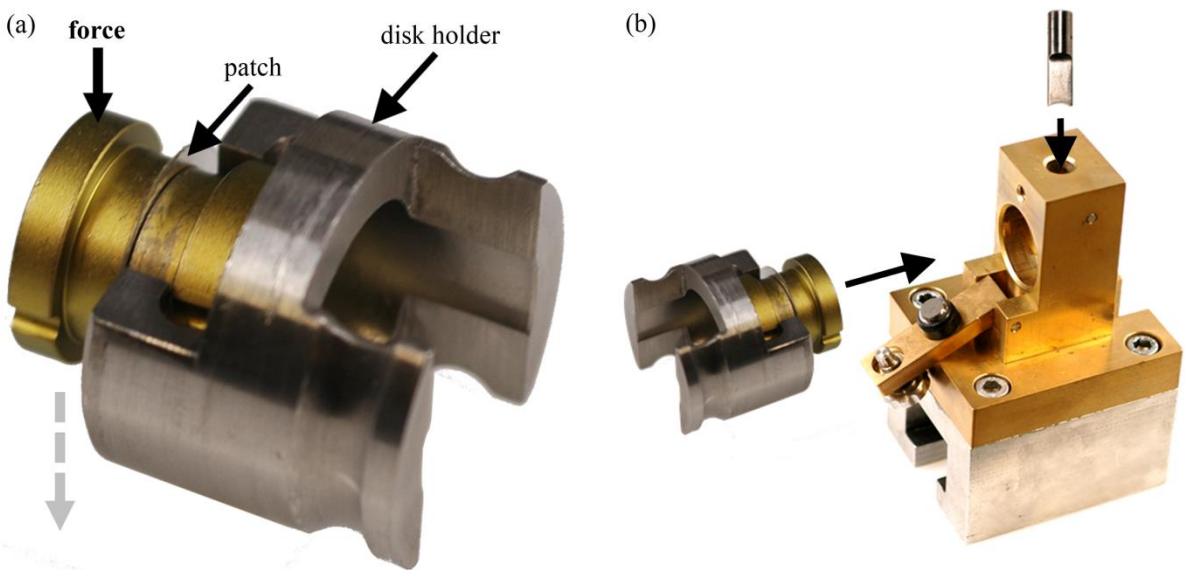

Figure 6. The disk/patch/disk construct is placed in the holder. Then force is being applied from above to the disk on the left site, while the right part of the device is rigidly fixed, leading to a well-controlled shear testing (a). The disk holder is placed in another holder for rigid fixation and the force is applied from above by a pin (b).

3.4. Characterisation of patch properties

In order to investigate, if the attachment by PACA affected the structural properties in PVA patches of different thicknesses, the patches (∅ = 15 mm) were peeled off from the test implant surface after gluing. Three samples from each group were analysed for glue penetration within the patch.

Due to their brittleness, the PVA patches with included HA nanoparticles were analysed by Raman Microscopy for glue penetration without being peeled off from the implant surfaces. Three samples per group were analysed.

3.4.1. Small- and Wide Angle X-ray Scattering

Small-angle and wide-angle X-ray scattering (SAXS and WAXS) measurements were made by using a pinhole SAXS camera (NanoSTAR, Bruker AXS, Karlsruhe, Germany). This device has a sealed X-ray tube operating at 1.2 kW, from where CuKα radiation (wavelength λ=0.154 nm) was selected and collimated by a graded multilayer. Two-dimensional (2D) scattering patterns were collected with an area detector at sample–detector distances of 50 and 1050 mm, covering a complete range in the length of the scattering vector q of 0.1 nm^{-1} < q < 25 nm^{-1}, where q is defined by $q = 4\pi \sin\theta/\lambda$ (2θ is the scattering angle). 2D SAXS and WAXS patterns were collected for all samples, corrected for background scattering and the obtained profiles were determined from the azimuthally averaged intensity I(q).

3.4.2. Raman Microscopy

The PVA patches were also analysed by depth profiling and mapping using Raman spectroscopy: A Bruker Senterra dispersive Raman spectrometer equipped with two lasers (785 and 532 nm) and a motorized x-, y-, and z-table was used for that purpose. Using a 50x magnification for the depth-profiling, a step size of 5 µm and 20 steps (resulting in a depth of 100 µm; except 25 µm sample that had 15 x 5µm steps) were employed to map an area of 500 x 500 µm (5 x 5 measurement points with distance of 100 µm) per patch. The power of the laser was adjusted to 5 mW for a wavelength of 532 nm and 128 scans with an aperture of

50 µm. For analysis of the RAMAN spectra for the PVA a CH-bond at 2900cm^{-1} and for PBCA the CN bond at 2250cm^{-1} were used for evaluation by the Bruker OPUS Software.
Identical settings were used to analyse the glued PVA/HA patches. Each sample was analysed in depth at several randomly selected locations (step size of 5 µm) and no mapping was performed because the presence of HA nanoparticles resulted in irregular intensities. For analysis of the RAMAN spectra for the HA a PO-bond at 963cm^{-1} was used. For better evaluation, the spectra were additionally normed on the PVA signal and presented as intensity vs. depth.

3.4.3. Infrared (IR)-Microscopy

To investigate the patches, fourier transform infrared spectroscopy was used. The analyses were made by a Bruker Tensor 27 IR-spectrometer with ATR equipment. Connected to the infrared spectrometer was an infrared microscope model HYPERION 2000. This microscope was used to examine specific points at the sample surfaces after the formation process. For the measurements and the mappings an ATR objective (magnification 20x) was used. These analyses were made on the visual-reflectance mode using 32 scans at a resolution of 4 cm^{-1}. For the mapping a raster size of 13 x 9 measurement points in an area of 350 x 250 µm was performed. This resulted in a distance between each measurement point of 27 µm in x- and y-direction for a diameter of 20 µm of the imprinted ATR crystal. For analysis of the IR-spectra the significant bonds of PVA at 3280 cm^{-1} (OH) and 2911 cm^{-1} (CH) and of PBCA at 1747 cm^{-1} (CO) were assessed by the Bruker OPUS Software.
In case of SAXS, WAXS, Raman and IR Microscopy, pretreated patches without any PACA or HA present were used as controls-valid for pretreated PVA patches glued by CA.

On the other hand, amorphous PVA patches only and HA powder alone without any CA were used as controls for Raman microscopy-valid for PVA/HA patch analysis.

3.5. Preservation of the molecular bioactivity in the patch

To determine the activity of bioactive molecules, 10 mg of HRP (Horseradish Peroxidase Type VI-A, Sigma-Aldrich, Germany), were used as model drug and were added to 10 g of 15% PVA (6-98) solution. The solution was then incubated by rolling onto a tube roller for

12 hours at room temperature. The PVA+HRP solution was then casted in a mould and was subjected to 3 cycles of freezing and thawing. The film was dried overnight at room temperature and then stored at 4° C. Next, the film was punched in order to prepare patches that were glued over the test surfaces. Finally, 50 µl of HRP substrate (Cheluminate-HRP PicoDetect, Applichem, Germany,) was pipetted over each tested patch in triplicates. The resulting chemiluminescent signal was detected by a chemiluminescence imaging system (G: Box, VWR, Germany).

3.6. Protein Release Profiles

The protein release from the patch was evaluated to quantify whether the expected protein burst release would be blocked by the gluing procedure. For that purpose, stock solutions (100 mg/ml) of BSA (bovine serum albumin, Sigma-Aldrich, Germany) corresponding to 5, 10 and 15 mg were added to 10 g of 5 %, 10 % and 15 % PVA solution, respectively. In order to achieve a homogeneous BSA distribution within the PVA, the solution was then incubated by rolling onto a tube roller for 12 hours at room temperature and was used to prepare pretreated patches.

Three samples of each investigated group were each placed in 2 ml PBS (1x) and were incubated in an oven at 37-38° C. At day 1, 3, 5, 7, and 14, 1 ml of the PBS was removed out of the tube, stored at -20° C, and additional 1 ml of fresh PBS was added back to the sample. The amount of the released BSA was quantified by Coomassie Plus Assay (Thermo Fisher Scientific, Germany) according to the manufacturer's instructions for using a microplate reader (Bio-Rad, Model 680, Germany).

3.7. Biocompatibility testing

To investigate the biocompatibility of the PVA patches that were glued by CA, primary human fibroblasts were first seeded in 6 well plates at a density of $2.3x10^4$ per well (2ml of DMEM + 10% Fetal Calf serum + 1% Penicillin/Streptomycin, Invitrogen GmbH). The cells were actually seeded 1 day before being exposed to the samples. The patches were pretreated with UV light (neoLab UV Hand Lamp Type 6 KLU: 254 nm + 366 nm) for 2 hours from

both sides for sterilization to be achieved. Three samples of each group were glued over test implant surfaces and placed in a cell culture insert with the patch facing downwards. Thereafter, the inserts were immediately placed in the cell culture plates to establish interaction with the fibroblasts. Once the inserts were placed within the wells, an additional 1 ml of cell media was added to increase the volume in the well and allow an optimal wetting of the glued patches. Thus, the cells were exposed to the patches via the cell medium but were not in a direct contact.

At day 1 after being exposed to the glued patch, the cells were tested for early cytotoxicity effect using FACS analyses. For that purpose, the cells were trypsinized (PAA Laboratories GmbH, Germany) and brought into suspension in buffer solution (PBS (1x) PAA Laboratories GmbH, Germany). Just before the actual measurement, 5 µl of 7-Aminoactinomycin D (BD Biosciences, Germany) was added to the cells and cells were incubated for 10 minutes at room temperature.

In order to determine the biocompatibility by comparing the initial cell viability and the viability at later stages, Alamar Blue viability assay (Biozol GmbH, Germany) staining was performed at day 1, 3 and 7. Briefly, 1 ml of Alamar Blue was dissolved in DMEM (1:10) and was added to the cells. After incubation period of 3 hours, the Alamar Blue solution was removed from the cells and 180µl were pipetted in a 96 well plate. For quantification of the cell viability, absorbance at 570/595 nm was measured using a micro plate reader (Bio-Rad, Model 680, Germany).

3.8. Drug release profile by microparticles embedded into the PVA patch

The Dexamethasone release from the PLGA microparticles (∅≈50 µm, 7.5 wt% Dexamethasone (micronized, Fagron, Barsbüttel, Germany) prepared by the Center for Biomaterial Development, Helmholtz-Zentrum Geesthacht-Teltow) was quantified in order to evaluate whether the release profile would be influenced by their incorporation in PVA patch and if the gluing of the patch has any effect. Therefore, 80 mg of microparticles were dispersed by pipetting into 10 g of 5 wt% Mowiol 6-98. The dispersion was then incubated on a tube roller for 15 minutes at room temperature and followed by casting in the mould, drying and preparation of patches (8 mm (∅)). In order to prepare amorphous and patches with increased crystallinity, the patches were prepared as described before in the patch

preparation section. Then the patches were glued over the sand papered Titanium alloy-Synthes disks by 1µl PBCA after 1minute of humidity exposure and 1 minute of pressing.

Not glued patches and microparticles alone served as control release groups. Six samples of each group were each placed in 2 ml PBS (1x) and incubated in an oven at 37-38° C. At day 1, 3, 5, 7, 14, 21 and 28, 1 ml of the PBS was removed, stored at -20° C, and additional 1 ml of PBS was added to the sample. In order to evaluate the total amount of Dexamethasone loading in the patches, they were dissolved in 2 ml of DMSO in ultrasound bath for 10 minutes. Then 100 µl of the DMSO fraction was dissolved in 900 µl of 100% Ethanol and was used for HPLC measurement. The amount of the released Dexamethasone from the patches (glued or not), from the microparticles alone and the dissolved patches, was quantified by high performance liquid chromatography-HPLC (Agilent Technologies 1200 series) with a flow rate of 1 ml/min, 10 µl injection volume, eluent A: HPLC water with 0.1% trifluoroacetic acid (TFA), and eluent B: Acetonitrile.

3.9. The influence of HA nanoparticles on the Dexamethasone release from the PVA patches

In order to evaluate the effect of HA nanoparticles in the PVA patches on the Dexamethasone release, first layer (HA/PVA 1.5) was prepared as described before. Due to the low solubility of Dexamethasone in water (<100 mg/100 ml), 10.6 mg of Dexamethasone (micronized, Fagron, Barsbüttel, Germany), were dispersed in 2 ml of distilled water by vortex and followed by 15 minutes in ultrasound batch at 40° C. Then two separate PVA/HA dispersions including Dexamethasone were prepared in 3 steps as it follows: Step 1. 100 mg HA nanoparticles were added in 4.4 g distilled water followed by dispersing in an ultrasonic bath at 40° C for 15 minutes; Step 2. 755µl Dexamethasone dispersion (corresponding to 4 mg Dexamethasone) was filled up with distilled water until 1 g of weight was reached and was added to the HA dispersion; Step 3. Two grams of 15 wt% Mowiol 6-98 solution (300mg PVA) were added to the HA/Dexamethasone dispersion followed by treatment in ultrasonic bath at 40° C for 30 minutes and then incubated on a tube roller for 24 hours before being casted in the mould. One of the dispersions was casted over the HA/PVA 1.5 layer to achieve double-layered (HA/PVA 1.5 + 300/100 PVA/HA) film and the other dispersion was casted alone to achieve single-layered (300/100 PVA/HA) film. The films were dried and prepared

as 8 mm (∅) patches. Then the patches were glued over the sand papered Titanium alloy-Synthes disks by 1µl PBCA after 1minute of humidity exposure and 1 minute of pressing.

Not glued patches served as control release groups. Six samples of each group were each placed in 2 ml PBS (1x) and incubated in an oven at 37-38° C. At day 1, 3, 5, 7 and 14, 1 ml of the PBS was removed, stored at -20° C, and additional 1 ml of fresh PBS was added to the sample. In order to define the total amount of Dexamethasone loading in the patches, they were dissolved in 2 ml of distilled water by vortex. The amount of the released Dexamethasone from the patches (glued or not), including Dexamethasone from dissolved patches, was quantified by high performance liquid chromatography-HPLC (Agilent Technologies 1200 series) with a flow rate of 1 ml/min, 10 µl injection volume, eluent A: HPLC water with 0.1% trifluoroacetic acid (TFA), and eluent B: Acetonitrile.

4. Results

4.1. Shear Strength of the implant coating

A new platform for local drug delivery by implant coating was established. To establish such a new local drug release platform, a reproducible preparation of PVA patches was realized first. Immediately before their use, each patch had to be exposed to a controlled level of humidity. The water molecules absorbed by the patch are acting as an initiator for polymerization of the CA adhesive. Pressing the humidified patch against a not polymerized CA adhesive, that was spread over a test implant surface, resulted in rapid adhesive polymerization and patch attachment. After successful patch gluing to the tested implant surfaces, the binding strength and the influence of the gluing conditions were evaluated. Therefore, shear strength testing was employed to determine the influence of the implants surface (Titanium, CrNi steel, PMMA), type of PACA (PECA, PBCA, POCA), the pretreatment of patches by freeze/thaw cycles, the pressing time (1 or 10 minutes), and the exposure time in the humidity chamber (0, 1, 3, 5 minutes) on the mechanical stability of the patch-substrate bonding. In addition, the influence of HA nanoparticles presence into the PVA patches on the shear strength was also investigated.

4.1.1. Influence of disk material and surface roughness on the shear strength

SEM (Fig. 7) and Optical Profilometry (Table 3) were used in order to find correlation between the micro-roughness of the test implant surfaces and the shear strength of the coating.

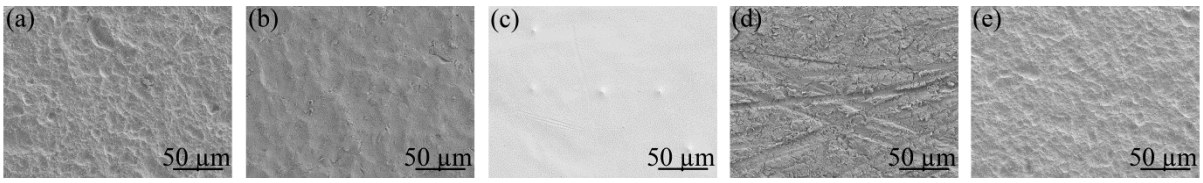

Figure 7. Scanning Electron Microscopy of tested implant surfaces: Ti-Synthes (a), Ti-AAP (b), CrNi-AAP (c), PMMA (d), Ti-Synthes-multiple use (e).

Table 3.

Correlation between the micro-roughness and the shear strength for different implant surfaces. Values Ra represent mean surface roughness values and Rq represent root mean squared (rms) surface roughness.

	Ti-Synthes	Ti-AAP	CrNi-AAP	PMMA	Ti-Synthes-multiple use
Ra (µm)	0.424 ± 0.004	0.196 ± 0.013	0.039 ± 0.020	0.243 ± 0.007	0.4 ± 0.009
Rq (µm)	0.534 ± 0.009	0.256 ± 0.017	0.056 ± 0.027	0.310 ± 0.009	0.504 ± 0.010
Shear Strength (MPa)	11.74±0.83	13.91±2.48	15.32±1.99	4.6±1	16.98±1.48

Even though there was a difference in the surface micro-roughness, the shear strength measured for the different Ti surfaces was not significantly different. The gluing to the

surface that had lowest micro-roughness values, CrNi-AAP, was significantly stronger than the gluing on Ti Synthes (p=0.002), but not significantly different from the gluing on Ti-AAP. For the PMMA surface, the shear strength values were much lower compared to the metal test implant surfaces. It was expected that the re-using of the titanium disks (Synthes) would generate surface impurities and that would result in lower shear strengths. To determine that effect, the patches were glued to cleaned and re-used disks with PBCA by 1 minute of humidity exposure and 1 minute of pressing. Surprisingly, even though there was almost no change in the surface-micro-roughness, higher shear strength was observed for those titanium disk substrates (Synthes) that were used multiple times (Table 3).

4.1.2. Influence of pressing time on the shear strength

It was concluded that the pressing time had a correlation with the patch pretreatment and the type of CA after 1 minute of patch humidity exposure. To be more specific, the gluing strength by PECA was significantly increased for PVA patches that were pretreated by freeze/thaw cycles (Fig. 8a). The highest shear strength was 23.4±1.5 MPa for PECA and 17.7±1.3 MPa for PBCA. However, an increase in pressing time resulted in decrease of the shear strength of patches that received no pretreatment. On the other hand, no effect was observed for pretreated patches that were glued by PBCA. No gluing was observed for POCA at 1 minute of pressing. Even though the pressing time was increased, the shear strength obtained for POCA was much lower than compared to PECA and PBCA.

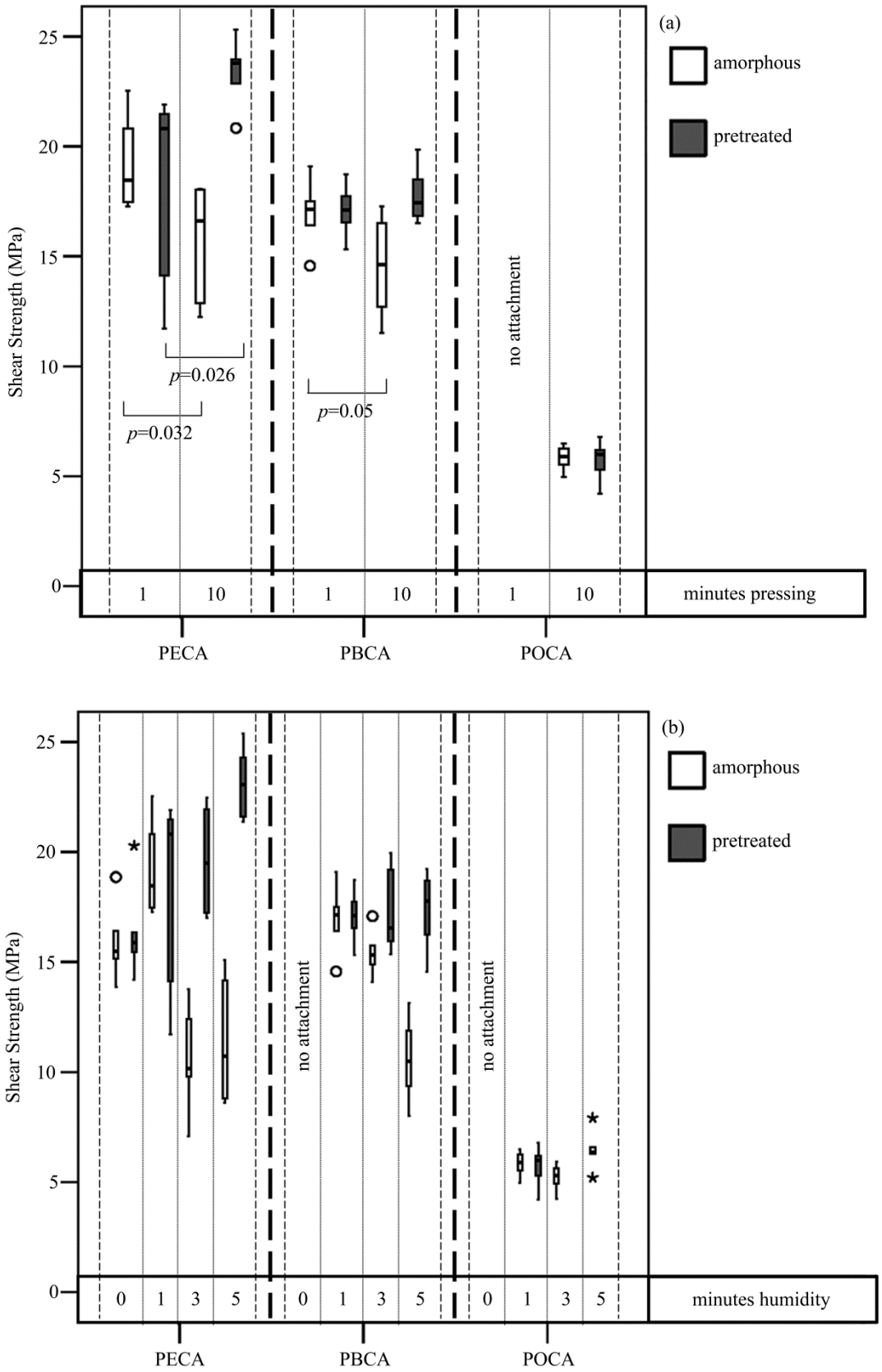

Figure 8. The shear strength at 1 minute of humidity exposure. Correlation between the type of CA, the patch properties and the pressing time (a). The shear strength and the effect of

humidity exposure (b). ° indicate outliers and * indicate far outliers. Sample description in Table 1 (Shear Strength).

4.1.3. Influence of humidity on the shear strength

Since the humidity exposure time seemed be of a great importance, the patches were exposed to 0, 1, 3, and 5 minutes of humidity. A pressing time of one minute was selected for PECA and PBCA, and 10 minutes for POCA. The results revealed that the increase in the humidity exposure increased the shear strength of PECA. Surprisingly, most of the disks broke for PMCA (methyl CA) that was originally chosen to be the strongest of all tested adhesives. To give more precise explanation, 4 out of 6 at minute 1, 2 out of 6 at minute 3, and all 6 samples at minute 5 of humidity exposure broke at the patch side glued by PMCA and not at the expected side glued by PECA. Therefore, the actual shear strength of pretreated PVA attached by PECA is even higher than the values being presented here. Furthermore, an increase in the time of humidity exposure did not cause any effect in the pretreated patches attached by PBCA. The increase in the humidity exposure time decreased the shear strength in amorphous patches that were attached by both PECA and PBCA. Only if PECA was used, polymerization was achieved without any humidity being provided to the patch. In addition, the gluing by POCA generated lowest values and thus was not in the focus of the subsequent investigations (Fig. 8b).

4.1.4. Influence of HA nanoparticles in the PVA patch on the shear strength

The addition of HA nanoparticles to the PVA resulted in changes of the PVA patch morphology. The transparent PVA patches turned into milky white and their morphology depended on the HA to PVA ratio. The first layer in the double-layered patch (HA/PVA 1.5) resulted in uniform particle distribution and compact structure of the layer (Fig. 9a). On the other hand, the second layer (300/100 PVA/HA) had formation of HA nanoparticle clusters within the PVA (Fig. 9a). The clustered structure was also observed if the same formulation that was used to produce single-layered patch (300/100 PVA/HA) (Fig. 9b).

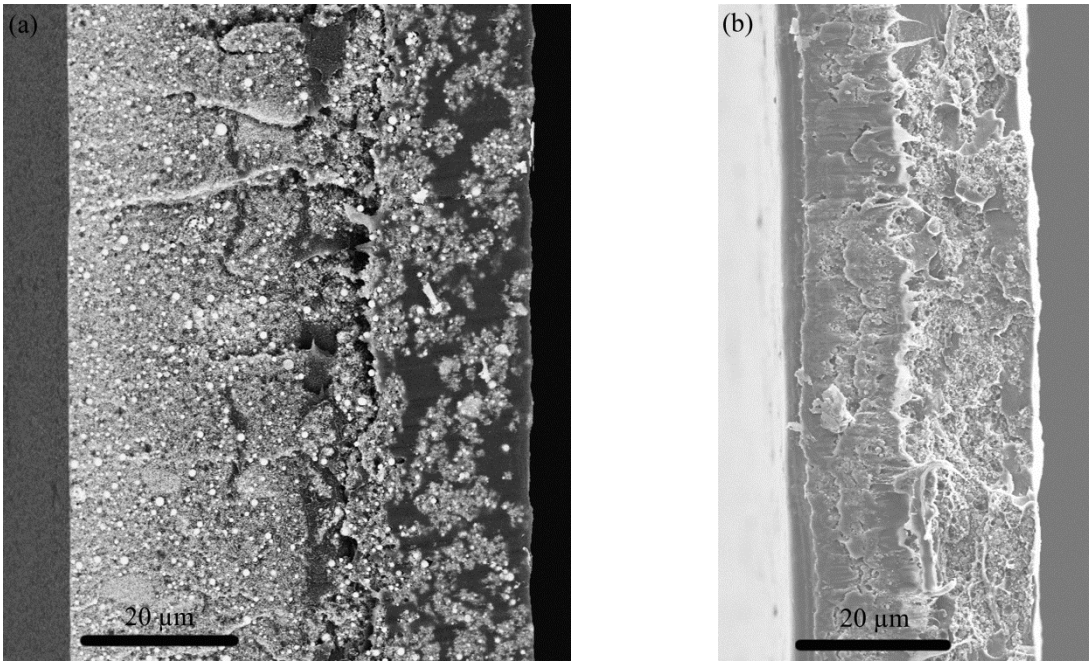

Figure 9. Double-layered patch (HA/PVA 1.5 + 300/100 PVA/HA), left-first layer (HA/PVA 1.5), right-second layer (300/100 PVA/HA) (a), Single-layered patch (300/100 PVA/HA) (b). Sample description in Table 2 (SEM).

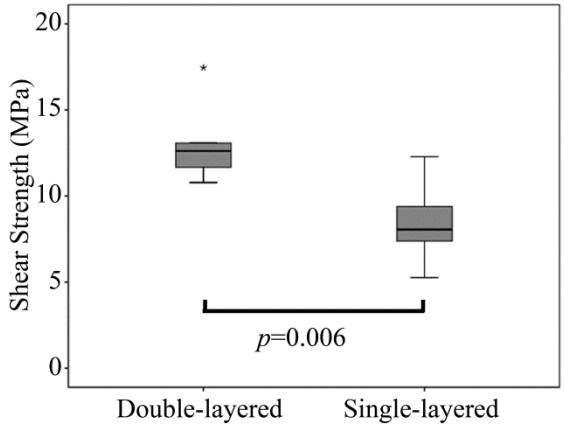

Figure 10. Shear Strength of the double-layered patch (HA/PVA 1.5 + 300/100 PVA/HA)-left and single-layered patch (300/100 PVA/HA)-right. Sample description in Table 2 (Shear Strength).

The patch morphology changes due to the addition of HA nanoparticles did not result in any significant influence on the shear strength. To explain, the 58.8±3.9 µm thick double-layered patch (HA/PVA 1.5 + 300/100 PVA/HA) had comparable shear strength (Fig. 10) to the 80 µm thick pretreated PVA patch without no HA included (Table 3, Ti Synthes values). That

was not the case with the 31.7±4.6 µm thick single-layered (300/100 PVA/HA) patch where significant decrease in the shear strength was observed when compared to the double-layered patches (Fig. 10). This result is probably due to the failure of the patch itself rather than the PBCA.

4.2. Patch properties after gluing over the implant surface

The polymerization of CA adhesive in contact with humidified PVA patches of different thicknesses as listed in Table 1 (biomaterial properties), was expected to result in interaction between the two polymers. Small Angle X-ray Scattering (SAXS) and Wide Angle X-ray Scattering (WAXS) were used to evaluate how the PACA affected the morphology of the PVA patch. The results revealed that a decrease in the patch thickness leads, as expected, to a decrease in the signal intensity I, but the comparison between non-glued and glued patches did not have any significant differences in the semi-crystallinity of PVA since the wave scattering vectors q of the intensity peaks were comparable (Fig. 11). To be more precise, neither crystallinity nor crystal structure of the PVA as investigated by WAXS nor size and arrangement of crystalline domains determined by SAXS (Fig. 12) in PVA did show significant differences that were caused by the glue.

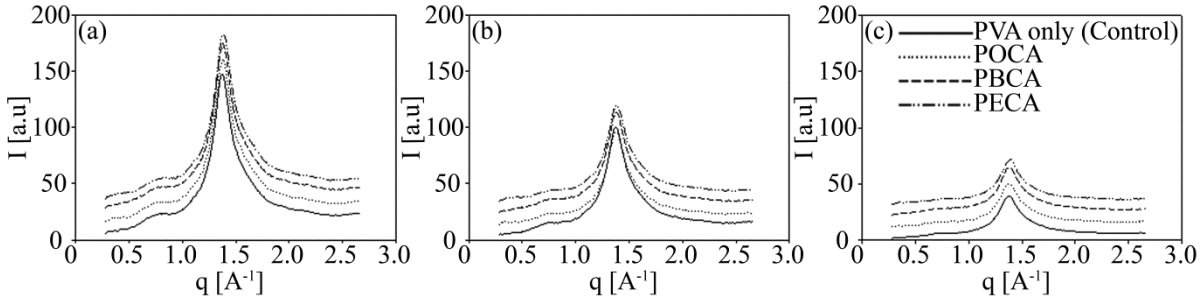

Figure 11. WAXS spectra of PVA patches depending on the presence of PECA, PBCA POCA with a variation of sample thickness, which was 80 µm (a), 58 µm (b), and 27 µm (c). Curves have been shifted along the y-axis (arbitrary units) to allow visual differentiation. Sample description in Table 1 (Biomaterial properties).

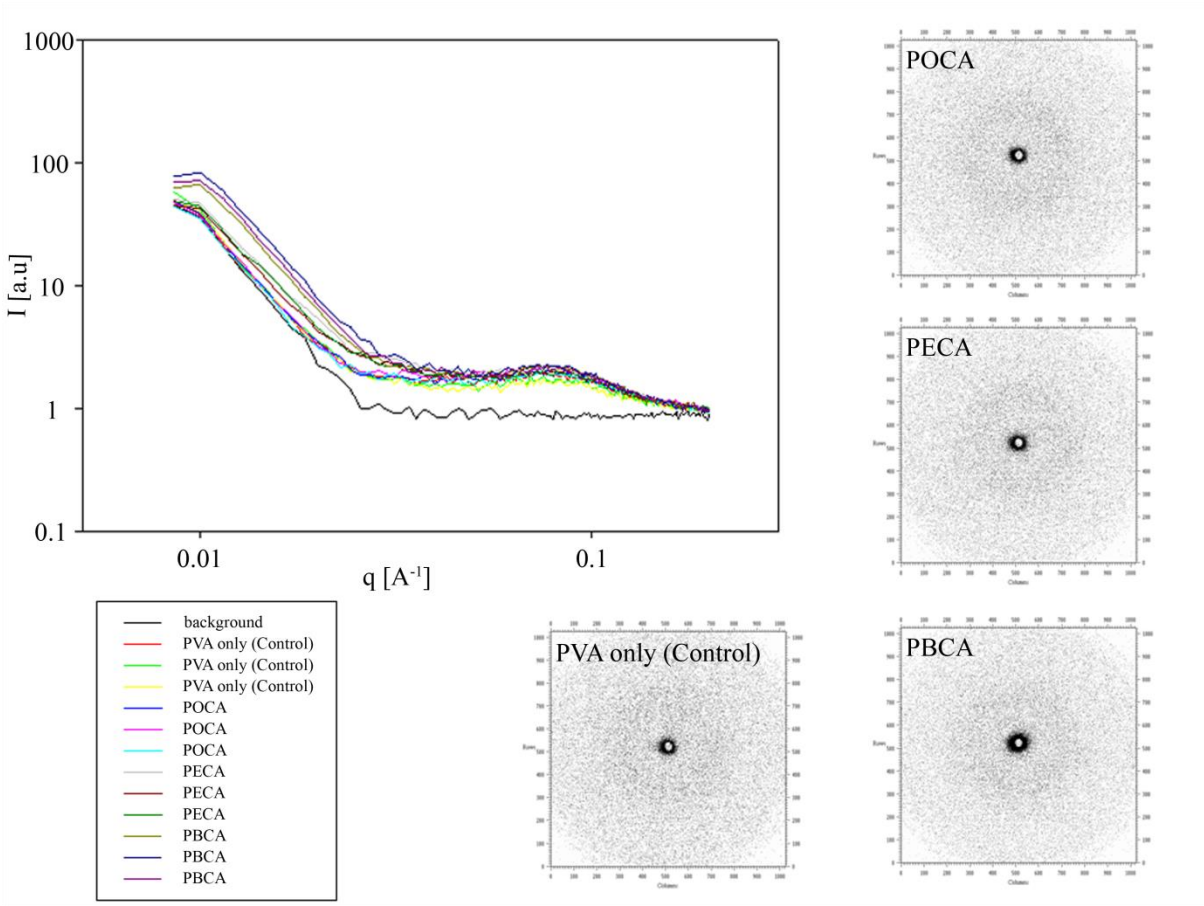

Figure 12. SAXS spectra of 80 µm thick PVA patches, their size and arrangement of crystalline domains depending on the presence of PECA, PBCA POCA (each line correlates to one sample). Sample description in Table 1 (Biomaterial properties).

The liquid CA monomers can penetrate into the PVA network and polymerize within the patch. Therefore, PVA patches of different thickness pretreated by freeze/thaw cycles were glued by PBCA (1 minute humidity exposure and 1 minute pressing) and were later carefully peeled off in order to be analyzed by Raman microscopy for depth profiling and by IR microscopy. PBCA was chosen for this purpose because unlike PECA, it is already a FDA approved product for topical skin use and it is a stronger adhesive under the selected conditions compared to POCA. The control samples (pure PVA) showed no presence of PBCA in all cases. By deep profiling, it was shown that PBCA was permeating into the patch (Fig. 13a). In fact, light microscopy illustrated that the test samples were inhomogeneous with contrast differences (Fig. 13b). Raman mapping revealed the fact that in some regions no PBCA was present. Furthermore, overlaying signals were present in the bulk within sharply defined regions (Fig. 13c and 13d). Additionally, IR microscopy of the surface

confirmed the inhomogeneity by the fluctuation of the intensity of the specific IR signals. To be more specific, distinct regions of PVA and PBCA were investigated at the surface of the patch confirming that the distribution of PBCA was depending on the distribution of PVA (Fig. 14).

Highly crystalline HA nanoparticles were included in the PVA in order to prevent the CA monomers penetration into the patch. The results obtained by depth profiling showed that the CN bond at 2250cm^{-1} is missing in the spectra, meaning that no PBCA was penetrating in both double-layered patch (HA/PVA 1.5 + 300/100 PVA/HA) (Fig. 15a) and single-layered patch (300/100 PVA/HA) (Fig. 15b). In addition, no PBCA was detected at the lowest depth point that actually came in contact with the adhesive during the pressing (Fig. 16).

Even though no penetration of PBCA was observed within the both double-layered patch (HA/PVA 1.5 + 300/100 PVA/HA) and single-layered patch (300/100 PVA/HA), the presence of highly crystalline HA nanoparticles into the PVA resulted in improved patch attachment over the implant test surfaces in a wet state (Fig. 17). To explain, 80μm thick PVA patches with no HA included tend to detach from the surface shortly after swelling in PBS at 37-38° C. The only exception was the case with Titanium alloy-AAP and PMMA-Charite surfaces where patches tend to remain attached for more than 4 weeks (data not shown). On the other hand, double-layered patches (HA/PVA 1.5 + 300/100 PVA/HA) and single-layered patches (300/100 PVA/HA) detached after swelling only from the Titanium alloy-Synthes surface. After 7 days of incubation, 2 out of 3 single-layered patches detached only from the CrNi steel-AAP (Fig. 17). The rest of the patches remained attached on the surfaces for more than 4 weeks.

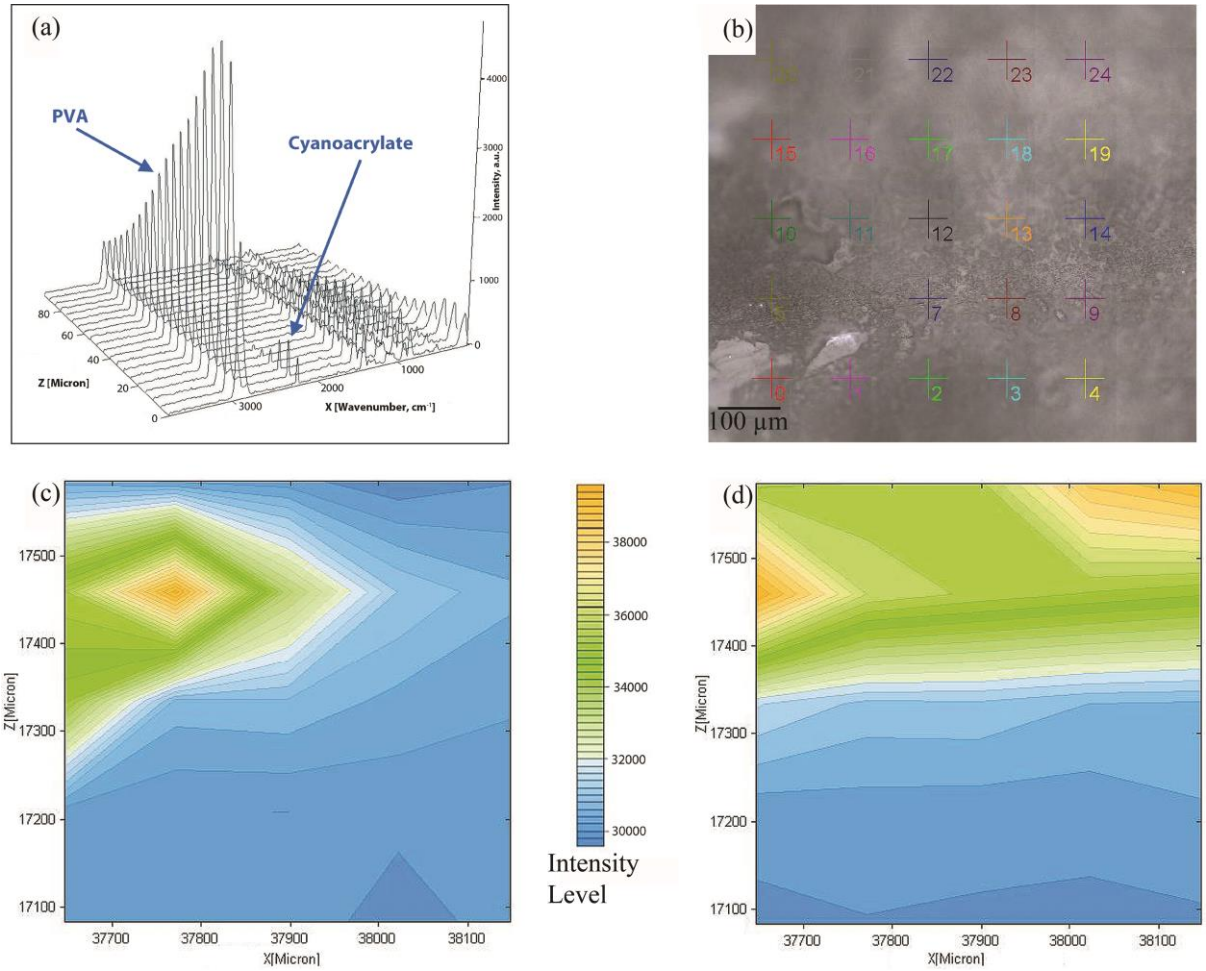

Figure 13. Raman Microscopy: Inhomogeneous penetration of the PBCA into the bulk of the 80µm thick PVA patch: depth-profile (a), VIS photograph with location of measurement points (b), mapping of the PBCA signal (c) and mapping of PVA signal (d). Sample description in Table 1 (Biomaterial properties).

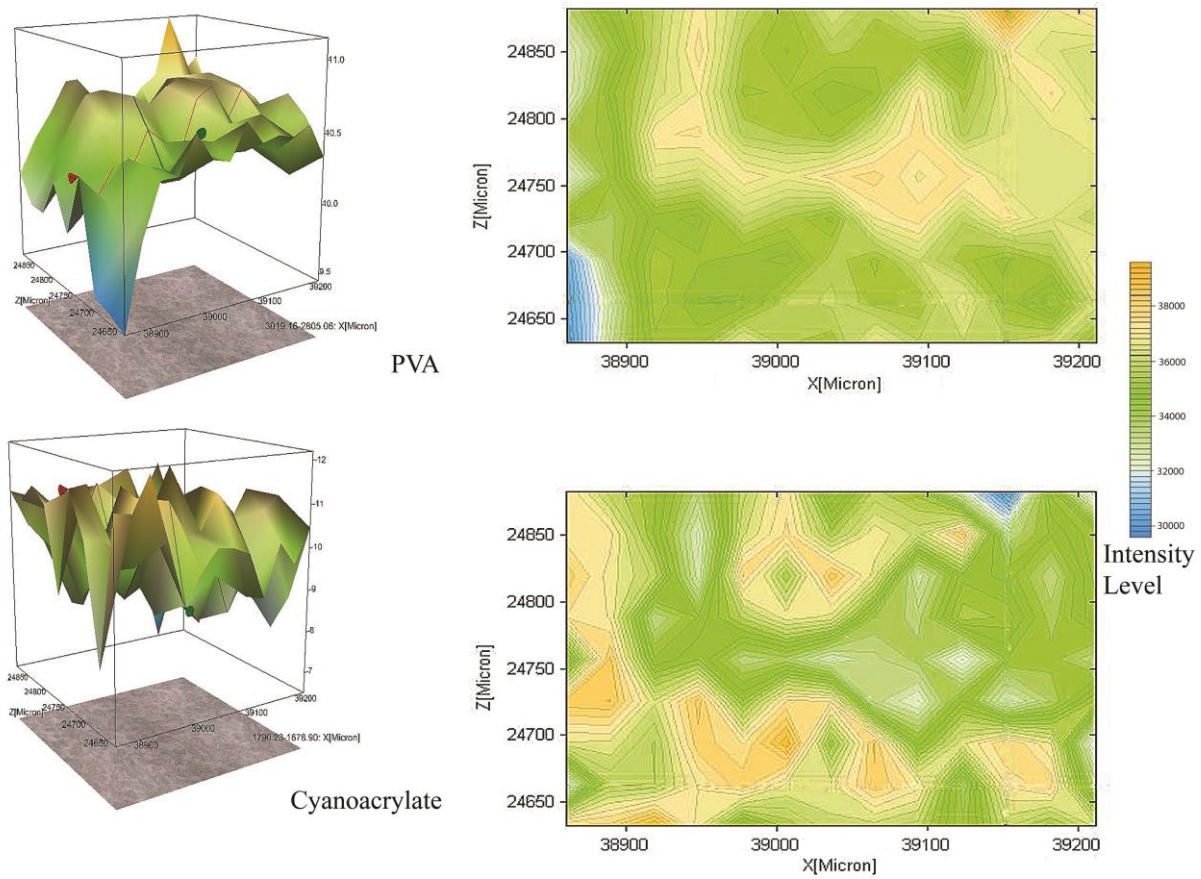

Figure 14. IR Microscopy - Intensity distribution (including VIS-image) of PVA (upper) and PBCA (lower) in the bulk material (mapping size 350 µm x 250 µm with 13 x 9 measurement points). Sample description in Table 1 (Biomaterial properties).

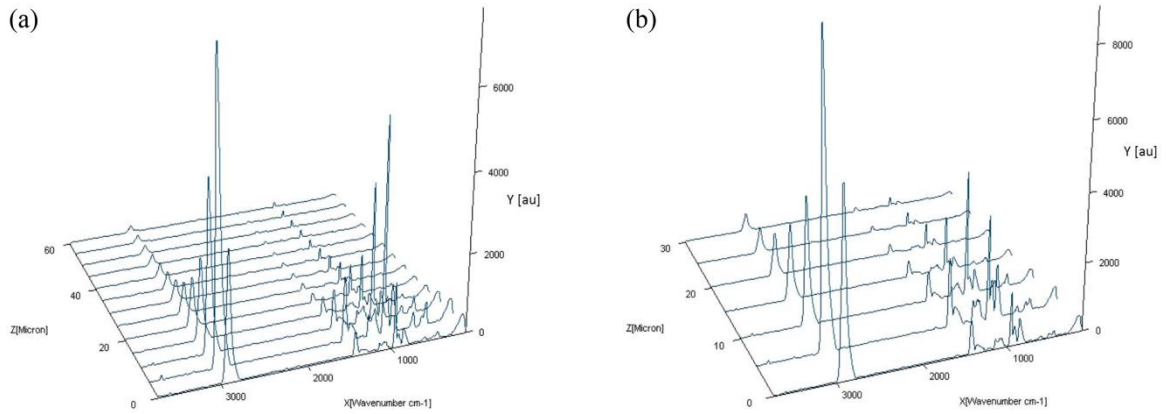

Figure 15. PBCA does not penetrate into both double-layered patch (HA/PVA 1.5 + 300/100 PVA/HA) (a) and single-layered patch (300/100 PVA/HA) (b) because the CN bond at 2250cm^{-1} is missing in the spectra. Sample description in Table 2 (Raman Microscopy).

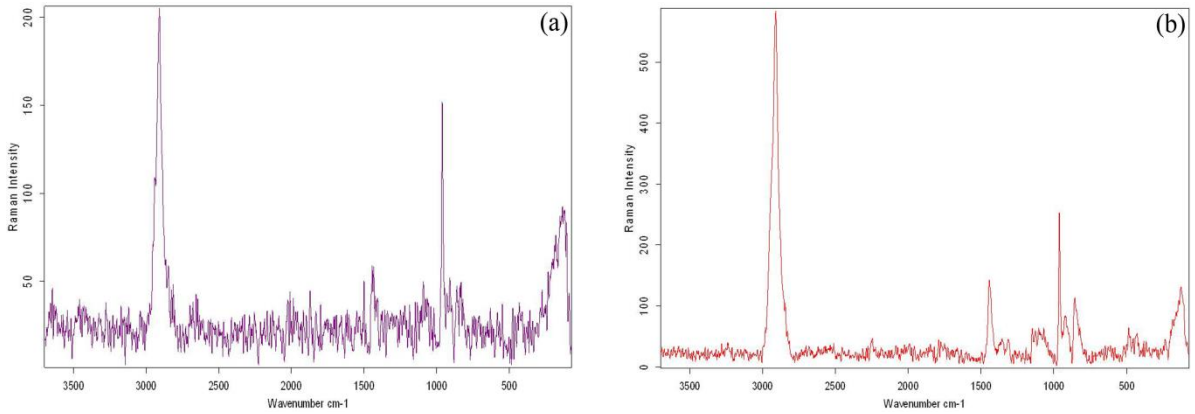

Figure 16. PBCA is absent at the lowest depth of the glued double-layered patch (HA/PVA 1.5 + 300/100 PVA/HA) (a) and single-layered patch (300/100 PVA/HA) (b) because the CN bond at 2250cm^{-1} is missing in the spectra. Sample description in Table 2 (Raman Microscopy).

4.3. Preservation of the molecular bioactivity in the patch

Since bioactive molecules are supposed to be loaded into the patch, the influence of the penetration of CA adhesive into the patch on the bioactivity of incorporated molecules was examined. The CA monomers could potentially interact with the bioactive molecules and then cause their inactivity or even lead to the formation of toxic agents. In order to investigate that behaviour, Horseradish Peroxidase (HRP) was selected as model protein drug. HRP was added into PVA patches that were subsequently glued to disk specimens. The results showed that after adding HRP chemiluminiscence substrate over the HRP patches, almost immediately a chemiluminescent signal was observed. That indicated preserved HRP enzymatic activity and conversion of the HRP substrate into the product. More important, the chemiluminescent signal from the attached samples was detectable long after 10 minutes. In contrast, the signal from the positive control patches (not glued) disappeared after 1 minute (Fig. 18).

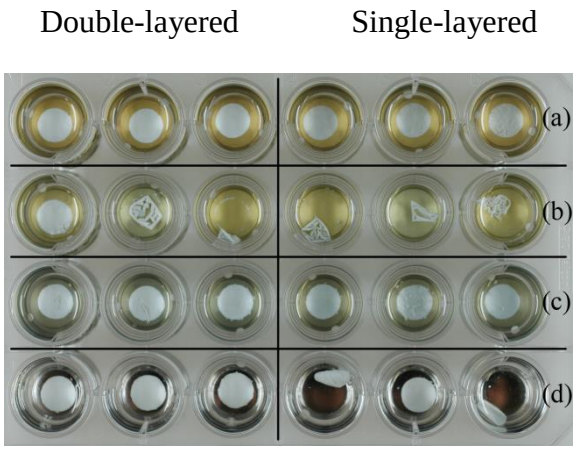

Figure 17. Wet-detachment of double-layered patches (HA/PVA 1.5 + 300/100 PVA/HA)-left and single-layered patches (300/100 PVA/HA)-right, at 7 days of incubation, glued over Ti-Synthes-multiple use (a), Ti-Synthes (b), Ti-AAP (c), CrNi-AAP (d). Sample description in Table 2 (Wet-detachment test).

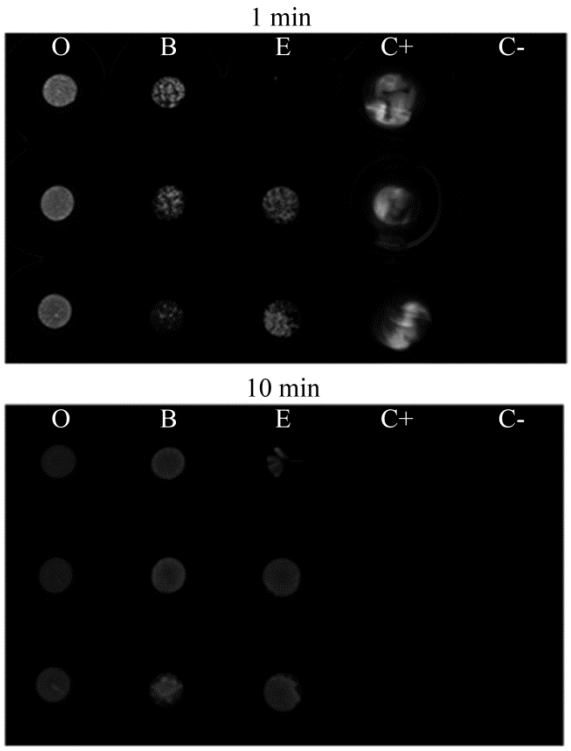

Figure 18. Chemiluminescent signal generated by the HRP activity: POCA (O), PBCA (B), PECA (E), Positive control-not glued (C+), Negative control –not glued, without HRP (C-). Sample description in Table 1 (Preservation of molecule bioactivity).

4.4. Protein Release Profiles

It is known that the BSA undergoes burst release profile out of PVA hydrogels that are treated by freeze/thaw cycles [218]. The penetrating CA adhesive could affect the protein release out of the patch. Therefore, a formulation of PVA patches had to be realized in such a way, that the protein release would be minimally influenced by the gluing to a metallic surface. BSA was selected as a model drug and was loaded into the PVA patches. Different formulations by controlling the PVA molecular weight, BSA concentration and patch thickness were produced. The release profile of BSA was monitored over a period of 14 days.

Just as expected, a burst BSA release was observed followed by a gradual slow release profile. Depending on the formulation, the majority of the BSA (41.6% to 90.7%) was released during the first 24 h (Fig. 19).

The molecular weight of the PVA molecules had an effect on the protein release from patches of 80 µm thickness. After day 1, the higher Mw patches (Mowiol 6-98) had a faster release (64.47%) compared to the lower Mw PVA patches (52.3% for PVA-Sigma and 53% for Mowiol 4-98). At day 14, 72.3%, 64.1% and 76.8% of BSA was released for PVA-Sigma, Mowiol 4-98 and Mowiol 6-98 respectively (Fig. 19a).

Further analyses explained the influence of the BSA concentration onto the 80 µm thick patches made out of PVA 6-98: The reduction of the BSA dose from 15 mg to 10 mg in the PVA solution that was used to prepare the patches had a decrease of the release from 64.5% to 41.7% BSA release during the first 24 hours. At day 14, the cumulative release profile of BSA dropped from 76.8% to 56.0%. On contrary, further reduction of BSA dose to 5 mg in the PVA solution that was used for patch preparation, had an opposite effect. The released BSA amount during the first 24 hours increased up to 90.8% and was followed up by a gradual release during the observation period (Fig. 19b).

A decrease in the patch thickness by keeping constant ratio of PVA 6-98: BSA (100:1) also resulted in differences of the BSA release (Fig. 19c). Reduction of the thickness from 80 µm to 58 µm led to an increase in the BSA release from 64.5% to 75.3% during the first day. A further reducing of the thickness to 27 µm led to a further increase in the BSA release for up to 89.3%. In both cases, small or no further BSA release was detected after day 3.

4.5. Biocompatibility testing

The degradation products of PACA adhesives might represent a problem in terms of biocompatibility [143]. Thus, the PVA patches were investigated after attaching to the metal surface for any potential cytotoxic effect in a time period up to 7 days. FACS analysis was used to define the ratio between the living and dead/dying cells after 1 day exposure to samples containing PVA and PACAs. The results revealed no early cytotoxicity in any of the groups (Fig. 20a). The lack of any early cytotoxic effect was also confirmed by Alamar Blue viability assay. At day 1, the cells that were exposed to the ethyl PECA showed slightly less

viability when compared to the other groups. Anyway, the cells proliferated during the studied period and no delayed cytotoxic effect was observed in any of the groups (Fig. 20b).

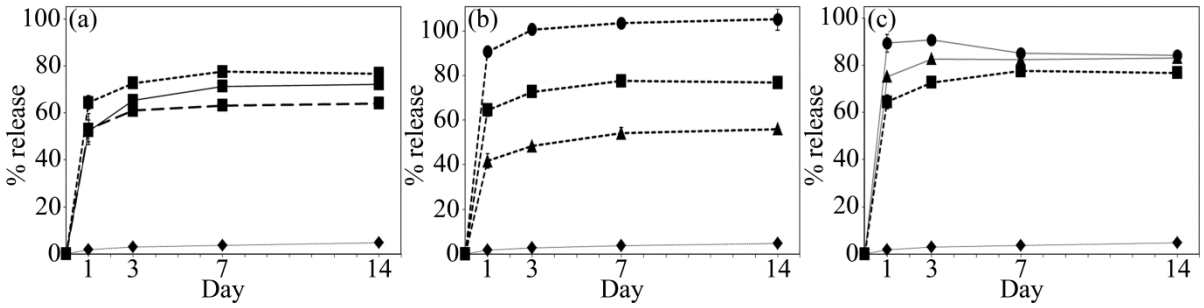

Figure 19. Influence of patch parameters on the BSA release. The effect of PVA Mw (a). The effect of BSA concentration in the patch (b). The effect of patch thickness (c). —■— 1,5g PVA-Sigma + 15mgBSA (80µm); –■– 1,5g Mowiol 4-98 + 15mgBSA (80µm); ·-■-· 1,5g Mowiol 6-98 + 15mgBSA (80µm); -·▲-· 1,5g Mowiol 6-98 + 10mgBSA (80µm); -·●-· 1,5g Mowiol 6-98 + 5mgBSA (80µm); —▲— 1g Mowiol 6-98 + 10mgBSA (58µm); —●— 0,5g Mowiol 6-98 + 5mgBSA (27µm); ◆ Control (1,5g Mowiol 6-98). Sample description in Table 1 (Protein release).

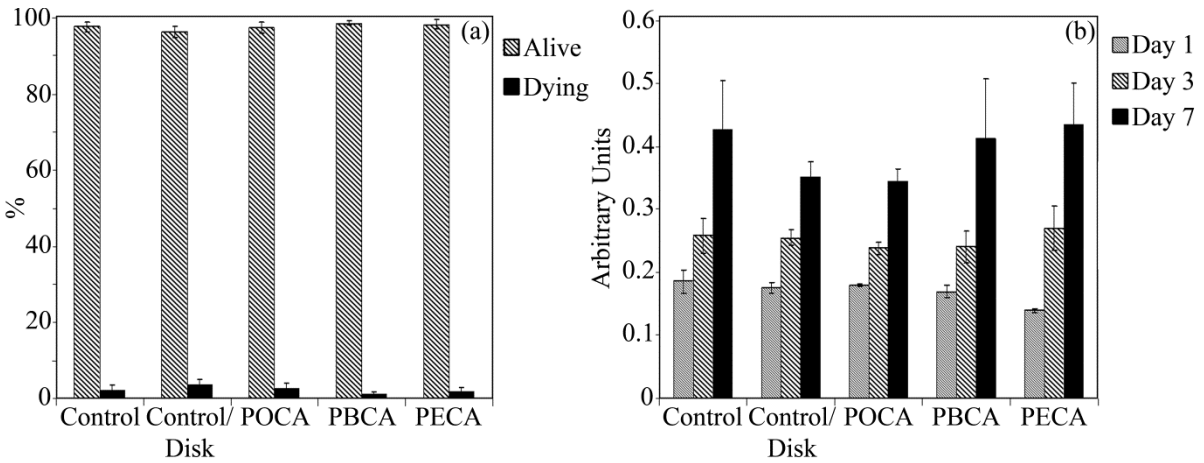

Figure 20. FACS analysis shows no initial cytotoxicity (a). Alamar Blue assay shows no early and delayed cytotoxicity (b). Sample description in Table 1 (Biocompatibility).

4.6. Drug release profile by microparticles embedded into the PVA patch

The penetrating PBCA into the PVA patches can also have inhibitory effect on the drug release profile even though it is controlled by a drug loaded microparticles. Therefore, Dexamethasone loaded PLGA microparticles were incorporated within amorphous and pretreated PVA patches followed by gluing over the test implant surfaces. The results showed that the drug release profile was mainly controlled by the microparticles. In all cases burst drug release was observed at the first day even though different initial amounts were released. The not glued patches were dissolved almost immediately after their placement in PBS but showed decreased dexamethasone release at day 1 (75.95±2.64 % for amorphous, 75.9±38.3 % for pretreated patches) when compared to the release from the control group-microparticles alone (89.7±9.2 %). Gluing of these patches resulted in even further decreased release during the day 1 (57.2±1.6 % for amorphous, 60.84±24.5 % for pretreated patches). The burst release was followed by a gradual slow release during the observed period of 28 days. The only exception was the glued amorphous patch group where the release reached 73.6±2.1 % at day 3 and no further release was detected during the 4 weeks of observation period.

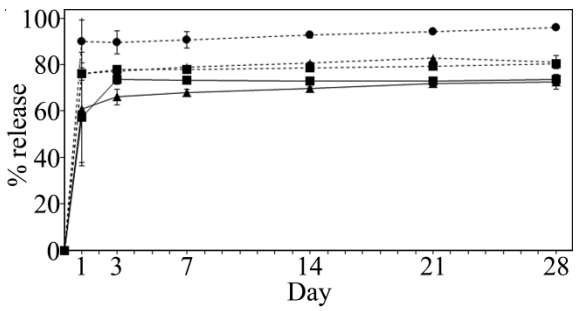

Figure 21. Dexamethasone release from PLGA particles embedded in PVA film. —■— amorphous/glued; —▲— pretreated/glued; --■-- amorphous/not glued; --▲-- pretreated/not glued; --●-- control/MPs only.

4.7. The influence of HA nanoparticles on the Dexamethasone release from PVA patches

HA nanoparticles were incorporated into the PVA patch in order to prevent the PBCA penetration and eliminate any potential reaction with incorporated bioactive molecules. Yet,

the presence of HA nanoparticles might affect the drug release profile provided by the patches. Therefore, Dexamethasone was loaded in double-layered (HA/PVA 1.5 + 300/100 PVA/HA) and single-layered (300/100 PVA/HA) patches. The results showed that a complete Dexamethasone release was achieved from the not glued patches (double- and single-layered) during the first day. Gluing of these patches resulted in similar drug release profile. To be more specific, double-layered patches released 86±20 % at day 1 followed by a complete release at day 3. The big standard deviation in this group is probably due to the Dexamethasone penetration into the first layer of the patch during the preparation procedure. On the other hand, single-layered patches showed 92.8±2.6 % release during the first day followed by a gradual and very slow release during the observed period of 14 days (Fig. 22).

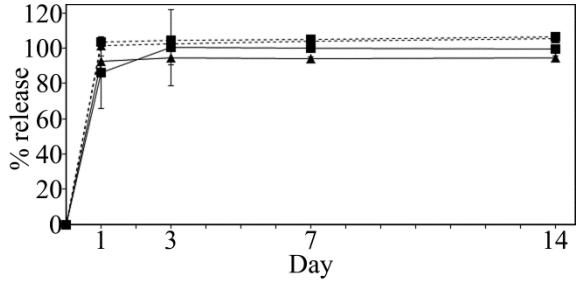

Figure 22. Dexamethasone release from PVA/HA patches: —■— double-layered/glued; —▲— single-layered/glued; --■-- double-layered; --▲-- single-layered.

5. Discussion

In this thesis it was hypothesized that a humidified PVA patch could initiate rapid CA polymerization and therefore could provide a platform to combine standard surgical implants with adjustable coating localization and selection of drugs and their corresponding dosage-all in one step as required for intra-operative use. If such intra-operative local drug delivery platform is to be developed, it has to fulfil certain criteria such as immediate patch attachment, controlled drug delivery and not detaching from the implant surface. The goal of the present study was to establish a novel implant coating platform that can provide a combination of drugs, customization of the dosage, and a free choice over the selected localization of a drug release. To realize this, an intra-operative customization is mandatory. This was realized by a PVA patch that is attached by gluing to the implant surface. Humidity loaded into the PVA patch was used as an initiator of the rapid CA adhesive polymerization

and enabled a fast intra-operatively applicable coating. The implant coating platform technology was verified in provision of a strongly attached coating that can deliver bioactive molecules and is non-cytotoxic. Further improvement of this technology was achieved by incorporation of HA nanoparticles into the PVA patch.

Current drug delivery implant coating strategies like antimicrobial sleeves [138], inorganic [65] and non-ceramic coatings [67] have major drawbacks and cannot be used as solutions for intra-operative usage. In fact, most of the research in the field of drug delivery by implant coating does not concentrate on the coating techniques but on improvement of already existing technologies and finding possible applications of newly developed biomaterials without paying attention to the clinical requirements [1]. Therefore, this study was initiated to design and evaluate a new implant coating platform with possibility for intra-operative customization.

5.1. Preparation of the PVA patches

The incorporation of drug loaded PLGA microspheres [134] or nanoparticles [181] in a PVA hydrogel that is pretreated by freeze-thawing seems to be a good strategy to realize the desired drug release profiles. It is widely accepted that the pretreatment by repeated freeze-thawing leads to formation of three phases: low PVA concentration water phase, amorphous phase and crystalline phase [219, 220] Therefore, PVA patches were prepared by a casting method, which in most experimental groups included repeated freeze/thaw cycles in order to induce crystallization of the PVA. The resulting polymer crystallites act as netpoints, thus affecting the mechanical properties when compared to non-treated materials and without the need to use potentially toxic chemical cross-linkers and hazardous solvents [219]. Upon contact with water which is a polar solvent, PVA swells to form a hydrogel and provides a burst release of incorporated molecules [218]. That observation can be beneficial when a rapid initial release for high drug concentration is needed such as in the case of antibiotics to prevent infections. One possible drawback is that the patch has a pre-defined coating area and drug loading. Therefore, a set of different drug loaded patches should be available for selection during the operation time. Most important, by this technology only the drug loaded patches and not the full implant are affected by a limited shelf-life.

5.2. CA adhesives and their potential for intraoperative solution

In addition to drug delivery provided by the payload of the patch, an intraoperative solution is necessary to realize a rapid patch attachment to the implant surfaces. Medical CA adhesives seem to be very interesting candidates due to the formation of strong adhesive bonds and their rapid anionic polymerization in the presence of water molecules. They are currently used as tissue adhesives for various applications like wound closure [221], arterial embolization [222] and orthodontic adhesive [223]. The CA adhesives have limited FDA approval because of their degradation products such as formaldehyde and alkyl cyanoacetate [143]. However, the actual in vivo degradation mechanism and related biocompatibility issues are still under debate [224]. In some cases, PACAs demonstrated cytotoxic effects in vitro [225-228] as well as some adverse effects in vivo [229]. Nevertheless, number of in vivo investigations showed that longer alkyl side chain PACAs can be safe for use. For example, PBCA caused minimal histotoxic effect and demonstrated good bone graft-cartilage binding ability [230]. PBCA has also appeared to be successful in nasal septum fixation without causing infection, foreign body reaction, necrosis or histotoxicity [231]. Fixation of zygomatic bone fracture in rabbits by PBCA resulted in tissue reaction similar to the non-fixated control. Actually, in the glued group the fixation was successful while the control group had displaced fractures [232]. A case report confirmed the beneficial effect of PBCA in fixation of acute osteochondral fractures [215], healing without any complications and promising clinical outcome in humans [214]. Furthermore, it was concluded that POCA was superior when compared to suture in stabilization of cartilage grafts in rabbits [233]. POCA was used for tibial fracture fixation in rabbit that resulted in adhesive degradation and bone union [234].

5.3. Shear Strength of the implant coating

In order to evaluate the quality of patch attachment over the test implant surfaces we have investigated various gluing parameters including: the type of the CA, the time of pressing, the phase state of the patch (amorphous/semi-crystalline) and the duration of exposure in the humidity chamber. The results that were obtained from shear testing revealed that the values can be comparable to that of hydroxyapatite coatings [235]. The CA adhesives with longer

alkyl side chain in principle can form more flexible polymers, which decreases their adhesive strength [236]. This is consistent with our results since PECA had higher shear strength values than patch attachment by PBCA, whereas POCA showed lowest values. More important, an increase in the pressing time and PVA pretreatment appeared to be beneficial when patches were glued by PECA and PBCA. Increased pressing time for amorphous patches resulted in a decrease of the shear strength. However, that observation is not valid for the pretreated PVA patches (Fig. 8a). In addition, an increase in the time of humidity exposure had effect with the pretreated patches. An increase in humidity exposure time for amorphous patches resulted in a decrease of the shear strength. However, that was not a case with the pretreated PVA patches (Fig. 8b).

The current study provides no data regarding the amount of water uptake by the PVA patches. It is known that the water uptake by the PVA is lower if the crystallinity is increased due to the physical netpoints that are formed as result of the freeze-thawing [190]. In fact, the crystalline phase in the freeze-thawed PVA restricts the motion of the amorphous chains [219]. Especially for PVA with a high degree of hydrolysis of acetyl side chains and a reduced solubility, i.e., an expected higher crystallinity, crystalline domains are acting as diffusion barrier for water penetration thus affecting the water uptake process. Consequently, after a certain time of humidity exposure, the amorphous patches would be expected to have absorbed higher amount of water than the pretreated ones. As a result, the increased amount of water can affect the PACA polymerization kinetics (nucleation vs. chain growth) and molecular weight, which might be the reason for the decreased shear resistance. Furthermore, the attachment of PVA patches over various test implant surfaces did not have any direct correlation with the surface micro-roughness (Table 3). It was expected that re-using might generate impurities over the metal surface which in turn would generate lower shear values. Surprisingly, the results showed that the newly used metals surfaces generated lower values than the re-used, even though the re-using did not influence their micro-roughness (Table 3). Further investigations concerning the surface chemistry are required in order to explain this effect. On the other hand, the results obtained from attachment on the PMMA surface showed much lower values than compared to the attachment on the metal surfaces. The main reason for that behaviour might be the mechanical properties of the material itself. In this case PMMA is much softer material compared to the metal surfaces and the mechanical interlocking of the adhesive within the surface is probably distorted during shear testing.

5.4. Characterization of the patch properties

The initiation of CA polymerization by the PVA patch brought up certain concern regarding possible alterations of the patch. SAXS and WAXS analysis did not reveal any morphological difference between the glued and not glued patches (Fig. 11, 12). Obviously, no morphological changes were caused by the PACA, or they could not be detected by these methods because of the low amount of adhesive used in the procedure. Therefore, Raman microscopy was used to evaluate if the liquid CA monomers penetrate the PVA network and polymerize within. The results showed inhomogeneous distribution of polymerized PBCA within the PVA patch (Fig. 13). This result can possibly be addressed to the semi-crystallinity of the PVA network and its three phase structure formed by the freeze/thawing cycles that makes penetration and swelling possible [219, 220]. In fact, the presence of low PVA concentration water phase, amorphous phase, and crystalline phase might lead to a difference in the speed of penetration of CA monomers (the crystalline phase acts as diffusion barrier). Consequently, partially separated regions of both materials are being formed and the PBCA distribution is correlated to the morphology of the PVA network (Fig. 14).

5.5. Preservation of the molecular bioactivity in the patch

Sensitive drugs could be chemically modified by the penetrating and highly reactive CA monomers [237]. The functional groups from the CA may covalently bind the bioactive molecules incorporated into the patch and subsequently cause their inactivation. On the other hand, incorporation of sensitive molecules such as HRP into a polymeric film stabilizes their structure and therefore protects their bioactivity [238]. It is also known that PVA can contribute for stabilization of the HRP activity [239]. This study showed that HRP loaded patches before and after the CA attachment preserved the enzymatic activity. Specifically, the addition of HRP substrate over the HRP loaded patches led to the generation of enzymatic product. However, the patch attachment by PACA adhesives delayed the HRP enzymatic reaction (Fig. 18). Consistent with these results, it can take up to a few minutes for the substrate of HRP to penetrate the polymeric film [238]. Our WAXS and SAXS data showed no changes in the crystalline structure of the patch due to the gluing by PACA. On the other hand, the formation of glassy hydrophobic PACA in the PVA patch and present as domains

(Fig. 13) may reduce the diffusivity of hydrophilic molecules in the patch. In fact, that might have reduced the HRP substrate penetration into the patch, which in turn led to delayed HRP substrate conversion into product. Based on this assumption, the delayed enzymatic reaction might be attributed to the difference in the speed of substrate diffusion into the PVA patches. Also a partial inactivation of HRP is possible and could have a similar effect. The difference in the contact area between attached and not attached patches (controls) also seem to be parameter of a great importance.

5.6. Protein Release Profiles

The penetrating CA can not only damage bioactive molecules but may also hinder their release out of the patch by acting as a diffusion barrier. On the other hand, incorporated substances such as drugs will be excluded from the crystallites in the freeze-thawed PVA, which could affect the release properties. Since proteins are known to exhibit burst diffusion out of pretreated PVA hydrogels [218], a PVA patch formulation had to be prepared in such a way that the burst protein release would be minimally altered by the gluing to a test implant surface. As expected, the burst BSA release was examined during the first 24 hours and it was followed by a gradual slow release during the studied period (Fig. 19). As a result, the higher molecular weight of PVA (Fig. 19a), low BSA dose (Fig. 19b) and reduced patch thickness (Fig. 19c) resulted in highest burst release. Formulation like this can be used to incorporate pre-loaded and pre-validated drug delivery particles in the PVA patches and their release profile will be minimally affected by the gluing. Consequently, the drug release profile can mainly be controlled by one or multiple types of drug delivery particles [134, 181]. That provides a wide choice of drugs, doses and release profiles to be applied as intra-operative solution.

5.7. Drug release profile by microparticles embedded into the PVA patch

For that purpose, Dexamethasone loaded PLGA microparticles were included in amorphous and pretreated PVA patches. The PLGA microparticles/PVA patches were prepared as patch with reduced thickness and out of higher molecular weight PVA. It seems that the drug

release profile from these patches is mainly controlled by the embedded microparticles because in all cases most of the Dexamethasone was released during the first day. Still, the gluing showed effect as the amount of released Dexamethasone in the glued patches was lower when compared to the non-glued patches (Fig. 21). That is probably due to the difference in the contact area between attached and not attached patches as well as CA monomers penetration and polymerization within the patch. Therefore, additional work had to be done in order to prevent the CA penetration and prevent their influence on the drug release profile.

5.8. Biocompatibility testing

No CA adhesive is currently FDA approved for internal use in the human body. It is widely known that the shorter alkyl side chain in the CAs like PECA, leads to a higher cytotoxic effect than compared to the PBCA and POCA [143]. Nevertheless, the combination with PVA patch was expected to significantly improve the biocompatibility of all the tested CAs. It was hypothesized that the release of degradation products from the PACA will be delayed by the interaction with the PVA patch. In this study the amount of degradation products being released was not measured but the biocompatibility of the PACA attached PVA patches was tested. The results indicated no presence of any cytotoxic effect at early and delayed time points (Fig. 20).

5.9. Influence of the HA nanoparticles in the PVA patch

It has to be noted that under prolonged exposure to aqueous solutions like phosphate buffered saline (PBS) at 37° C, even though showing high shear strength in the dry state, the PVA patches tend to detach from some of the tested metal surface within only a minutes. This might represent a problem if the patch location is not stabilized by surrounding tissue structures e.g. in the situation of plates used for bone fracture fixation. In contrast, the application on endoprosthetic shafts that are anchored in the bone structure seems to be less critical. The presence of a passive oxide layer on the metal surface probably leads only to mechanical interlocking of the PACA network within the surface micro-roughness rather than

to covalent interaction with the implant surface. Accordingly, the PVA swelling may cause mechanical deformations in the patch and that might be the reason for detachment from some of the tested metal surfaces. On the other hand, if the passivating oxide layer is being removed, the patches showed to stay attached for more than a month (data not shown). However, onto PMMA surfaces, the PVA patches were able to stay attached for at least 4 weeks even though the shear strength in the dry state was much lower compared to the metal surfaces (data not shown). Since the removal of the passivating oxide layer is not desirable solution for orthopaedic implants, additional improvement of the patch attachment is mandatory for certain applications on passivated metal surfaces.

In order to overcome issues such as patch detachment in a wet state, the CA monomers penetration and their potential interaction with the loaded drugs, HA nanoparticles were used to influence the morphology of the PVA patch. Therefore, various formulations of PVA and HA nanoparticles were used to prepare single- and double-layered patches. The goal was to determine which PVA to HA nanoparticles ratio can be used to prepare the first layer of the double-layered patches that should come in contact with the CA monomers during the gluing. The purpose of this layer is to be strongly attached to the implants surface, to prevent the CA penetration and to avoid pronounced swelling that seems to be responsible for the patch detachment the surface. Such layer can be achieved by higher ratio of HA nanoparticles to PVA (e.g. HA/PVA=1.5). In such case, the first layer has compact structure due to the uniform nanoparticle distribution within the PVA (Fig. 9). In order to prepare the second or drug delivery layer, a higher ratio of PVA to HA nanoparticles (e.g. PVA/HA=3) can be used. Here, the HA nanoparticles form clusters (Fig. 9) which imparts stability and drugs can diffuse from in-between the clusters.

The results obtained from the shear testing revealed that the addition of HA nanoparticles to the PVA does not significantly influence the shear strength. That behaviour is valid for double-layered patches (HA/PVA 1.5 + 300/100 PVA/HA) (Fig. 10) and is comparable to the PVA patches of similar thickness (Table 3, Ti-Synthes). On the other hand, single-layered patches (300/100 PVA/HA) showed significant decrease in the shear strength that is probably due to the failure of the patch itself rather than the adhesive. The lower thickness of the single-layered patches and their brittleness caused from the presence of HA nanoparticles might be an explanation for this result.

Since the penetrating CA monomers can inactivate bioactive molecules and can also affect their diffusion from the patch, it was of a great importance to prevent the CA penetration

within the patch. That was achieved by the presence of highly crystalline HA nanoparticles that act as a barrier for the CA monomers permeation into the patch (Fig. 15). Not only limited, but the penetration of CA was entirely prevented as the signal coming from the lowest depth of the glued patch lacks the CN bond (Fig. 16).

Nevertheless, both single- and double-layered PVA/HA patches showed improved attachment in a wet state when compared to the PVA patches (Fig. 17). In fact, the patches were detaching from the newly used Titanium alloy-Synthes almost immediately after swelling. On the other hand, the multiple use of this surface led to different behaviour and the patches did not detach. This is in agreement with the shear strength results where the new metals surfaces generated lower values than the re-used, even though the re-using did not cause any influence to the micro-roughness (Table 3). This is probably due to the changes in the surface chemistry and further investigations need to be performed in order to explain this observation.

5.10. The influence of the HA nanoparticles on the Dexamethasone release from the PVA patch

The drug release properties of PVA/HA patches remained in main focus throughout the whole study as the patches themselves, or their gluing should not interfere with the drug release profile provided by a drug loaded particles embedded within the patch. The single- and double-layered PVA/HA patches were able to achieve complete Dexamethasone release in only 1 day (Fig. 22). Furthermore, gluing of these patches onto implant surface only slightly influenced the release profile. For example, with the double-layered patches complete release was achieved after 3 days (Fig. 22). The main explanation for this effect might be the possible Dexamethasone penetration into the first layer of the patch during the preparation procedure. Actually, if a second dispersion that includes Dexamethasone in casted over the first layer, then that layer absorbs the water, it swells and might partially absorbs some of the Dexamethasone. The absorbed Dexamethasone by the first layer probably needs longer time to diffuse out of the patch. On the other hand, the single-layered patches released almost the complete amount during the first day followed by a gradual and slow release (Fig. 22). That is probably due to the Dexamethasone entrapment into the HA nanoparticle clusters and requires longer diffusion time. Also electrostatic interactions with the HA nanoparticles

might act as diffusion barrier. Nevertheless, formulations of this kind can include drug delivery particles in order to control the release profiles and can be processed as a single layer or as a second layer of double-layered patch.

6. Summary

An intra-operative custom made implant coating for drug delivery was developed in this thesis. In that approach, a drug delivery polyvinyl alcohol based patch is glued to implant surfaces by a CA adhesive. To initiate polymerization of the adhesive, the patch is first exposed to a controlled level of humidity. We observed that humidified patches, when pressed in the standardized setup against CA that is deposited on model implant surfaces, were suitable to initiate the nucleophilic polymerization of CA and resulted in a rapid patch attachment to the test implant surfaces. These patches were strongly attached onto the test implant surfaces with the shear strength depending on several factors like the type of the CA, the time of pressing, the properties of the patch, the type of test implant surface and the amount of humidity exposure. The liquid CA monomers penetrated and polymerized within the PVA patch. Nevertheless, no morphological changes of the PVA patch could be observed. Furthermore, the enzymatic activity of the embedded HRP molecules remained preserved. The glued PVA patch was able to provide protein release in all the cases. This platform technology gives the opportunity to realize different drug delivery formulations, including fast release or delayed release from embedded pre-loaded and pre-validated particles that are necessary for an optimized patient treatment in terms of a personalized medicine approach. For example, this strategy was able to support the release profile provided by the Dexamethasone loaded PLGA microparticles. A further continuation of research on this technology is supported by the observation that the combination of PACA and PVA patches did not show any cytotoxic effects in vitro. The addition of HA nanoparticles within the patch managed to overcome the disadvantages such as detachment in a wet state, penetration of CA monomers into the patch and still providing the opportunity for a drug loaded particles that are potentially embedded within to control the release profile.

In this thesis we present the first results of Dexamthasone release by an intra-operative custom made implant coating approach. This could find potential use in a total knee replacement surgery where patches can be directly attached onto the PMMA spacers in order

to locally deliver anti-inflammatory and analgesic drugs. Such treatment can support the post-operative pain management and significantly improve the patient situation. Finally, this platform could find use in growth factors delivery directly from the coated metal implant surface.

7. Zusammenfassung

In dieser Arbeit wurde eine intra-operative zur Wirkstofffreisetzung maßgeschneiderte Implantat-Beschichtung entwickelt. In diesem Ansatz wird mittels Cyanoacrylat (CA) ein wirkstofffreisetzender, auf Polyvinylalkohol basierender Film auf die Oberfläche der Implantate aufgeklebt. Um die Polymerisation des Klebstoffs zu initiieren, wird der Film zunächst einer kontrollierten Luftfeuchtigkeit ausgesetzt. Es wurde beobachtet, dass befeuchtete Filme, die in einem standardisierten Prozess auf eine mit CA benetzte Implantat-Testoberfläche aufgepresst wurden, in der Lage waren, die nucleophile Polymerisation von CA zu initiieren. Dies führte zu einer schnellen Verklebung des Filmes mit der Implantat-Testoberfläche. Die Filme zeigten generell eine mechanisch stabile Verbindung mit den Implantat-Testoberfläche wobei die Scherfestigkeit von verschiedenen Faktoren abhing: der Art des CA, der Anpresszeit, den Eigenschaften des Films, der Art der Implantat-Testoberfläche und dem Feuchtigkeitsgrad im Film. Die flüssigen CA Monomere durchdrangen den PVA Film und polymerisierten innerhalb des Films. Dennoch konnten keine morphologischen Veränderungen des Films beobachtet werden. Darüber hinaus blieb die enzymatische Aktivität eingebetteter HRP-Moleküle erhalten. In allen Fällen konnte eine Proteinfreisetzung durch den aufgeklebten PVA Film beobachtet werden. Diese Plattformtechnologie bietet die Möglichkeit, verschiedenste Arten von Wirkstoffen freizusetzen, einschließlich einer schnellen oder verzögerten Freisetzung aus eingebetteten Partikeln. Diese Partikel können im Vorhinein mit Wirkstoffen beladenen und validiert werden. Die Flexibilität der Technologie ist für eine optimierte Behandlung von Patienten im Sinne der individualisierten Medizin notwendig. Exemplarisch konnte der entwickelte Ansatz genutzt werden, um das Freisetzungsprofil von Dexamethason beladenen PLGA-Mikropartikeln auch nach Einbettung in den Film zu erhalten. Die Kombination von PACA und PVA-Filmen zeigte in vitro keine zytotoxischen Effekte. Dies motiviert eine weiterführende Erforschung der entwickelten Technologie. Durch die Einbettung von HA-

Nanopartikeln in den Film, wurden anfängliche Probleme wie das Ablösen des Films bei Flüssigkeitsbenetzung und das Eindringen von CA Monomeren in den Film überwunden, ohne die Möglichkeit zu verlieren, den Wirkstofffreisetzungsverlauf über eingebettete Partikel zu kontrollieren.

In dieser Arbeit werden die ersten Ergebnisse für eine Dexamethasone-Freisetzung aus einer intra-operativ aufzubringenden, maßgeschneiderten Implantat-Beschichtung präsentiert. Dieser Ansatz könnte bei der Totalendoprothetik des Kniegelenks eine Verwendung finden, wo entsprechende Filme direkt auf PMMA Abstandshaltern befestigt werden könnten, um lokal entzündungshemmende und schmerzstillende Medikamente freizusetzen. Eine solche Behandlung kann postoperative Schmerzen vermindern und die Situation des Patienten deutlich verbessern. Schließlich könnte diese Technologie bei der Wachstumsfaktor-Freisetzung von beschichteten Metallimplantat-Oberflächen Verwendung finden.

References

1. Trajkovski, B., et al., *Intra-operatively customized implant coating strategies for local and controlled drug delivery to bone.* Advanced Drug Delivery Reviews, doi:10.1016/j.addr.2012.05.016, 2012(0).
2. Duda, G.N., S. Benusch, and N.P. Haas, *[Clinical research in partnership: musculoskeletal surgery].* Chirurg, 2010. 81(4): p. 352-8.
3. Katz, J.N., *Lumbar spinal fusion. Surgical rates, costs, and complications.* Spine, 1995. 20(24 Suppl): p. 78S-83S.
4. Della Rocca, G.J., K.S. Leung, and H.C. Pape, *Periprosthetic fractures: epidemiology and future projections.* J Orthop Trauma, 2011. 25 Suppl 2: p. S66-70.
5. Lad, S.P., et al., *Trends in pathological vertebral fractures in the United States: 1993 to 2004.* J Neurosurg Spine, 2007. 7(3): p. 305-10.
6. Weinstein, J.N., et al., *United States' trends and regional variations in lumbar spine surgery: 1992-2003.* Spine (Phila Pa 1976), 2006. 31(23): p. 2707-14.
7. Deyo, R.A., et al., *United States trends in lumbar fusion surgery for degenerative conditions.* Spine (Phila Pa 1976), 2005. 30(12): p. 1441-5; discussion 1446-7.
8. Bergmann, G., et al., *Realistic loads for testing hip implants.* Biomed Mater Eng, 2010. 20(2): p. 65-75.
9. Boden, S.D. and J.H. Schimandle, *Biologic enhancement of spinal fusion.* Spine, 1995. 20(24 Suppl): p. 113S-123S.
10. Giannoudis, P.V., T.A. Einhorn, and D. Marsh, *Fracture healing: the diamond concept.* Injury, 2007. 38 Suppl 4: p. S3-6.
11. Sloan, A., et al., *The effects of smoking on fracture healing.* Surgeon, 2010. 8(2): p. 111-6.
12. Reid, J.J., J.S. Johnson, and J.C. Wang, *Challenges to bone formation in spinal fusion.* J Biomech, 2011. 44(2): p. 213-20.
13. Wessinghage, D. and E. Kisslinger, *[Long-term results after cemented total hip arthroplasty in chronic polyarthritis].* Orthopade, 1998. 27(6): p. 381-91.
14. Thillemann, T.M., et al., *Postoperative use of bisphosphonates and risk of revision after primary total hip arthroplasty: a nationwide population-based study.* Bone, 2010. 46(4): p. 946-51.
15. Pedersen, A.B., et al., *Risk factors for revision due to infection after primary total hip arthroplasty. A population-based study of 80,756 primary procedures in the Danish Hip Arthroplasty Registry.* Acta Orthop, 2010. 81(5): p. 542-7.
16. accessible via http://cdc.gov/nchs, accessed 29. Feb. 2012.
17. AAOS. *(American Association of Orthopaedic Surgeons) Burden of Musculoskeletal Diseases in the United States: Prevalence, Societal and Economic Costs*. 2011 [cited 2012 29 Feb]; Available from: www.boneandjointburden.org/pdfs/BMUS_chpt6_injuries.pdf.
18. Rajaee, S.S., et al., *Spinal fusion in the United States: analysis of trends from 1998 to 2008.* Spine (Phila Pa 1976), 2012. 37(1): p. 67-76.
19. Cahill, K.S., et al., *Prevalence, complications, and hospital charges associated with use of bone-morphogenetic proteins in spinal fusion procedures.* Jama, 2009. 302(1): p. 58-66.
20. Haentjens, P., G. Lamraski, and S. Boonen, *Costs and consequences of hip fracture occurrence in old age: an economic perspective.* Disabil Rehabil, 2005. 27(18-19): p. 1129-41.
21. Ismail, A.A., et al., *Incidence of limb fracture across Europe: results from the European Prospective Osteoporosis Study (EPOS).* Osteoporos Int, 2002. 13(7): p. 565-71.
22. van Staa, T.P., et al., *Epidemiology of fractures in England and Wales.* Bone, 2001. 29(6): p. 517-22.
23. Ahmed, L.A., et al., *The gender- and age-specific 10-year and lifetime absolute fracture risk in Tromso, Norway.* Eur J Epidemiol, 2009. 24(8): p. 441-8.
24. Kannus, P., et al., *Rate of proximal humeral fractures in older Finnish women between 1970 and 2007.* Bone, 2009. 44(4): p. 656-9.
25. Bruyere, O., et al., *Post-fracture management of patients with hip fracture: a perspective.* Curr Med Res Opin, 2008. 24(10): p. 2841-51.
26. *European Markets for Spinal Fusion Instrumentation Products #A314*, 2011, Medtech Insight, Elsevier Business Intelligence: Irvine. p. 1-162.
27. Giannoudis, P.V. and C. Tzioupis, *Clinical applications of BMP-7: the UK perspective.* Injury, 2005. 36 Suppl 3: p. S47-50.
28. Salvati, E.A., et al., *Infection rates after 3175 total hip and total knee replacements performed with and without a horizontal unidirectional filtered air-flow system.* J Bone Joint Surg Am, 1982. 64(4): p. 525-35.
29. Poss, R., et al., *Factors influencing the incidence and outcome of infection following total joint arthroplasty.* Clin Orthop Relat Res, 1984(182): p. 117-26.
30. Grogan, T.J., et al., *Deep sepsis following total knee arthroplasty. Ten-year experience at the University of California at Los Angeles Medical Center.* J Bone Joint Surg Am, 1986. 68(2): p. 226-34.
31. Urquhart, D.M., et al., *Incidence and risk factors for deep surgical site infection after primary total hip arthroplasty: a systematic review.* J Arthroplasty, 2010. 25(8): p. 1216-22 e1-3.
32. Webb, B.G., D.M. Lichtman, and R.A. Wagner, *Risk factors in total joint arthroplasty: comparison of infection rates in patients with different socioeconomic backgrounds.* Orthopedics, 2008. 31(5): p. 445.
33. Cole, C.D., et al., *Comparison of low back fusion techniques: transforaminal lumbar interbody fusion (TLIF) or posterior lumbar interbody fusion (PLIF) approaches.* Curr Rev Musculoskeletal Med, 2009. 2(2): p. 118-26.
34. Jacobs, W.C., A. Vreeling, and M. De Kleuver, *Fusion for low-grade adult isthmic spondylolisthesis: a systematic review of the literature.* Eur Spine J, 2006. 15(4): p. 391-402.
35. Smith, J.S., et al., *Rates of infection after spine surgery based on 108,419 procedures: a report from the Scoliosis Research Society Morbidity and Mortality Committee.* Spine (Phila Pa 1976), 2011. 36(7): p. 556-63.
36. Bacon, W.E., *Secular trends in hip fracture occurrence and survival: age and sex differences.* J Aging Health, 1996. 8(4): p. 538-53.
37. Strube, P., et al., *Sex-specific compromised bone healing in female rats might be associated with a decrease in mesenchymal stem cell quantity.* Bone, 2009. 45(6): p. 1065-72.

38. Strube, P., et al., *Influence of age and mechanical stability on bone defect healing: Age reverses mechanical effects.* Bone, 2008. 42(4): p. 758-64.
39. Mehta, M., et al., *Influence of Gender and Fixation Stability on Bone Defect Healing in Middle-aged Rats: A Pilot Study.* Clin Orthop Relat Res, 2011. 469(11): p. 3102-10.
40. Mehta, M., et al., *Influences of age and mechanical stability on volume, microstructure, and mineralization of the fracture callus during bone healing: is osteoclast activity the key to age-related impaired healing?* Bone, 2010. 47(2): p. 219-28.
41. Lienau, J., et al., *Initial vascularization and tissue differentiation are influenced by fixation stability.* J Orthop Res, 2005. 23(3): p. 639-45.
42. Pedersen, A.B., et al., *Risk of revision of a total hip replacement in patients with diabetes mellitus: a population-based follow up study.* J Bone Joint Surg Br, 2010. 92(7): p. 929-34.
43. Thillemann, T.M., et al., *Use of diuretics and risk of implant failure after primary total hip arthroplasty: a nationwide population-based study.* Bone, 2009. 45(3): p. 499-504.
44. Thillemann, T.M., et al., *The risk of revision after primary total hip arthroplasty among statin users: a nationwide population-based nested case-control study.* J Bone Joint Surg Am, 2010. 92(5): p. 1063-72.
45. Schurch, M.A., et al., *A prospective study on socioeconomic aspects of fracture of the proximal femur.* J Bone Miner Res, 1996. 11(12): p. 1935-42.
46. Tzioupis, C. and P.V. Giannoudis, *Prevalence of long-bone non-unions.* Injury, 2007. 38 Suppl 2: p. S3-9.
47. Garrison, K.R., et al., *Clinical effectiveness and cost-effectiveness of bone morphogenetic proteins in the non-healing of fractures and spinal fusion: a systematic review.* Health Technol Assess, 2007. 11(30): p. 1-150, iii-iv.
48. Coles, C.P. and M. Gross, *Closed tibial shaft fractures: management and treatment complications. A review of the prospective literature.* Can J Surg, 2000. 43(4): p. 256-62.
49. Garrison, K.R., et al., *Bone morphogenetic protein (BMP) for fracture healing in adults.* Cochrane Database Syst Rev, 2010(6): p. CD006950.
50. Kraus, K.H. and C. Kirker-Head, *Mesenchymal stem cells and bone regeneration.* Vet Surg, 2006. 35(3): p. 232-42.
51. Bielby, R., E. Jones, and D. McGonagle, *The role of mesenchymal stem cells in maintenance and repair of bone.* Injury, 2007. 38 Suppl 1: p. S26-32.
52. Bruder, S.P., D.J. Fink, and A.I. Caplan, *Mesenchymal stem cells in bone development, bone repair, and skeletal regeneration therapy.* J Cell Biochem, 1994. 56(3): p. 283-94.
53. Peters, A., et al., *Locally applied osteogenic predifferentiated progenitor cells are more effective than undifferentiated mesenchymal stem cells in the treatment of delayed bone healing.* Tissue Eng Part A, 2009. 15(10): p. 2947-54.
54. Jones, E. and X. Yang, *Mesenchymal stem cells and bone regeneration: current status.* Injury, 2011. 42(6): p. 562-8.
55. Kim, S.E., et al., *Enhancement of ectopic bone formation by bone morphogenetic protein-2 delivery using heparin-conjugated PLGA nanoparticles with transplantation of bone marrow-derived mesenchymal stem cells.* J Biomed Sci, 2008. 15(6): p. 771-7.
56. Silva, G.A., et al., *Materials in particulate form for tissue engineering. 2. Applications in bone.* J Tissue Eng Regen Med, 2007. 1(2): p. 97-109.
57. Devescovi, V., et al., *Growth factors in bone repair.* Chir Organi Mov, 2008. 92(3): p. 161-8.
58. Phillips, A.M., *Overview of the fracture healing cascade.* Injury, 2005. 36 Suppl 3: p. S5-7.
59. Lissenberg-Thunnissen, S.N., et al., *Use and efficacy of bone morphogenetic proteins in fracture healing.* Int Orthop, 2011. 35(9): p. 1271-80.
60. Issa, J.P., et al., *Sustained release carriers used to delivery bone morphogenetic proteins in the bone healing process.* Anat Histol Embryol, 2008. 37(3): p. 181-7.
61. Kim, M. and S. Choe, *BMPs and their clinical potentials.* BMB Rep, 2011. 44(10): p. 619-34.
62. Laflamme, C. and M. Rouabhia, *Effect of BMP-2 and BMP-7 homodimers and a mixture of BMP-2/BMP-7 homodimers on osteoblast adhesion and growth following culture on a collagen scaffold.* Biomed Mater, 2008. 3(1): p. 15008.
63. Lee, S.H. and H. Shin, *Matrices and scaffolds for delivery of bioactive molecules in bone and cartilage tissue engineering.* Adv Drug Deliv Rev, 2007. 59(4-5): p. 339-59.
64. Wang, C.K., et al., *Controlled-release of rhBMP-2 carriers in the regeneration of osteonecrotic bone.* Biomaterials, 2009. 30(25): p. 4178-86.
65. de Jonge, L.T., et al., *Organic-inorganic surface modifications for titanium implant surfaces.* Pharm Res, 2008. 25(10): p. 2357-69.
66. Macdonald, M.L., et al., *Tissue integration of growth factor-eluting layer-by-layer polyelectrolyte multilayer coated implants.* Biomaterials, 2011. 32(5): p. 1446-53.
67. Strobel, C., G. Schmidmaier, and B. Wildemann, *Changing the release kinetics of gentamicin from poly(D,L-lactide) implant coatings using only one polymer.* Int J Artif Organs, 2011. 34(3): p. 304-16.
68. Couto, D.S., et al., *Lessons from innovation in drug-device combination products.* Adv Drug Deliv Rev, 2011.
69. Wu, P. and D.W. Grainger, *Drug/device combinations for local drug therapies and infection prophylaxis.* Biomaterials, 2006. 27(11): p. 2450-2467.
70. Faster, L.N., *Faster approvals seen for drug and device combination products*, in *BBI Newsletter*2003. p. 26(9):249.
71. Beth, W., *Medical Devices and Combination Products*, in *Using the Pharmaceutical Literature*2006, Informa Healthcare. p. 233-297.
72. Willie, B.M., et al., *Designing biomimetic scaffolds for bone regeneration: why aim for a copy of mature tissue properties if nature uses a different approach?* Soft Matter, 2010. 6(20): p. 4976.
73. Schmidmaier, G., et al., *Quantitative assessment of growth factors in reaming aspirate, iliac crest, and platelet preparation.* Bone, 2006. 39(5): p. 1156-63.
74. Carreon, L.Y., et al., *Platelet gel (AGF) fails to increase fusion rates in instrumented posterolateral fusions.* Spine (Phila Pa 1976), 2005. 30(9): p. E243-6; discussion E247.

75. Benglis, D., M.Y. Wang, and A.D. Levi, *A comprehensive review of the safety profile of bone morphogenetic protein in spine surgery.* Neurosurgery, 2008. 62(5 Suppl 2): p. ONS423-31; discussion ONS431.
76. Argintar, E., S. Edwards, and J. Delahay, *Bone morphogenetic proteins in orthopaedic trauma surgery.* Injury, 2011. 42(8): p. 730-4.
77. Lovell, T.P., et al., *Augmentation of spinal fusion with bone morphogenetic protein in dogs.* Clin Orthop Relat Res, 1989(243): p. 266-74.
78. Zdeblick, T.A., et al., *Cervical interbody fusion cages. An animal model with and without bone morphogenetic protein.* Spine, 1998. 23(7): p. 758-65; discussion 766.
79. Schimandle, J.H., S.D. Boden, and W.C. Hutton, *Experimental spinal fusion with recombinant human bone morphogenetic protein-2.* Spine, 1995. 20(12): p. 1326-37.
80. Sandhu, H.S., et al., *Experimental spinal fusion with recombinant human bone morphogenetic protein-2 without decortication of osseous elements.* Spine, 1997. 22(11): p. 1171-80.
81. Boden, S.D., et al., *Posterolateral lumbar intertransverse process spine arthrodesis with recombinant human bone morphogenetic protein 2/hydroxyapatite-tricalcium phosphate after laminectomy in the nonhuman primate.* Spine (Phila Pa 1976), 1999. 24(12): p. 1179-85.
82. Burkus, J.K., et al., *Anterior lumbar interbody fusion using rhBMP-2 with tapered interbody cages.* J Spinal Disord Tech, 2002. 15(5): p. 337-49.
83. Boden, S.D., et al., *Use of recombinant human bone morphogenetic protein-2 to achieve posterolateral lumbar spine fusion in humans: a prospective, randomized clinical pilot trial: 2002 Volvo Award in clinical studies.* Spine (Phila Pa 1976), 2002. 27(23): p. 2662-73.
84. Dimar, J.R., et al., *Clinical outcomes and fusion success at 2 years of single-level instrumented posterolateral fusions with recombinant human bone morphogenetic protein-2/compression resistant matrix versus iliac crest bone graft.* Spine (Phila Pa 1976), 2006. 31(22): p. 2534-9; discussion 2540.
85. Glassman, S.D., et al., *The efficacy of rhBMP-2 for posterolateral lumbar fusion in smokers.* Spine (Phila Pa 1976), 2007. 32(15): p. 1693-8.
86. Haid, R.W., Jr., et al., *Posterior lumbar interbody fusion using recombinant human bone morphogenetic protein type 2 with cylindrical interbody cages.* Spine J, 2004. 4(5): p. 527-38; discussion 538-9.
87. Joseph, V. and Y.R. Rampersaud, *Heterotopic bone formation with the use of rhBMP2 in posterior minimal access interbody fusion: a CT analysis.* Spine (Phila Pa 1976), 2007. 32(25): p. 2885-90.
88. Buttermann, G.R., *Prospective nonrandomized comparison of an allograft with bone morphogenic protein versus an iliac-crest autograft in anterior cervical discectomy and fusion.* Spine J, 2008. 8(3): p. 426-35.
89. Vaidya, R., et al., *Complications of anterior cervical discectomy and fusion using recombinant human bone morphogenetic protein-2.* Eur Spine J, 2007. 16(8): p. 1257-65.
90. Shields, L.B., et al., *Adverse effects associated with high-dose recombinant human bone morphogenetic protein-2 use in anterior cervical spine fusion.* Spine (Phila Pa 1976), 2006. 31(5): p. 542-7.
91. Smucker, J.D., et al., *Increased swelling complications associated with off-label usage of rhBMP-2 in the anterior cervical spine.* Spine (Phila Pa 1976), 2006. 31(24): p. 2813-9.
92. Allen, R.T., et al., *Bone morphogenetic protein-2 (BMP-2) in the treatment of pyogenic vertebral osteomyelitis.* Spine (Phila Pa 1976), 2007. 32(26): p. 2996-3006.
93. Aryan, H.E., et al., *Corpectomy followed by the placement of instrumentation with titanium cages and recombinant human bone morphogenetic protein-2 for vertebral osteomyelitis.* J Neurosurg Spine, 2007. 6(1): p. 23-30.
94. Burkus, J.K., H.S. Sandhu, and M.F. Gornet, *Influence of rhBMP-2 on the healing patterns associated with allograft interbody constructs in comparison with autograft.* Spine (Phila Pa 1976), 2006. 31(7): p. 775-81.
95. Martin, G.J., Jr., et al., *Posterolateral intertransverse process spinal arthrodesis with rhBMP-2 in a nonhuman primate: important lessons learned regarding dose, carrier, and safety.* J Spinal Disord, 1999. 12(3): p. 179-86.
96. Mindea, S.A., P. Shih, and J.K. Song, *Recombinant human bone morphogenetic protein-2-induced radiculitis in elective minimally invasive transforaminal lumbar interbody fusions: a series review.* Spine (Phila Pa 1976), 2009. 34(14): p. 1480-4; discussion 1485.
97. Villavicencio, A.T., et al., *Safety of transforaminal lumbar interbody fusion and intervertebral recombinant human bone morphogenetic protein-2.* J Neurosurg Spine, 2005. 3(6): p. 436-43.
98. Pradhan, B.B., et al., *Graft resorption with the use of bone morphogenetic protein: lessons from anterior lumbar interbody fusion using femoral ring allografts and recombinant human bone morphogenetic protein-2.* Spine (Phila Pa 1976), 2006. 31(10): p. E277-84.
99. Kanatani, M., et al., *Stimulatory effect of bone morphogenetic protein-2 on osteoclast-like cell formation and bone-resorbing activity.* J Bone Miner Res, 1995. 10(11): p. 1681-90.
100. Nishiyama, K., et al., *Stimulatory effect of growth hormone on bone resorption and osteoclast differentiation.* Endocrinology, 1996. 137(1): p. 35-41.
101. Hsu, H.P., et al., *Comparing ectopic bone growth induced by rhBMP-2 on an absorbable collagen sponge in rat and rabbit models.* J Orthop Res, 2006. 24(8): p. 1660-9.
102. Nair, L.S. and C.T. Laurencin, *Polymers as biomaterials for tissue engineering and controlled drug delivery.* Adv Biochem Eng Biotechnol, 2006. 102: p. 47-90.
103. Solchaga, L.A., et al., *Augment(R) Bone Graft Products Compare Favorably to Autologous Bone Graft in an Ovine Model of Lumbar Interbody Spine Fusion.* Spine (Phila Pa 1976), 2011.
104. Gruskin, E., et al., *Demineralized bone matrix in bone repair: History and use.* Adv Drug Deliv Rev, (DOI 10.1016/j.addr.2012.06.008).
105. Bae, H.W., et al., *Intervariability and intravariability of bone morphogenetic proteins in commercially available demineralized bone matrix products.* Spine (Phila Pa 1976), 2006. 31(12): p. 1299-306; discussion 1307-8.
106. Holt, D.J. and D.W. Grainger, *Demineralized bone matrix as a vehicle for delivering endogenous and exogenous therapeutics in bone repair.* Advanced Drug Delivery Reviews, (0): p. published on line (April 9, 2012), doi10.1016/j.addr.2012.04.002, (2012).

107. Aebli, N., et al., *Effects of bone morphogenetic protein-2 and hyaluronic acid on the osseointegration of hydroxyapatite-coated implants: an experimental study in sheep.* J Biomed Mater Res A, 2005. 73(3): p. 295-302.
108. Sachse, A., et al., *Osteointegration of hydroxyapatite-titanium implants coated with nonglycosylated recombinant human bone morphogenetic protein-2 (BMP-2) in aged sheep.* Bone, 2005. 37(5): p. 699-710.
109. Schnettler, R., et al., *Enhancement of bone formation in hydroxyapatite implants by rhBMP-2 coating.* J Biomed Mater Res B Appl Biomater, 2009. 90(1): p. 75-81.
110. Sumner, D.R., et al., *Locally delivered rhTGF-beta2 enhances bone ingrowth and bone regeneration at local and remote sites of skeletal injury.* J Orthop Res, 2001. 19(1): p. 85-94.
111. Sumner, D.R., et al., *Locally delivered rhBMP-2 enhances bone ingrowth and gap healing in a canine model.* J Orthop Res, 2004. 22(1): p. 58-65.
112. Liu, Y., K. de Groot, and E.B. Hunziker, *BMP-2 liberated from biomimetic implant coatings induces and sustains direct ossification in an ectopic rat model.* Bone, 2005. 36(5): p. 745-57.
113. Liu, Y., et al., *The influence of BMP-2 and its mode of delivery on the osteoconductivity of implant surfaces during the early phase of osseointegration.* Biomaterials, 2007. 28(16): p. 2677-86.
114. Liu, Y., et al., *Delivery mode and efficacy of BMP-2 in association with implants.* J Dent Res, 2007. 86(1): p. 84-9.
115. Lucke, M., et al., *Gentamicin coating of metallic implants reduces implant-related osteomyelitis in rats.* Bone, 2003. 32(5): p. 521-31.
116. Schmidmaier, G., et al., *Biodegradable poly(D,L-lactide) coating of implants for continuous release of growth factors.* J Biomed Mater Res, 2001. 58(4): p. 449-55.
117. Schmidmaier, G., et al., *Bone morphogenetic protein-2 coating of titanium implants increases biomechanical strength and accelerates bone remodeling in fracture treatment: a biomechanical and histological study in rats.* Bone, 2002. 30(6): p. 816-22.
118. Wildemann, B., et al., *Local delivery of growth factors from coated titanium plates increases osteotomy healing in rats.* Bone, 2004. 34(5): p. 862-8.
119. Han, D., et al., *Optimal delivery systems for bone morphogenetic proteins in orthopedic applications should model initial tissue repair structures by using a heparin-incorporated fibrin-fibronectin matrix.* Med Hypotheses, 2008. 71(3): p. 374-8.
120. Patel, S., E.C. Rodriguez-Merchan, and F.S. Haddad, *The use of fibrin glue in surgery of the knee.* J Bone Joint Surg Br, 2010. 92-B(10): p. 1325-1331.
121. Shikanov, A., A. Ezra, and A.J. Domb, *Poly(sebacic acid-co-ricinoleic acid) biodegradable carrier for paclitaxel--effect of additives.* J Control Release, 2005. 105(1-2): p. 52-67.
122. Krasko, M.Y., et al., *Gentamicin extended release from an injectable polymeric implant.* J Control Release, 2007. 117(1): p. 90-6.
123. Saito, N., et al., *Synthetic biodegradable polymers as drug delivery systems for bone morphogenetic proteins.* Advanced Drug Delivery Reviews, 2005. 57(7): p. 1037.
124. Stadlinger, B., et al., *Effect of biological implant surface coatings on bone formation, applying collagen, proteoglycans, glycosaminoglycans and growth factors.* J Mater Sci Mater Med, 2008. 19(3): p. 1043-9.
125. Chung, Y.I., et al., *Enhanced bone regeneration with BMP-2 loaded functional nanoparticle-hydrogel complex.* J Control Release, 2007. 121(1-2): p. 91-9.
126. Jeon, O., et al., *Long-term and zero-order release of basic fibroblast growth factor from heparin-conjugated poly(L-lactide-co-glycolide) nanospheres and fibrin gel.* Biomaterials, 2006. 27(8): p. 1598-607.
127. Jeon, O., et al., *Long-term delivery enhances in vivo osteogenic efficacy of bone morphogenetic protein-2 compared to short-term delivery.* Biochem Biophys Res Commun, 2008. 369(2): p. 774-80.
128. Yilgor, P., et al., *Incorporation of a sequential BMP-2/BMP-7 delivery system into chitosan-based scaffolds for bone tissue engineering.* Biomaterials, 2009. 30(21): p. 3551-9.
129. Kempen, D.H., et al., *Retention of in vitro and in vivo BMP-2 bioactivities in sustained delivery vehicles for bone tissue engineering.* Biomaterials, 2008. 29(22): p. 3245-52.
130. Niu, X., et al., *Porous nano-HA/collagen/PLLA scaffold containing chitosan microspheres for controlled delivery of synthetic peptide derived from BMP-2.* J Control Release, 2009. 134(2): p. 111-7.
131. Chen, F.M., et al., *Novel glycidyl methacrylated dextran (Dex-GMA)/gelatin hydrogel scaffolds containing microspheres loaded with bone morphogenetic proteins: formulation and characteristics.* J Control Release, 2007. 118(1): p. 65-77.
132. Allison, S.D., *Analysis of initial burst in PLGA microparticles.* Expert Opin Drug Deliv, 2008. 5(6): p. 615-28.
133. Xie, H. and J.W. Smith, *Fabrication of PLGA nanoparticles with a fluidic nanoprecipitation system.* J Nanobiotechnology, 2010. 8: p. 18.
134. Bhardwaj, U., et al., *PLGA/PVA hydrogel composites for long-term inflammation control following s.c. implantation.* Int J Pharm, 2010. 384(1-2): p. 78-86.
135. Galeska, I., et al., *Controlled release of dexamethasone from PLGA microspheres embedded within polyacid-containing PVA hydrogels.* AAPS J, 2005. 7(1): p. E231-40.
136. Henslee, A.M., et al., *Biodegradable composite scaffolds incorporating an intramedullary rod and delivering bone morphogenetic protein-2 for stabilization and bone regeneration in segmental long bone defects.* Acta Biomater, 2011. 7(10): p. 3627-37.
137. Fulmer, M.T., et al., *US Patent Application 20080262630 - Drug-Impregnated Encasement*, 2008.
138. von Plocki, S.C., et al., *Biodegradable Sleeves for Metal Implants to Prevent Implant-Associated Infection: An Experimental In Vivo Study in Sheep.* Vet Surg, 2012.
139. Forster, H., et al., *Bactericidal activity of antimicrobial coated polyurethane sleeves for external fixation pins.* J Orthop Res, 2004. 22(3): p. 671-7.
140. Duda, G.N., M. Manav, and P. Strube, *US Patent Application 20090182425 - Sheet or Tubular Structure Consisting of Elastic Biocompatible Material and its Use*, 2009.
141. Wang, Y., et al., *Effect of chondroitin sulfate modification on rhBMP-2 release kinetics from collagen delivery system.* J Biomed Mater Res A, 2010. 92(2): p. 693-701.
142. Mattamal, G.J., *U.S. FDA Perspective on the Regulation of Cyanoacrylate Polymer Tissue Adhesives in Clinical Applications.* Materials Science Forum, 2007. 539-543: p. pp 692-697.

143. Mattamal, G.J., *US FDA perspective on the regulations of medical-grade polymers: cyanoacrylate polymer medical device tissue adhesives.* Expert Rev Med Devices, 2008. 5(1): p. 41-9.
144. Reece, T.B., T.S. Maxey, and I.L. Kron, *A prospectus on tissue adhesives.* Am J Surg, 2001. 182(2 Suppl): p. 40S-44S.
145. Ryou, M. and C.C. Thompson, *Tissue Adhesives: A Review.* Techniques in Gastrointestinal Endoscopy, 2006. 8(1): p. 33-37.
146. Traver, M.A. and D.G. Assimos, *New generation tissue sealants and hemostatic agents: innovative urologic applications.* Rev Urol, 2006. 8(3): p. 104-11.
147. Prausnitz, M.R. and R. Langer, *Transdermal drug delivery.* Nat Biotechnol, 2008. 26(11): p. 1261-8.
148. Scheindlin, S., *Transdermal drug delivery: PAST, PRESENT, FUTURE.* Mol Interv, 2004. 4(6): p. 308-12.
149. Basmanav, F.B., G.T. Kose, and V. Hasirci, *Sequential growth factor delivery from complexed microspheres for bone tissue engineering.* Biomaterials, 2008. 29(31): p. 4195-204.
150. Sawyer, A.A., et al., *The stimulation of healing within a rat calvarial defect by mPCL-TCP/collagen scaffolds loaded with rhBMP-2.* Biomaterials, 2009. 30(13): p. 2479-88.
151. Nie, T., et al., *Production of heparin-functionalized hydrogels for the development of responsive and controlled growth factor delivery systems.* J Control Release, 2007. 122(3): p. 287-96.
152. Gharibjanian, N.A., et al., *Release kinetics of polymer-bound bone morphogenetic protein-2 and its effects on the osteogenic expression of MC3T3-E1 osteoprecursor cells.* Plast Reconstr Surg, 2009. 123(4): p. 1169-77.
153. Zhao, Y., et al., *The osteogenic effect of bone morphogenetic protein-2 on the collagen scaffold conjugated with antibodies.* J Control Release, 2010. 141(1): p. 30-7.
154. Engstrand, T., et al., *A novel biodegradable delivery system for bone morphogenetic protein-2.* Plast Reconstr Surg, 2008. 121(6): p. 1920-8.
155. Cai, S., et al., *Injectable glycosaminoglycan hydrogels for controlled release of human basic fibroblast growth factor.* Biomaterials, 2005. 26(30): p. 6054-67.
156. Seal, B.L. and A. Panitch, *Physical polymer matrices based on affinity interactions between peptides and polysaccharides.* Biomacromolecules, 2003. 4(6): p. 1572-82.
157. Yang, H.S., et al., *Heparin-Conjugated Fibrin as an Injectable System for Sustained Delivery of Bone Morphogenetic Protein-2.* Tissue Eng Part A, 2010.
158. Zhang, L., E.M. Furst, and K.L. Kiick, *Manipulation of hydrogel assembly and growth factor delivery via the use of peptide-polysaccharide interactions.* J Control Release, 2006. 114(2): p. 130-42.
159. Bergman, K., et al., *Injectable cell-free template for bone-tissue formation.* J Biomed Mater Res A, 2009. 91(4): p. 1111-8.
160. Capila, I. and R.J. Linhardt, *Heparin-protein interactions.* Angew Chem Int Ed Engl, 2002. 41(3): p. 391-412.
161. Pinto Reis, C., et al., *Nanoencapsulation I. Methods for preparation of drug-loaded polymeric nanoparticles.* Nanomedicine, 2006. 2(1): p. 8-21.
162. Tamilvanan, S., et al., *Manufacturing techniques and excipients used during the design of biodegradable polymer-based microspheres containing therapeutic peptide/protein for parenteral controlled drug delivery.* PDA J Pharm Sci Technol, 2008. 62(2): p. 125-54.
163. Woo, B.H., et al., *Enhancement of bone growth by sustained delivery of recombinant human bone morphogenetic protein-2 in a polymeric matrix.* Pharm Res, 2001. 18(12): p. 1747-53.
164. Patel, Z.S., et al., *Biodegradable gelatin microparticles as delivery systems for the controlled release of bone morphogenetic protein-2.* Acta Biomater, 2008. 4(5): p. 1126-38.
165. Patel, Z.S., et al., *Dual delivery of an angiogenic and an osteogenic growth factor for bone regeneration in a critical size defect model.* Bone, 2008. 43(5): p. 931-40.
166. Wang, G., et al., *Preparation of BMP-2 containing bovine serum albumin (BSA) nanoparticles stabilized by polymer coating.* Pharm Res, 2008. 25(12): p. 2896-909.
167. Jha, A.K., et al., *Perlecan domain I-conjugated, hyaluronic acid-based hydrogel particles for enhanced chondrogenic differentiation via BMP-2 release.* Biomaterials, 2009. 30(36): p. 6964-75.
168. Kirby, G.T.S., et al., *PLGA-Based Microparticles for the Sustained Release of BMP-2.* Polymers, 2011. 3(1): p. 571-586.
169. Ji, Y., et al., *Transplanted bone morphogenetic protein/poly(lactic-co-glycolic acid) delayed-release microcysts combined with rat micromorselized bone and collagen for bone tissue engineering.* J Int Med Res, 2009. 37(4): p. 1075-87.
170. Jongpaiboonkit, L., T. Franklin-Ford, and W.L. Murphy, *Mineral-Coated Polymer Microspheres for Controlled Protein Binding and Release.* Advanced Materials, 2009. 21(19): p. 1960.
171. Wolfgang Friess, M.S., *Release mechanisms from gentamicin loaded poly(lactic-<I>co</I>-glycolic acid) (PLGA) microparticles.* Journal of Pharmaceutical Sciences, 2002. 91(3): p. 845-855.
172. Kempen, D.H., et al., *Effect of local sequential VEGF and BMP-2 delivery on ectopic and orthotopic bone regeneration.* Biomaterials, 2009. 30(14): p. 2816-25.
173. Zhang, S., M.R. Doschak, and H. Uludag, *Pharmacokinetics and bone formation by BMP-2 entrapped in polyethylenimine-coated albumin nanoparticles.* Biomaterials, 2009. 30(28): p. 5143-55.
174. Zhang, S., et al., *Polyethylenimine-coated albumin nanoparticles for BMP-2 delivery.* Biotechnol Prog, 2008. 24(4): p. 945-56.
175. Garty, S., et al., *Peptide-modified "smart" hydrogels and genetically engineered stem cells for skeletal tissue engineering.* Biomacromolecules, 2010. 11(6): p. 1516-26.
176. Chen, F.M., et al., *In vitro cellular responses to scaffolds containing two microencapulated growth factors.* Biomaterials, 2009. 30(28): p. 5215-24.
177. Yilgor, P., N. Hasirci, and V. Hasirci, *Sequential BMP-2/BMP-7 delivery from polyester nanocapsules.* J Biomed Mater Res A, 2009.
178. Bessa, P.C., et al., *Thermoresponsive self-assembled elastin-based nanoparticles for delivery of BMPs.* J Control Release, 2009.
179. Stammen, J.A., et al., *Mechanical properties of a novel PVA hydrogel in shear and unconfined compression.* Biomaterials, 2001. 22(8): p. 799-806.
180. Ammar, M.R., et al., *Adhesion improvement of poly (vinyl alcohol) coating on silicon substrate.* Surface and Coatings Technology, 2009. 203(16): p. 2202.

181. Liu, J., et al., *Controlled release of insulin from PLGA nanoparticles embedded within PVA hydrogels.* Journal of Materials Science: Materials in Medicine, 2007. 18(11): p. 2205.
182. Hassan, C.M. and N.A. Peppas, *Structure and Morphology of Freeze/Thawed PVA Hydrogels.* Macromolecules, 2000. 33(7): p. 2472.
183. Chiellini, E., et al., *Biodegradation of poly (vinyl alcohol) based materials.* Progress in Polymer Science, 2003. 28(6): p. 963.
184. Jiang, Y., et al., *In-vivo studies on intraperitoneally administrated poly(vinyl alcohol).* J Biomed Mater Res B Appl Biomater. 93(1): p. 275-84.
185. Krumova, M., et al., *Effect of crosslinking on the mechanical and thermal properties of poly(vinyl alcohol).* Polymer, 2000. 41(26): p. 9265.
186. Wang, J. and M. Satoh, *Novel PVA-based polymers showing an anti-Hofmeister Series property.* Polymer, 2009. 50(15): p. 3680.
187. Mondino, A.V., et al., *Physical properties of gamma irradiated poly(vinyl alcohol) hydrogel preparations.* Radiation Physics and Chemistry, 1999. 55(5-6): p. 723.
188. Bourke, S.L., et al., *A photo-crosslinked poly(vinyl alcohol) hydrogel growth factor release vehicle for wound healing applications.* AAPS PharmSci, 2003. 5(4): p. E33.
189. Chaouat, M., et al., *A Novel Cross-linked Poly(vinyl alcohol) (PVA) for Vascular Grafts.* Advanced Functional Materials, 2008. 18(19): p. 2855.
190. Jeck, S., P. Scharfer, and M. Kind, *Water sorption in physically crosslinked poly(vinyl alcohol) membranes: An experimental investigation of Schroeder's paradox.* Journal of Membrane Science, 2009. 337(1-2): p. 291.
191. Wan, W.K., et al., *Optimizing the tensile properties of polyvinyl alcohol hydrogel for the construction of a bioprosthetic heart valve stent.* J Biomed Mater Res, 2002. 63(6): p. 854-61.
192. Ma, R.-y. and D.-s. Xiong, *Synthesis and properties of physically crosslinked poly (vinyl alcohol) hydrogels.* Journal of China University of Mining and Technology, 2008. 18(2): p. 271-274.
193. Yang, X., et al., *Investigation of PVA/ws-chitosan hydrogels prepared by combined [gamma]-irradiation and freeze-thawing.* Carbohydrate Polymers, 2008. 73(3): p. 401.
194. Varshney, L., *Role of natural polysaccharides in radiation formation of PVA-hydrogel wound dressing.* Nuclear Instruments and Methods in Physics Research Section B: Beam Interactions with Materials and Atoms, 2007. 255(2): p. 343.
195. Jiang, T., et al., *Heparinized poly(vinyl alcohol)--small intestinal submucosa composite membrane for coronary covered stents.* Biomed Mater, 2009. 4(2): p. 025012.
196. Westedt, U., et al., *Paclitaxel releasing films consisting of poly(vinyl alcohol)-graft-poly(lactide-co-glycolide) and their potential as biodegradable stent coatings.* J Control Release, 2006. 111(1-2): p. 235-46.
197. Thomas, L.V., et al., *A biodegradable and biocompatible PVA-citric acid polyester with potential applications as matrix for vascular tissue engineering.* J Mater Sci Mater Med, 2009. 20 Suppl 1: p. S259-69.
198. Zheng, Y., et al., *Performance of novel bioactive hybrid hydrogels in vitro and in vivo used for artificial cartilage.* Biomed Mater, 2009. 4(1): p. 015015.
199. Wang, M., et al., *In vitro and in vivo study to the biocompatibility and biodegradation of hydroxyapatite/poly(vinyl alcohol)/gelatin composite.* J Biomed Mater Res A, 2008. 85(2): p. 418-26.
200. Pan, Y., D. Xiong, and F. Gao, *Viscoelastic behavior of nano-hydroxyapatite reinforced poly(vinyl alcohol) gel biocomposites as an articular cartilage.* J Mater Sci Mater Med, 2008. 19(5): p. 1963-9.
201. Kobayashi, M., Y.S. Chang, and M. Oka, *A two year in vivo study of polyvinyl alcohol-hydrogel (PVA-H) artificial meniscus.* Biomaterials, 2005. 26(16): p. 3243-8.
202. Asran, A.S., S. Henning, and G.H. Michler, *Polyvinyl alcohol-collagen-hydroxyapatite biocomposite nanofibrous scaffold: Mimicking the key features of natural bone at the nanoscale level.* Polymer. 51(4): p. 868.
203. Kumar, J. and S.F. D'Souza, *Preparation of PVA membrane for immobilization of GOD for glucose biosensor.* Talanta, 2008. 75(1): p. 183.
204. Hyon SH, *Poly(vinyl alcohol) hydrogels as soft contact lens material.* Journal of Biomaterials Science, Polymer Edition, 1994. 5: p. 397.
205. Maluccio, M.A., et al., *Transcatheter arterial embolization with only particles for the treatment of unresectable hepatocellular carcinoma.* J Vasc Interv Radiol, 2008. 19(6): p. 862-9.
206. Orienti, I., et al., *Hydrogels Formed by Crosslinked Poly(vinyl alcohol) as Sustained Drug Delivery Systems.* Arch Pharm (Weinheim), 2002. 335(2): p. 89-93.
207. Mc Gann, M.J., et al., *The synthesis of novel pH-sensitive poly(vinyl alcohol) composite hydrogels using a freeze/thaw process for biomedical applications.* Int J Pharm, 2009. 372(1-2): p. 154-61.
208. Coluccio, M.L., et al., *Enzymatic erosion of bioartificial membranes to control drug delivery.* Macromol Biosci, 2006. 6(6): p. 403-11.
209. Sinha, A. and A. Guha, *Biomimetic patterning of polymer hydrogels with hydroxyapatite nanoparticles.* Materials Science and Engineering: C, 2009. 29(4): p. 1330-1333.
210. Supova, M., *Problem of hydroxyapatite dispersion in polymer matrices: a review.* J Mater Sci Mater Med, 2009. 20(6): p. 1201-13.
211. Fenglan, X., et al., *Preparation and characterization of nano-hydroxyapatite/poly(vinyl alcohol) hydrogel biocomposite.* J Mater Sci Mater Med, 2004. 39(18): p. 5669-5672.
212. Sheikh, F., et al., *Synthesis of poly(vinyl alcohol) (PVA) nanofibers incorporating hydroxyapatite nanoparticles as future implant materials.* Macromolecular Research, 2010. 18(1): p. 59-66.
213. Zeng, S., et al., *Preparation and characterization of nano-hydroxyapatite/poly(vinyl alcohol) composite membranes for guided bone regeneration.* J Biomed Nanotechnol, 2011. 7(4): p. 549-57.
214. Gul, R., et al., *Osteochondral fractures in the knee treated with butyl-2-cyanoacrylate glue. A case report.* Acta Orthop Belg, 2006. 72(5): p. 641-3.
215. Yilmaz, C. and F. Kuyurtar, *Fixation of a talar osteochondral fracture with cyanoacrylate glue.* Arthroscopy, 2005. 21(8): p. 1009.
216. Papatheofanis, F.J., *Contribution of hydroxyapatite to the tensile strength of the isobutyl-2-cyanoacrylate-bone bond.* Biomaterials, 1989. 10(3): p. 185-6.
217. Petrie, E.M., *Handbook of Adhesives and Sealants*, 2000, McGraw-Hill.

218. Hassan, C.M., J.E. Stewart, and N.A. Peppas, *Diffusional characteristics of freeze/thawed poly(vinyl alcohol) hydrogels: applications to protein controlled release from multilaminate devices.* Eur J Pharm Biopharm, 2000. 49(2): p. 161-5.
219. Hassan, C. and N. Peppas, *Structure and Applications of Poly(vinyl alcohol) Hydrogels Produced by Conventional Crosslinking or by Freezing/Thawing Methods. Biopolymers · PVA Hydrogels, Anionic Polymerisation Nanocomposites*, 2000, Springer Berlin / Heidelberg. p. 37-65.
220. Ricciardi, R., et al., *X-ray Diffraction Analysis of Poly(vinyl alcohol) Hydrogels, Obtained by Freezing and Thawing Techniques.* Macromolecules, 2004. 37(5): p. 1921.
221. Charters, A., *Wound glue: a comparative study of tissue adhesives.* Accid Emerg Nurs, 2000. 8(4): p. 223-7.
222. Park, J.H., et al., *Transcatheter arterial embolization of arterial esophageal bleeding with the use of N-butyl cyanoacrylate.* Korean J Radiol, 2009. 10(4): p. 361-5.
223. Manfrin, T.M., et al., *Analysis in vitro of direct bonding system with cyanoacrylate ester and orthodontic wires.* Dent Traumatol, 2009. 25(2): p. 229-32.
224. Tripodo, G., C. Wischke, and A. Lendlein, *Highly Flexible Poly(ethyl-2-cyanoacrylate) Based Materials Obtained by Incorporation of Oligo(ethylene glycol)diglycidylether.* Macromolecular Symposia, 2011. 309-310(1): p. 49-58.
225. Hee Park, D., et al., *In vitro degradation and cytotoxicity of alkyl 2-cyanoacrylate polymers for application to tissue adhesives.* Journal of Applied Polymer Science, 2003. 89(12): p. 3272-3278.
226. Ciapetti, G., et al., *Cytotoxicity testing of cyanoacrylates using direct contact assay on cell cultures.* Biomaterials, 1994. 15(1): p. 63-7.
227. Thumwanit, V. and U. Kedjarune, *Cytotoxicity of polymerized commercial cyanoacrylate adhesive on cultured human oral fibroblasts.* Aust Dent J, 1999. 44(4): p. 248-52.
228. Evans, C.E., G.C. Lees, and I.A. Trail, *Cytotoxicity of cyanoacrylate adhesives to cultured tendon cells.* J Hand Surg Br, 1999. 24(6): p. 658-61.
229. Ekelund, A. and O.S. Nilsson, *Tissue adhesives inhibit experimental new bone formation.* Int Orthop, 1991. 15(4): p. 331-4.
230. Toriumi, D.M., et al., *Histotoxicity of cyanoacrylate tissue adhesives. A comparative study.* Arch Otolaryngol Head Neck Surg, 1990. 116(5): p. 546-50.
231. Alkan, S., et al., *The efficacy of N-2-butyl cyanoacrylate in the fixation of nasal septum to the anterior nasal spine in rabbits: experimental study.* Eur Arch Otorhinolaryngol, 2007. 264(12): p. 1425-30.
232. Dadas, B., et al., *Treatment of tripod fracture of zygomatic bone by N-2-butyl cyanoacrylate glue fixation, and its effects on the tissues.* Eur Arch Otorhinolaryngol, 2007. 264(5): p. 539-44.
233. Brown, P.N., H.S. McGuff, and A.D. Noorily, *Comparison of N-octyl-cyanoacrylate vs suture in the stabilization of cartilage grafts.* Arch Otolaryngol Head Neck Surg, 1996. 122(8): p. 873-7.
234. Lu, B., et al., *Octyl-a-cyanoacrylate adhesive in the treatment of tibial transverse fracture in rabbits.* Chin J Traumatol, 2005. 8(4): p. 240-4.
235. Sun, L., et al., *Material fundamentals and clinical performance of plasma-sprayed hydroxyapatite coatings: a review.* J Biomed Mater Res, 2001. 58(5): p. 570-92.
236. Ninan, L., et al., *Adhesive strength and curing rate of marine mussel protein extracts on porcine small intestinal submucosa.* Acta Biomater, 2007. 3(5): p. 687-94.
237. Yordanov, G. and C. Dushkin, *Preparation of poly(butylcyanoacrylate) drug carriers by nanoprecipitation using a pre-synthesized polymer and different colloidal stabilizers.* Colloid & Polymer Science, 2010. 288(9): p. 1019-1026.
238. Lu, S., et al., *Stabilization of enzymes in silk films.* Biomacromolecules, 2009. 10(5): p. 1032-42.
239. Boyd, S., K. Letcher, and H. Yamazaki, *Stabilization effect of polyvinyl alcohol on horseradish peroxidase, glucose oxidase, β-galactosidase and alkaline phosphatase.* Biotechnology Techniques, 1996. 10(9): p. 693-698.

Abbreviations

∅ - diameter

ALP - alkaline phosphatase

bFGF - basic fibroblast growth factor

BMP's - bone morphogenetic proteins

BMP-2; -4; -5; -6; -7; -8; -9; -10 - Bone Morphogenetic Protein 2; 4; 5; 6; 7; 8; 9; 10

BSA - bovine serum albumin

CA - cyanoacrylate

CH - carbon-hydrogen bond

CMC - carboxymethyl cellulose

CN - cyano group

CO - carbonyl group

CrNi - chromium-nickel steel

CS - chondroitin sulphate

DBM - Demineralized Bone Matrix

Dex-GMA - glycidyl methacrylated dextran

DMSO - dimethyl sulfoxide

FACS - Flow cytometry

GF`s - growth factors

HA - hydroxyapatite

HAP - hydroxyapatites

HPLC - high performance liquid chromatography

HRP - Horseradish Peroxidase

IGF-I - insulin-like growth factor I

IGFs - insulin-like growth factors

IR microscopy - Infrared microscopy

LbL - layer-by-layer

LMWH-PEG - low molecular weight heparin-functionalised star-PEG

MAPK - Mitogen-activated protein kinase

MMP - matrix metalloproteinase

MPa - megapascal

MSC's - mesenchymal stem cells

NMP - n-methyl-pyrrolidone

OCP - Office for Combination Products

OH - hydroxyl group

P(SA-RA) - poly(sebacic-co-ricinoleic-esteranhydride)

PACA - poly(alkyl-2-cyanoacrylate)

PBCA - poly(n-butyl cyanoacrylate)

PBS - phosphate buffered saline

PDGF - platelet derived growth factor

PDLF's - periodontal ligament fibroblasts

PDLLA - poly-DL-lactide

PECA - poly(ethyl cyanoacrylate)

PEG - polyethylene glycol

PEI - polyethyleneimine

PF4-PEG - Platelet factor 4-functionalised star-PEG

PGA - polyglycolide

PHBV - poly(3-hydroxybutyrate-co-3-hydroxyvalerate)

PLA - polylactide

PLA-DX-PEG - poly-d,l-lactic acid-para-dioxanone-polyethylene glycol

PLGA - poly(lactic-co-glycolic acid)

PLGA-PEG - poly(lactic-co-glycolic acid)-polyethylene glycol block copolymer

PLL - Poly-L-Lysine

PMCA - poly(methyl cyanoacrylate)

PMMA - polymethylmethacrylate

PO - phosphate-oxygen bond

POCA - poly(octyl cyanoacrylate)

PPF - polypropylene fumarate

PRP - platelet rich plasma

PVA - polyvinylalcohol

rhBMP-2 - recombinant human bone morphogenetic protein 2

rhBMP-7 - recombinant human bone morphogenetic protein 7

SAXS - Small Angle X-ray Scattering

SEM - Scanning Electron Microscopy

siRNA - small interfering RNA

ß-TCP - ß-tricalcium phosphate

TFA - trifluoroacetic acid

TGF-ß1 - transforming growth factor β1

TGFβ - transforming growth factor β

Ti - titanium

TIMP - tissue inhibitor of metalloproteinase

US FDA - Unated States Food and Drug Administration

VEGF - vascular endothelial growth factor

WAXS - Wide Angle X-ray Scattering